Multi-tiered Regulation of *luxR* Provides Precise Timing and Maintenance of the Quorum Sensing Response of *Vibrio fischeri*

Joshua W. Williams

Dissertation submitted to the faculty of the Virginia Polytechnic Institute and State University in partial fulfillment of the requirements for the degree of

Doctor of Philosophy
In
Biological Sciences

Ann M. Stevens, Committee Chair
Rahul V. Kulkarni, Committee Member
Timothy J. Larson, Committee Member
David L. Popham, Committee Member

June 4, 2009

Blacksburg, VA

Keywords: quorum sensing, bistability, hysteresis, CsrA, LuxR

Multi-tiered Regulation of *luxR* Provides Precise Timing and Maintenance of the Quorum Sensing Response of *Vibrio fischeri*

Joshua W. Williams

ABSTRACT

The quorum-sensing response of *Vibrio fischeri* involves a complex network of genes (encoding regulatory proteins as well as sRNAs), that govern host-association and production of bioluminescence. A key regulator of this system is LuxR, which is the transcriptional activator of the *lux* operon as well as several other genes in. LuxR also autoregulates its own transcription, which we have shown causes bistability and hysteresis in the quorum-sensing response. This behavior allows the system to maintain a stable and robust response in the face of environmental fluctuation or decreases in external autoinducer concentration caused by other sources. There are many factors that are known to regulate *luxR* expression, including the ArcA redox-responsive regulator, the cAMP-CRP secondary metabolism regulator, and components of the quorum-sensing pathway like LitR. Because of this, LuxR levels are critical in both the timing of quorum-sensing induction, as well as the maintenance of the response over time. This makes it a potential target for multiple levels of regulation in response to factors such as environmental and metabolic conditions, as well as other components of the quorum-sensing network.

Another important global regulatory protein in *V. fischeri* (and most other species of Gram-negative proteobacteria) is the post-transcriptional regulator CsrA. CsrA controls processes involved in carbon storage and utilization, as well as the transition

from exponential to stationary phase growth. We have demonstrated that CsrA is regulated by two sRNAs (CsrB1 and CsrB2) in *V. fischeri*. Because CsrA regulates changes in cell behavior and is an important metabolic regulator, there is a good possibility that it has some interactions with the quorum-sensing regulon, whose endproduct, bioluminescence, creates a large metabolic demand from the cell.

In an effort to determine at which point in the quorum-sensing regulatory network CsrA regulation is important, epistasis experiments were designed using factorial design, which is a subset of statistical analysis of variance (ANOVA). This method was used to generate a high degree of confidence in the data, so that even minor interactions in the regulatory networks could be established. By altering the levels of CsrA expression in various mutant strains of *V. fischeri*, we have demonstrated that CsrA acts by an unknown mechanism to increase the transcription of *luxR* when the quorum-sensing regulator LitR is absent. Our results also demonstrated that CsrA mediates this effect through repression of ArcA activity, which is known to act directly on the *luxR* and *luxI* intergenic region as a repressor. This indicates that CsrA may bypass the upstream parts of the quorum-sensing regulatory cascade that lead to *litR* activation, so that LitR and LuxR may be regulated differently in response to certain conditions.

This work has shown that the interactions between global regulons can coordinately control the amount of quorum-sensing induction by affecting the level of LuxR in the cell. The balance of these regulatory networks allows the cell to tightly regulate the quorum-sensing response. Thus, LuxR serves as a critical regulatory hub in the cell, at which multiple signals can be integrated in order to generate the appropriate cellular response.

Acknowledgements

I would like to first thank my advisor, Dr. Ann Stevens, for putting up with me for the last several years, and for all of her help in pursuit of my research goals. I would also like to thank the other members of my committee, Drs. Rahul Kulkarni, Tim Larson, and David Popham, who have also been a tremendous help throughout my research career at Va. Tech. I have a great amount of respect for each of my committee members, both as researchers and teachers, and have been fortunate to have their help and guidance throughout my Ph.D. studies.

I also thank my collaborators Andre Levchenko and Jimmy Ritter, who have been instrumental in my work involving mathematical modeling and statistical analysis, and who have made me wish I still remembered some calculus.

I would also like to acknowledge my colleagues in both the Stevens' lab and other micro-group labs, for making this a fun and collaborative work environment. I would especially like to thank Danny Schu and Wes Black, who aside from being good scientists, are also two of my best friends, which makes it a little easier to come to work every day.

Last, but certainly not least of all, I would like to thank my family. My wife Tara, who has always been supportive of me; my parents Tim and Joni, who have always encouraged me to do what makes me happy, and who taught me the value of hard work; and my aunt Joan, who has always been an important part of my life.

Table of Contents

List of Figures

Appendix I

List of Tables

Chapter 1

Literature review

Introduction to quorum sensing

Quorum sensing is a cell-density-dependent form of gene regulation utilized by certain species of Gram-positive and Gram-negative bacteria, which was first recognized in the regulation of bacterial bioluminescence (57). This mechanism of gene regulation is based on the production and accumulation of an inducing signal (21) (called an autoinducer (AI)) in the cellular environment, which is recognized by specific proteins that bind the AI and then cause either positive or negative transcriptional regulation of quorum-sensing controlled genes (78, 87) (Fig. 1.1). Quorum sensing is utilized by many different species of bacteria, and is important in the regulation of a variety of important processes, such as virulence factor production, host association, motility, biofilm formation, and genetic competence (13, 35, 52, 80).

Gram-negative species that utilize quorum sensing produce acyl-homoserine lactone autoinducers (AHL). These small, freely diffusible signals have varying fatty acid side-chain lengths and substitutions at the 3rd carbon in the chain. These variations allow for species-specific recognition by the AI-receptor protein. Many species of Gram-negative proteobacteria have one or more quorum-sensing circuits homologous to the LuxR/I circuit of *Vibrio fischeri*, which is a model organism for quorum-sensing regulation. In this type of network, the "R" protein serves as the autoinducer-dependent transcription factor, and the "I" protein catalyzes production of the acyl-HSL autoinducers. The concentration of the signal builds up in the extracellular environment, such that as local cell density increases, so does the concentration of the autoinducer. Once a critical threshold of [AI] is met, the quorum sensing circuit becomes induced, and genes under its control are then activated or repressed (Fig. 1.1; panel A).

It is not uncommon for more than one tier of quorum-sensing circuits to regulate an organism's cell density-dependent gene expression. Many organisms produce multiple HSLs and have more than one LuxR/I feedback loop (41, 43, 50, 52, 82). These complex networks involving multiple levels of regulation allow a bacterial population to control the expression of many different genes necessary to exert a given response to the environment in which the cells reside. These regulatory arrangements usually involve a hierarchical system, in which one system is the master regulator, and others are involved in the timing and modulation of the response under various conditions. Examples of these types of arrangements can be found in the *V. fischeri ain/lux* quorum-sensing circuits, which control the timing of host-association and luminescence production (51), and the *Pseudomonas aeruginosa las/rhl* system which controls the expression of virulence factors (62).

In addition to variation in the number of quorum-sensing circuits found in species of Gram-negative proteobacteria, there are also variations in the mechanisms used to exert transcriptional control of target genes. Some species such as *Vibrio cholerae* and *Vibrio harveyi* contain LuxR homologues that do not directly bind the autoinducer, but rather are controlled by a two-component signal transduction system, whose activity is controlled in an autoinducer-responsive manner (44, 45). Amongst the LuxR homologues that directly bind AI, there are also differences in how AI binding controls the activity of the "R" protein. In the case of *V. fischeri*, LuxR binds the AI and forms an active homodimer complex that can then bind to the DNA, and activate transcription (74, 75). In other species like *Erwinia carotovora* and *Pantoea stewartii*, the LuxR homologue is bound to the DNA in the absence of AI and typically functions to repress

quorum sensing controlled genes (1, 54, 85). Once AI accumulation occurs, the LuxR homolog binds the AI to form a complex that causes it to dissociate from the DNA, allowing transcription of the previously repressed genes (1, 54, 86). This mechanism of derepression is common in many plant pathogens that produce exopolysaccharide in a quorum-sensing dependent manner (63). Although many of the LuxR homologs found in Gram-negative proteobacteria are typically classified as either activators or repressors, it is important to note that they can act as both, depending on where they bind the DNA in the promoter region of the target gene (22, 46, 85).

Unlike Gram-negative quorum-sensing systems, Gram-positive organisms typically produce short peptide autoinducers, which are actively exported from the cell into the surrounding environment. Gram-positive quorum-sensing receptors are membrane-associated, and act as kinases once they recognize their specific AI peptide. Once activated, these kinases phosphorylate a specific response regulator, which then directs expression of quorum sensing controlled genes (Fig. 1.1; panel B). For reviews of quorum sensing in bacterial systems, see (27, 32, 36, 53, 65, 78).

The *Vibrio fischeri* quorum-sensing system

V. fischeri was one of the first species of bacteria that was found to use quorum-sensing gene regulation, and it has served as a model organism due to the fact that many other species have homologous quorum-sensing circuitry. *V. fischeri* is a marine symbiont of certain species of marine fish and squid, and when grown to high cell density, it produces a blue-green light that the host organism uses for counterillumination.

The major quorum-sensing circuit in *V. fischeri* is the LuxR-LuxI system. LuxR is the AI-dependent regulator of the quorum-sensing response. The N-terminal domain

of the protein binds the AI, and the C-terminal domain binds to DNA once the active complex has been formed with AI (11). LuxI is the AI synthase responsible for catalyzing the production of the N-3-oxo-C6-L-homoserine lactone (3-oxo-C6-HSL) autoinducer (23). The *lux* genes are arranged divergently, with *luxR* transcribed in the opposite direction of *luxICDABEG*. *luxCDABE* are the genes necessary for light production, which is one of the main processes controlled by *V. fischeri* quorum sensing. *luxCDE* encodes the proteins necessary for the production of the aldehyde substrate for the luminescence reaction. *luxAB* encodes the alpha and beta subunit of luciferase respectively, which is the enzyme that catalyzes the light producing reaction (23, 31). *luxG* encodes a proposed flavin reductase that reduces FMN which is used for reduction of the fatty-acid substrate used in luminescence production (58).

luxR and *luxICDABEG* are separated by a region of DNA containing binding sites for many regulatory proteins, including LuxR, LitR, CRP, and ArcA (6, 18, 19, 73, 74). LuxR specifically recognizes a 20 base pair inverted repeat sequence called the *lux* box, which is centered at -42.5 bp from the +1 site of *luxI* (14, 76). As 3-oxo-C6-HSL accumulates in the cell, LuxR forms a homodimer containing two molecules of the AI. Once this active complex is formed, LuxR is capable of binding to the *lux* box, and activating transcription of the *lux* operon (11, 76). This creates a positive feedback loop leading to increased production of 3-oxo-C6-HSL, which in turn causes increased activation of the *lux* operon and higher luminescence output (Fig. 1.2). Aside from the *lux* box found upstream of *luxI*, there are other LuxR-regulated genes in *V. fischeri* that contain weaker *lux* boxes which have slight divergences from the consensus sequence, or are spaced differently in relation to the +1 site of transcription. Genes with *lux* boxes

more similar to the consensus sequence are activated to a higher degree than those containing significant variation (3, 64). This allows LuxR to control many different genes once quorum-sensing induction has occurred.

In addition to the LuxR/I circuit, there are many other important quorum-sensing network genes that control the initial stages of induction. A second AI synthase protein, AinS, produces N-octanoyl-L-homoserine lactone (C8-HSL) (29, 41, 42). C8-HSL is recognized by the membrane-associated AinR, which is proposed to begin a phosphorylation cascade culminating in the phosphorylation and inactivation of the quorum sensing repressor LuxO, based on the activities of homologous proteins from *V. harveyi* (45). LuxO, when in a non-phosphorylated state, activates production of the small RNA *qrr1*, which represses LitR (84). LitR is a transcriptional activator of *luxR*, and also plays a key role in regulating colonization genes necessary for *V. fischeri* to associate with its squid host *Euprymna scolopes* (25). Aside from relieving repression of the *lux* genes through activation of this phosphorylation cascade, C8-HSL can also weakly interact with LuxR to form an active complex, leading to transcriptional activation of *luxI*. This complex network is arranged so that there is a sequential induction process of genes necessary to colonize the host, followed by the induction of genes responsible for producing bioluminescence (51, 84) (Fig 1.2).

The cAMP-CRP complex is known to activate transcription of LuxR, indicating that metabolic state may also be important in determining the overall activation state of the *lux* operon (18, 19). This is an important aspect to consider, due to the high energy demand that the process of bioluminescence places on the cell. The reduction of the fatty acid substrate for the luciferase enzyme consumes a large amount of ATP (7, 8), and

therefore is a logical point of regulation based on metabolic state. It is also an important factor to consider in relation to *V. fischeri*'s symbiotic association with the squid *Euprymna scolopes*. It has been proposed that the host-bacterium interaction may cause the host epithelial cells of the light organ to excrete cAMP (17). This may be due to the production of an ADP-ribosyltransferase by *V. fischeri*, which in many pathogens is known to induce changes in the host cell (66). *V. fischeri* is capable of utilizing cAMP as a sole carbon source, due to the presence of a high-activity 3',5'-cyclic phosphodiesterase in its periplasm (17), which may give it a competitive advantage in colonizing the light organ, and may also induce luminescence through activation of *luxR* by cAMP-CRP.

The luminescence reaction also consumes a large amount of oxygen, and has been shown to be regulated by the ArcA/B system (6), which controls gene expression in response to redox state. As cells enter into stationary phase, their environment becomes more reduced, and the ArcA/B system activates genes important under these conditions, such as terminal electron-transport chain complexes that use alternate electron acceptors. The quorum-sensing system also becomes fully activated as the cells transition from late exponential to stationary phase, which is the point where there is generally a high enough density of cells to produce an inducing concentration of AI. ArcA has been shown to negatively regulate the *luxI* promoter, and also to a lesser extent the *luxR* promoter, by binding in the intergenic region that separates them (6). This repression of the *lux* system may function to delay the induction process until a higher cell density is reached, which would work in concert with the buildup of AI. Repression may also help modulate the response so that an appropriate level of light output is maintained.

It has also been proposed in previous work that LuxR is capable of both positive and negative autoregulation of its own transcription (10, 20, 72, 73). This positive autoregulation when combined with the positive feedback loop based on LuxI activation and AI accumulation, can lead to a rapid increase in luminescence once the appropriate conditions have been met. It is also important to note that this autoinduction of *luxR* can impact expression of other genes in *V. fischeri* that have been shown to be regulated by LuxR. The complexity and multi-level regulation of *luxR* transcription indicate that it is a critical component to the overall timing and maintenance of the quorum-sensing response. By increasing the concentration of the master regulator of the quorum-sensing response, the cell becomes more sensitive to slight increases in AI concentration, and can therefore become rapidly induced once the critical threshold of AI has been met. Conversely, by having multiple levels of negative regulation on *luxR*, the cell is able to precisely control under what conditions the quorum-sensing system becomes activated, so that it does not expend energy and produce light until it is in a high density setting like the light organ of the host. Chapters Two and Four of this thesis cover experimental analyses dealing with the regulation of *luxR* in relation to numerous transcription factors and inputs from multiple regulatory networks.

Hysteresis and multistability in positive feedback loops

Many bacterial systems involve transcriptional activation by an inducer-regulator complex that creates a positive feedback loop, leading to increased production of target proteins. In many cases, this causes a behavior called hysteresis, which simply means "history dependence". This history-dependence on exposure to the inducer creates the possibility for multiple states of genetic expression to exist for a particular inducer

molecule concentration. Once the inducer molecule has reached a critical threshold, target genes become activated, and positive feedback occurs. As a consequence, if the inducer concentration decreases, the system remains in a higher state of induction, or may be permanently locked in an "on" state (2, 24, 55, 59, 79, 81). A simple diagram of a hysteretic response is shown in Fig. 1.3.

Multistability and hysteresis has been demonstrated in many genetic systems, such as the *lac* operon in *E. coli* (61), control of the lambda phage lysis-lysogeny switch (60), and cell-cycle checkpoints in *Xenopus laevis* (71). Synthetic biology efforts have also taken advantage of hysteretic and bistable systems to engineer genetic switches in response to certain conditions (28, 33).

There have been numerous efforts to mathematically model the quorum-sensing system of *V. fischeri*, as well as many other quorum-sensing circuits. Many of these models predict that bistability is possible in the *luxI-luxR* genetic circuit, but there is some disagreement in the literature as to what leads to the hysteretic response during induction state switching. Several models propose that it is the LuxI-based increase in AI-production that causes the cell to enter a bistable range of gene expression, whereas others have stated that there must be a second positive feedback loop in order for this to occur (12, 15, 30, 33, 34, 56, 69, 91). The second proposed feedback loop in this quorum-sensing circuit is the LuxR autoregulation loop, which has been disregarded in some modeling efforts.

Hysteresis and bistability generally endow a genetic system with robustness in the occurrence of environmental fluctuation or variations in signal concentration. In cases where there is a genetic switch, such as in the *Bacillus subtilis* sporulation process (83),

or eukaryotic cell-cycle checkpoints, hysteretic gene expression allows the cells to become locked into a certain physiological state that cannot be reversed once a critical point has been reached in development. In more dynamic responses like quorum sensing, bistable gene expression is not a permanent phenomenon, but causes it to become more difficult to switch states once the critical concentration of the inducing signal has accumulated.

Another consequence of bistability in gene expression is that a population of cells may contain two or more sub-populations that are expressing different sets of genes, or are in different physiological states. This behavior is seen in processes such as biofilm formation, sporulation, and the presence of persister cells within a biofilm (9, 37, 83). The presence of these sub-populations may play a role in the emergence of antibiotic resistant strains of common pathogens, and may play an important role in survival of a species by increasing the chance for genetic variation to occur under selective conditions. It can be advantageous for a population if a small proportion of the cells remain in either a dormant state, or undergo an adaptation due to hysteretic gene expression, so that when conditions change or become lethal, some members of the species are better able to adapt and survive.

Chapter Two focuses on the experimental verification of hysteresis and bistability in the quorum sensing circuitry of *V. fischeri.* This work used both mathematical modeling and experimental approaches to determine what causes this behavior during the quorum-sensing induction process, as well as the factors that modulate the degree of the effect. This study focused solely on the *luxR/luxI* genetic circuit, but we were also interested in how this system interacts with other regulatory networks. Metabolic state of

the cell is a logical point of co-regulation of the quorum-sensing response, and because it is known that cAMP-CRP regulates *luxR*, we hypothesized that the carbon storage regulatory protein CsrA may also play a role in how the quorum-sensing network becomes activated.

Post-transcriptional regulation by the RNA-binding protein CsrA

CsrA (called RsmA in some species) is an RNA-binding protein that is an important global regulatory element involved in carbon utilization and the transition between exponential growth and stationary phases, that was first discovered as regulating glycogen metabolism in *Escherichia coli* (68). CsrA acts during exponential growth phase to activate expression of certain genes, while repressing others that are important in stationary phase. Some of the processes that are known to be regulated by CsrA include glycogen metabolism, gluconeogenesis, motility, and biofilm formation (reviewed in (67)).

Regulation by CsrA involves the recognition of specific RNA sequences as well as the presence of certain RNA secondary structures in the transcript, although the exact criteria for CsrA binding have not yet been established. In many CsrA-regulated transcripts, the presence of an ACA or GGA motif in certain positions in a stem-loop structure are present, but their arrangement and the structure of the stem-loop can create variations in CsrA-affinity (16, 40). CsrA can regulate the expression of a transcript by either blocking its translation by binding and occluding the ribosome binding site, or by destabilizing the transcript, leading to its degradation by RNases (4, 5, 48, 70). Many of the targets know to be regulated by CsrA are repressed, although it is suspected that it may also act to positively regulate genes as well. Simply using a bioinformatics

approach to scan genomes for CsrA-regulated genes has been difficult due to the variations in sequence and secondary structure requirements for CsrA recognition of a transcript, and the fact that there may be requirements for multiple CsrA-binding sites in order for CsrA to bind.

CsrA activity is controlled by several small non-coding RNAs (typically named CsrB or CsrC), which contain multiple stem-loops with RNA sequence and secondary structure that constitute a strong CsrA-binding motif (47, 88). These CsrA-regulating small RNAs typically bind multiple copies of the protein, forming an inactive complex (Fig. 1.4). The expression of the *csr* sRNAs is regulated by the BarA/UvrY two component signal transduction system in *E. coli* (GacS/GacA in *V. fischeri*), and indirectly by CsrA itself (77). CsrA activates BarA, which then activates UvrY allowing direct activation of *csrB*. CsrA also seems to have an indirect positive effect on UvrY expression mediated through an unknown mechanism. UvrY also has a positive autoregulatory mechanism due to its activation of BarA. This arrangement with multiple levels of feedback is important due to the fact that the balance of CsrA/B/C expression is crucial for maintaining the cell in the appropriate physiological state in response to nutrient availability and environmental stress.

CsrA has also been shown to regulate several important virulence factors in pathogenic species (26, 38, 39, 49), indicating that in addition to metabolism, it may also play a key role in adaptation to a host environment. GacA, which controls the production of the *csrB* sRNA regulators of CsrA, has been shown to play an important role in the control of host-colonization in *V. fischeri*, as well as its ability to utilize certain growth substrates (89, 90).

Chapter Three focuses on the identification of the *csrA/B* system in *V. fischeri* as well as the verification of their homologous function to the known *E. coli* system. Chapter Four is an experimental attempt to discover the points of co-regulation between the CsrA network and the quorum-sensing network in *V. fischeri*. This work used an epistasis approach to identify key points of interaction between these two networks, and how they impact the output of the *V. fischeri* quorum sensing response, luminescence.

Appendix II of this thesis contains methods and preliminary results from experiments involving CsrA purification and RNA-pulldown experiments that were not published, but that will be important for future work on this project.

References

1. **Andersson, R. A., A. R. Eriksson, R. Heikinheimo, A. Mae, M. Pirhonen, V. Koiv, H. Hyytiainen, A. Tuikkala, and E. T. Palva.** 2000. Quorum sensing in the plant pathogen *Erwinia carotovora* subsp. *carotovora*: the role of *expR*(Ecc). Mol Plant Microbe Interact **13:**384-93.
2. **Angeli, D., J. E. Ferrell, Jr., and E. D. Sontag.** 2004. Detection of multistability, bifurcations, and hysteresis in a large class of biological positive-feedback systems. Proc Natl Acad Sci U S A **101:**1822-7.
3. **Antunes, L. C., A. L. Schaefer, R. B. Ferreira, N. Qin, A. M. Stevens, E. G. Ruby, and E. P. Greenberg.** 2007. Transcriptome analysis of the *Vibrio fischeri* LuxR-LuxI regulon. J Bacteriol **189:**8387-91.
4. **Baker, C. S., L. A. Eory, H. Yakhnin, J. Mercante, T. Romeo, and P. Babitzke.** 2007. CsrA inhibits translation initiation of *Escherichia coli hfq* by binding to a single site overlapping the Shine-Dalgarno sequence. J Bacteriol **189:**5472-81.
5. **Baker, C. S., I. Morozov, K. Suzuki, T. Romeo, and P. Babitzke.** 2002. CsrA regulates glycogen biosynthesis by preventing translation of *glgC* in *Escherichia coli*. Mol Microbiol **44:**1599-610.
6. **Bose, J. L., U. Kim, W. Bartkowski, R. P. Gunsalus, A. M. Overley, N. L. Lyell, K. L. Visick, and E. V. Stabb.** 2007. Bioluminescence in *Vibrio fischeri* is controlled by the redox-responsive regulator ArcA. Mol Microbiol **65:**538-53.
7. **Boylan, M., A. F. Graham, and E. A. Meighen.** 1985. Functional identification of the fatty acid reductase components encoded in the luminescence operon of *Vibrio fischeri*. J Bacteriol **163:**1186-90.
8. **Boylan, M., C. Miyamoto, L. Wall, A. Graham, and E. Meighen.** 1989. Lux C, D and E genes of the *Vibrio fischeri* luminescence operon code for the reductase, transferase, and synthetase enzymes involved in aldehyde biosynthesis. Photochem Photobiol **49:**681-8.
9. **Chai, Y., F. Chu, R. Kolter, and R. Losick.** 2008. Bistability and biofilm formation in *Bacillus subtilis*. Mol Microbiol **67:**254-63.
10. **Chatterjee, J., C. M. Miyamoto, and E. A. Meighen.** 1996. Autoregulation of *luxR*: the *Vibrio harveyi lux*-operon activator functions as a repressor. Mol Microbiol **20:**415-25.
11. **Choi, S. H., and E. P. Greenberg.** 1992. Genetic dissection of DNA binding and luminescence gene activation by the *Vibrio fischeri* LuxR protein. J Bacteriol **174:**4064-9.
12. **Cox, C. D., G. D. Peterson, M. S. Allen, J. M. Lancaster, J. M. McCollum, D. Austin, L. Yan, G. S. Sayler, and M. L. Simpson.** 2003. Analysis of noise in quorum sensing. Omics **7:**317-34.
13. **de Kievit, T. R., and B. H. Iglewski.** 2000. Bacterial quorum sensing in pathogenic relationships. Infect Immun **68:**4839-49.
14. **Devine, J. H., Shadel, G.S., Baldwin, T.O.** 1989. Identification of the operator of the *lux* regulon of *Vibrio fischeri* strain ATCC7744. Proc. Natl. Acad. Sci., USA **86:**5688-5692.
15. **Dockery, J. D., and J. P. Keener.** 2001. A mathematical model for quorum sensing in *Pseudomonas aeruginosa*. Bull Math Biol **63:**95-116.

16. **Dubey, A. K., C. S. Baker, T. Romeo, and P. Babitzke.** 2005. RNA sequence and secondary structure participate in high-affinity CsrA-RNA interaction. Rna **11:**1579-87.
17. **Dunlap, P. V., and S. M. Callahan.** 1993. Characterization of a periplasmic 3':5'-cyclic nucleotide phosphodiesterase gene, *cpdP*, from the marine symbiotic bacterium *Vibrio fischeri*. J Bacteriol **175:**4615-24.
18. **Dunlap, P. V., Greenberg, E.P.** 1985. Control of *Vibrio fischeri* luminescence gene expression in *Escherichia coli* by cyclic AMP and cyclic AMP receptor protein. J. Bacteriol. **164:**45-50.
19. **Dunlap, P. V., Greenberg, E.P.** 1988. Control of *Vibrio fischeri lux* gene transcription by a cyclic AMP receptor protein-LuxR protein regulatory circuit. J. Bacteriol. **170:**4040-4046.
20. **Dunlap, P. V., and J. M. Ray.** 1989. Requirement for autoinducer in transcriptional negative autoregulation of the *Vibrio fischeri luxR* gene in *Escherichia coli*. J Bacteriol **171:**3549-52.
21. **Eberhard, A., A. L. Burlingame, C. Eberhard, G. L. Kenyon, K. H. Nealson, and N. J. Oppenheimer.** 1981. Structural identification of autoinducer of *Photobacterium fischeri* luciferase. Biochemistry **20:**2444-9.
22. **Egland, K. A., and E. P. Greenberg.** 2000. Conversion of the *Vibrio fischeri* transcriptional activator, LuxR, to a repressor. J Bacteriol **182:**805-11.
23. **Engebrecht, J., Silverman, M.** 1984. Identification of genes and gene products necessary for bacterial bioluminescence. Proc. Natl. Acad. Sci., USA **81:**4154-4158.
24. **Ferrell, J. E., Jr.** 2002. Self-perpetuating states in signal transduction: positive feedback, double-negative feedback and bistability. Curr Opin Cell Biol **14:**140-8.
25. **Fidopiastis, P., Miyamato, C., Jobling, M., Meighan, E., Ruby, G.** 2002. LitR, a new transcriptional activator in *Vibrio fischeri* regulates luminescence and symbiotic light organ colonization. Molec. Microbiol. **45:**131-143.
26. **Fields, J. A., and S. A. Thompson.** 2008. *Campylobacter jejuni* CsrA mediates oxidative stress responses, biofilm formation, and host cell invasion. J Bacteriol **190:**3411-6.
27. **Fuqua, W. C., S. C. Winans, and E. P. Greenberg.** 1994. Quorum sensing in bacteria: the LuxR-LuxI family of cell density-responsive transcriptional regulators. J Bacteriol **176:**269-75.
28. **Gardner, T. S., C. R. Cantor, and J. J. Collins.** 2000. Construction of a genetic toggle switch in *Escherichia coli*. Nature **403:**339-42.
29. **Gilson, L., Kuo, A., Dunlap, P.V.** 1995. AinS and a new family of autoinducer synthesis proteins. J. Bacteriol. **177:**6946-6951.
30. **Goryachev, A. B., D. J. Toh, and T. Lee.** 2006. Systems analysis of a quorum sensing network: design constraints imposed by the functional requirements, network topology and kinetic constants. Biosystems **83:**178-87.
31. **Gray, K. M., Greenberg, E.P.** 1992. Physical and functional maps of the luminescence gene cluster in an autoinducer-deficient *Vibrio fischeri* strain isolated from a squid light organ. J. Bacteriol. **174:**4384-4390.
32. **Greenberg, E. P.** 1997. Quorum sensing in Gram-negative bacteria. . ASM News **63:**371-378.

33. **Haseltine, E. L., and F. H. Arnold.** 2008. Implications of rewiring bacterial quorum sensing. Appl Environ Microbiol **74:**437-45.
34. **Hense, B. A., C. Kuttler, J. Muller, M. Rothballer, A. Hartmann, and J. U. Kreft.** 2007. Does efficiency sensing unify diffusion and quorum sensing? Nat Rev Microbiol **5:**230-9.
35. **Irie, Y., and M. R. Parsek.** 2008. Quorum sensing and microbial biofilms. Curr Top Microbiol Immunol **322:**67-84.
36. **Jayaraman, A., and T. K. Wood.** 2008. Bacterial quorum sensing: signals, circuits, and implications for biofilms and disease. Annu Rev Biomed Eng **10:**145-67.
37. **Jayaraman, R.** 2008. Bacterial persistence: some new insights into an old phenomenon. J Biosci **33:**795-805.
38. **Jones, M. K., E. B. Warner, and J. D. Oliver.** 2008. *csrA* inhibits the formation of biofilms by *Vibrio vulnificus*. Appl Environ Microbiol **74:**7064-6.
39. **Kerrinnes, T., Z. B. Zelas, W. Streckel, F. Faber, E. Tietze, H. Tschape, and S. Yaron.** 2008. CsrA and CsrB are required for the post-transcriptional control of the virulence-associated effector protein AvrA of *Salmonella enterica*. Int J Med Microbiol.
40. **Kulkarni, P. R., X. Cui, J. W. Williams, A. M. Stevens, and R. V. Kulkarni.** 2006. Prediction of CsrA-regulating small RNAs in bacteria and their experimental verification in *Vibrio fischeri*. Nucleic Acids Res **34:**3361-9.
41. **Kuo, A., Blough, N.V., Dunlap, P.V.** 1994. Multiple N-acyl-L-homoserine lactone autoinducers of luminescence in the marine symbiotic bacterium *Vibrio fischeri*. J. Bacteriol. **176:**7558-7565.
42. **Kuo, A., Callahan, S.M., Dunlap, P.V.** 1996. Modulation of luminescence operon expression by N-octanoyl-L-homoserine lactone in *ainS* mutants of *Vibrio fischeri*. J. Bacteriol. **178:**971-976.
43. **Latifi, A., M. Foglino, K. Tanaka, P. Williams, and A. Lazdunski.** 1996. A hierarchical quorum-sensing cascade in *Pseudomonas aeruginosa* links the transcriptional activators LasR and RhIR (VsmR) to expression of the stationary-phase sigma factor RpoS. Mol Microbiol **21:**1137-46.
44. **Lenz, D. H., K. C. Mok, B. N. Lilley, R. V. Kulkarni, N. S. Wingreen, and B. L. Bassler.** 2004. The small RNA chaperone Hfq and multiple small RNAs control quorum sensing in *Vibrio harveyi* and *Vibrio cholerae*. Cell **118:**69-82.
45. **Lilley, B. N., and B. L. Bassler.** 2000. Regulation of quorum sensing in *Vibrio harveyi* by LuxO and sigma-54. Mol Microbiol **36:**940-54.
46. **Lin, W., G. Kovacikova, and K. Skorupski.** 2005. Requirements for *Vibrio cholerae* HapR binding and transcriptional repression at the *hapR* promoter are distinct from those at the *aphA* promoter. J Bacteriol **187:**3013-9.
47. **Liu, M. Y., G. Gui, B. Wei, J. F. Preston, 3rd, L. Oakford, U. Yuksel, D. P. Giedroc, and T. Romeo.** 1997. The RNA molecule CsrB binds to the global regulatory protein CsrA and antagonizes its activity in *Escherichia coli*. J Biol Chem **272:**17502-10.
48. **Liu, M. Y., H. Yang, and T. Romeo.** 1995. The product of the pleiotropic *Escherichia coli* gene *csrA* modulates glycogen biosynthesis via effects on mRNA stability. J Bacteriol **177:**2663-72.

49. **Lucchetti-Miganeh, C., E. Burrowes, C. Baysse, and G. Ermel.** 2008. The post-transcriptional regulator CsrA plays a central role in the adaptation of bacterial pathogens to different stages of infection in animal hosts. Microbiology **154:**16-29.
50. **Lupp, C., and E. G. Ruby.** 2004. *Vibrio fischeri* LuxS and AinS: comparative study of two signal synthases. J Bacteriol **186:**3873-81.
51. **Lupp, C., M. Urbanowski, E. P. Greenberg, and E. G. Ruby.** 2003. The *Vibrio fischeri* quorum-sensing systems *ain* and *lux* sequentially induce luminescence gene expression and are important for persistence in the squid host. Mol Microbiol **50:**319-31.
52. **Miller, M. B., K. Skorupski, D. H. Lenz, R. K. Taylor, and B. L. Bassler.** 2002. Parallel quorum sensing systems converge to regulate virulence in *Vibrio cholerae*. Cell **110:**303-14.
53. **Milton, D. L.** 2006. Quorum sensing in *vibrios*: complexity for diversification. Int J Med Microbiol **296:**61-71.
54. **Minogue, T. D., M. Wehland-von Trebra, F. Bernhard, and S. B. von Bodman.** 2002. The autoregulatory role of EsaR, a quorum-sensing regulator in *Pantoea stewartii* ssp. *stewartii*: evidence for a repressor function. Mol Microbiol **44:**1625-35.
55. **Mitrophanov, A. Y., and E. A. Groisman.** 2008. Positive feedback in cellular control systems. Bioessays **30:**542-55.
56. **Muller, J., C. Kuttler, B. A. Hense, M. Rothballer, and A. Hartmann.** 2006. Cell-cell communication by quorum sensing and dimension-reduction. J Math Biol **53:**672-702.
57. **Nealson, K. H., T. Platt, and J. W. Hastings.** 1970. Cellular control of the synthesis and activity of the bacterial luminescent system. J Bacteriol **104:**313-22.
58. **Nijvipakul, S., J. Wongratana, C. Suadee, B. Entsch, D. P. Ballou, and P. Chaiyen.** 2008. LuxG is a functioning flavin reductase for bacterial luminescence. J Bacteriol **190:**1531-8.
59. **Ninfa, A. J., and A. E. Mayo.** 2004. Hysteresis vs. graded responses: the connections make all the difference. Sci STKE **2004:**pe20.
60. **Oppenheim, A. B., O. Kobiler, J. Stavans, D. L. Court, and S. Adhya.** 2005. Switches in bacteriophage lambda development. Annu Rev Genet **39:**409-29.
61. **Ozbudak, E. M., Thattai, M., Lim, H.N., Shraiman, B.I., von Oudenaarden, A.V. .** 2004. Multistability in the lactose utilization network of *Escherichia coli*. Nature **427:**737-740.
62. **Pesci, E. C., J. P. Pearson, P. C. Seed, and B. H. Iglewski.** 1997. Regulation of *las* and *rhl* quorum sensing in *Pseudomonas aeruginosa*. J Bacteriol **179:**3127-32.
63. **Pierson, L. S., 3rd, D. W. Wood, and E. A. Pierson.** 1998. Homoserine lactone-mediated gene regulation in plant-associated bacteria. Annu Rev Phytopathol **36:**207-25.
64. **Qin, N., S. M. Callahan, P. V. Dunlap, and A. M. Stevens.** 2007. Analysis of LuxR regulon gene expression during quorum sensing in *Vibrio fischeri*. J Bacteriol **189:**4127-34.
65. **Reading, N. C., and V. Sperandio.** 2006. Quorum sensing: the many languages of bacteria. FEMS Microbiol Lett **254:**1-11.

66. **Reich, K. A., and G. K. Schoolnik.** 1996. Halovibrin, secreted from the light organ symbiont *Vibrio fischeri*, is a member of a new class of ADP-ribosyltransferases. J Bacteriol **178:**209-15.
67. **Romeo, T.** 1998. Global regulation by the small RNA-binding protein CsrA and the non-coding RNA molecule CsrB. Mol Microbiol **29:**1321-30.
68. **Romeo, T., M. Gong, M. Y. Liu, and A. M. Brun-Zinkernagel.** 1993. Identification and molecular characterization of *csrA*, a pleiotropic gene from *Escherichia coli* that affects glycogen biosynthesis, gluconeogenesis, cell size, and surface properties. J Bacteriol **175:**4744-55.
69. **Sayut, D. J., P. K. Kambam, and L. Sun.** 2007. Noise and kinetics of LuxR positive feedback loops. Biochem Biophys Res Commun **363:**667-73.
70. **Schubert, M., K. Lapouge, O. Duss, F. C. Oberstrass, I. Jelesarov, D. Haas, and F. H. Allain.** 2007. Molecular basis of messenger RNA recognition by the specific bacterial repressing clamp RsmA/CsrA. Nat Struct Mol Biol **14:**807-13.
71. **Sha, W., Moore, J., Chen, K., Lassaletta, A.D., Yi, C., Tyson, J.J., Sible, J.C.** 2003. Hysteresis drives cell-cycle transitions in *Xenopus laevis* egg extracts. Proc. Natl. Acad. Sci., USA **100:**975-980.
72. **Shadel, G. S., and T. O. Baldwin.** 1992. Positive autoregulation of the *Vibrio fischeri luxR* gene. LuxR and autoinducer activate cAMP-catabolite gene activator protein complex-independent and -dependent *luxR* transcription. J Biol Chem **267:**7696-702.
73. **Shadel, G. S., Baldwin, T.O.** 1991. The *Vibrio fischeri* LuxR protein is capable of bidirectional stimulation of transcription and both positive and negative regulation of the *luxR* gene. J. Bacteriol. **173:**568-574.
74. **Shadel, G. S., Devine, J.H., Baldwin, T.O.** 1990. Control of the *lux* regulon of *Vibrio fischeri*. J. Bioluminescence and Chemiluminescence **5:**99-106.
75. **Stevens, A. M., and E. P. Greenberg.** 1997. Quorum sensing in *Vibrio fischeri*: essential elements for activation of the luminescence genes. J Bacteriol **179:**557-62.
76. **Stevens, A. M., Greenberg, E.P.** 1999. Transcriptional activation by LuxR: Cell-cell signaling in bacteria. Presented at the ASM conference, Washington, D.C.
77. **Suzuki, K., X. Wang, T. Weilbacher, A. K. Pernestig, O. Melefors, D. Georgellis, P. Babitzke, and T. Romeo.** 2002. Regulatory circuitry of the CsrA/CsrB and BarA/UvrY systems of *Escherichia coli*. J Bacteriol **184:**5130-40.
78. **Taga, M. E., and B. L. Bassler.** 2003. Chemical communication among bacteria. Proc Natl Acad Sci U S A **100 Suppl 2:**14549-54.
79. **Tian, T., and K. Burrage.** 2006. Stochastic models for regulatory networks of the genetic toggle switch. Proc Natl Acad Sci U S A **103:**8372-7.
80. **Tortosa, P., L. Logsdon, B. Kraigher, Y. Itoh, I. Mandic-Mulec, and D. Dubnau.** 2001. Specificity and genetic polymorphism of the *Bacillus* competence quorum-sensing system. J Bacteriol **183:**451-60.
81. **Tsai, T. Y., Y. S. Choi, W. Ma, J. R. Pomerening, C. Tang, and J. E. Ferrell, Jr.** 2008. Robust, tunable biological oscillations from interlinked positive and negative feedback loops. Science **321:**126-9.

82. **Ulrich, R. L., D. Deshazer, E. E. Brueggemann, H. B. Hines, P. C. Oyston, and J. A. Jeddeloh.** 2004. Role of quorum sensing in the pathogenicity of *Burkholderia pseudomallei*. J Med Microbiol **53:**1053-64.
83. **Veening, J. W., L. W. Hamoen, and O. P. Kuipers.** 2005. Phosphatases modulate the bistable sporulation gene expression pattern in *Bacillus subtilis*. Mol Microbiol **56:**1481-94.
84. **Visick, K. L.** 2005. Layers of signaling in a bacterium-host association. J Bacteriol **187:**3603-6.
85. **von Bodman, S. B., J. K. Ball, M. A. Faini, C. M. Herrera, T. D. Minogue, M. L. Urbanowski, and A. M. Stevens.** 2003. The quorum sensing negative regulators EsaR and ExpR(Ecc), homologues within the LuxR family, retain the ability to function as activators of transcription. J Bacteriol **185:**7001-7.
86. **von Bodman, S. B., D. R. Majerczak, and D. L. Coplin.** 1998. A negative regulator mediates quorum-sensing control of exopolysaccharide production in *Pantoea stewartii* subsp. *stewartii*. Proc Natl Acad Sci U S A **95:**7687-92.
87. **Waters, C. M., and B. L. Bassler.** 2005. Quorum sensing: cell-to-cell communication in bacteria. Annu Rev Cell Dev Biol **21:**319-46.
88. **Weilbacher, T., Kazushi, S., Dubey, A.K., Wang, X., Gudapaty, S., Morozov, I., Baker, C.S., Georgellis, D., Babitzke, P., Romeo, T.** 2003. A novel sRNA component of the carbon storage regulatory system of *Escherichia coli*. Molec. Microbiol. **43:**657-670.
89. **Whistler, C. A., T. A. Koropatnick, A. Pollack, M. J. McFall-Ngai, and E. G. Ruby.** 2007. The GacA global regulator of *Vibrio fischeri* is required for normal host tissue responses that limit subsequent bacterial colonization. Cell Microbiol **9:**766-78.
90. **Whistler, C. A., and E. G. Ruby.** 2003. GacA regulates symbiotic colonization traits of *Vibrio fischeri* and facilitates a beneficial association with an animal host. J Bacteriol **185:**7202-12.
91. **Williams, J. W., X. Cui, A. Levchenko, and A. M. Stevens.** 2008. Robust and sensitive control of a quorum-sensing circuit by two interlocked feedback loops. Mol Syst Biol **4:**234.

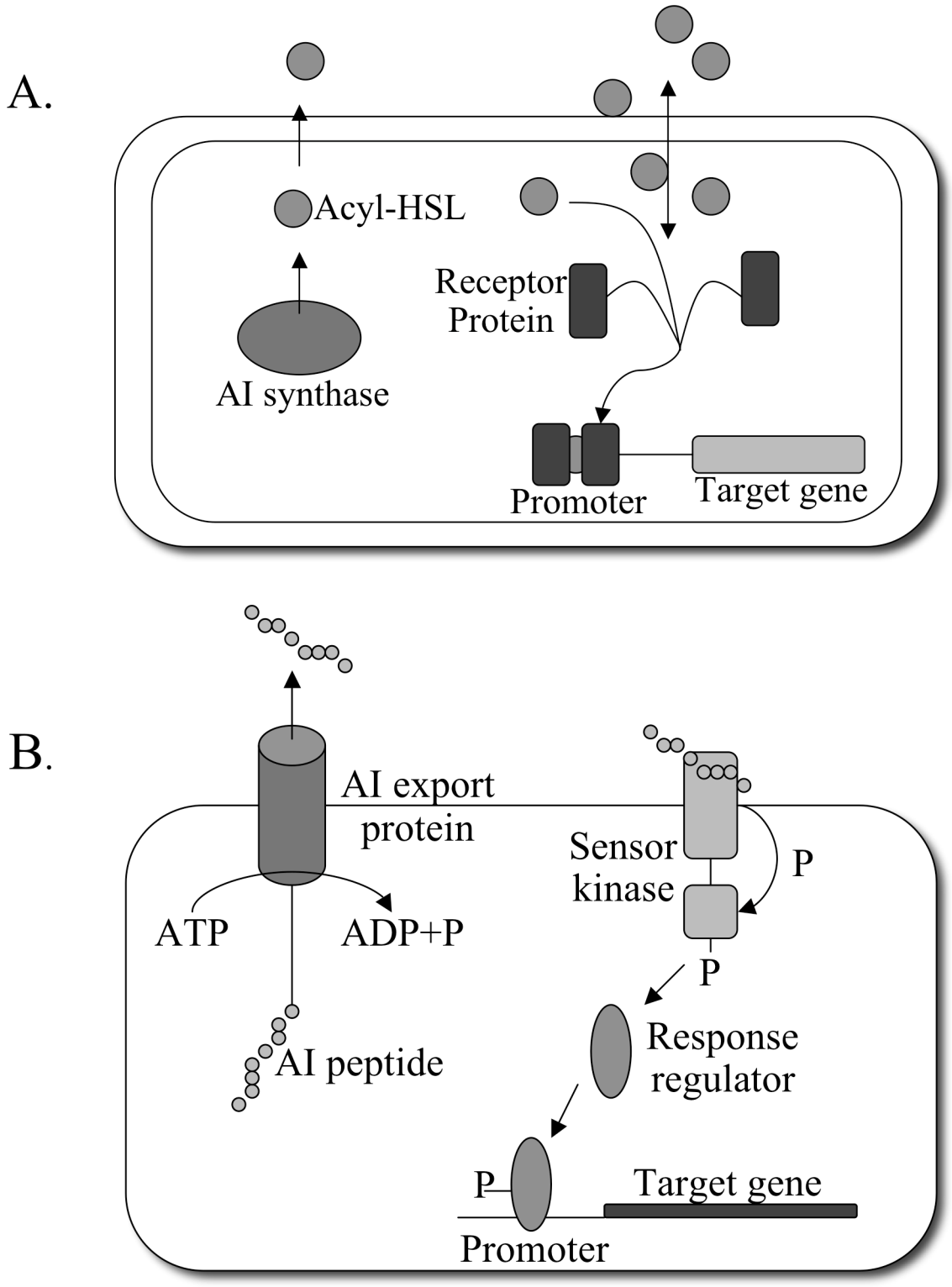

Figure 1.1: Quorum-sensing circuitry in Gram-negative and Gram-positive species (See text for details)

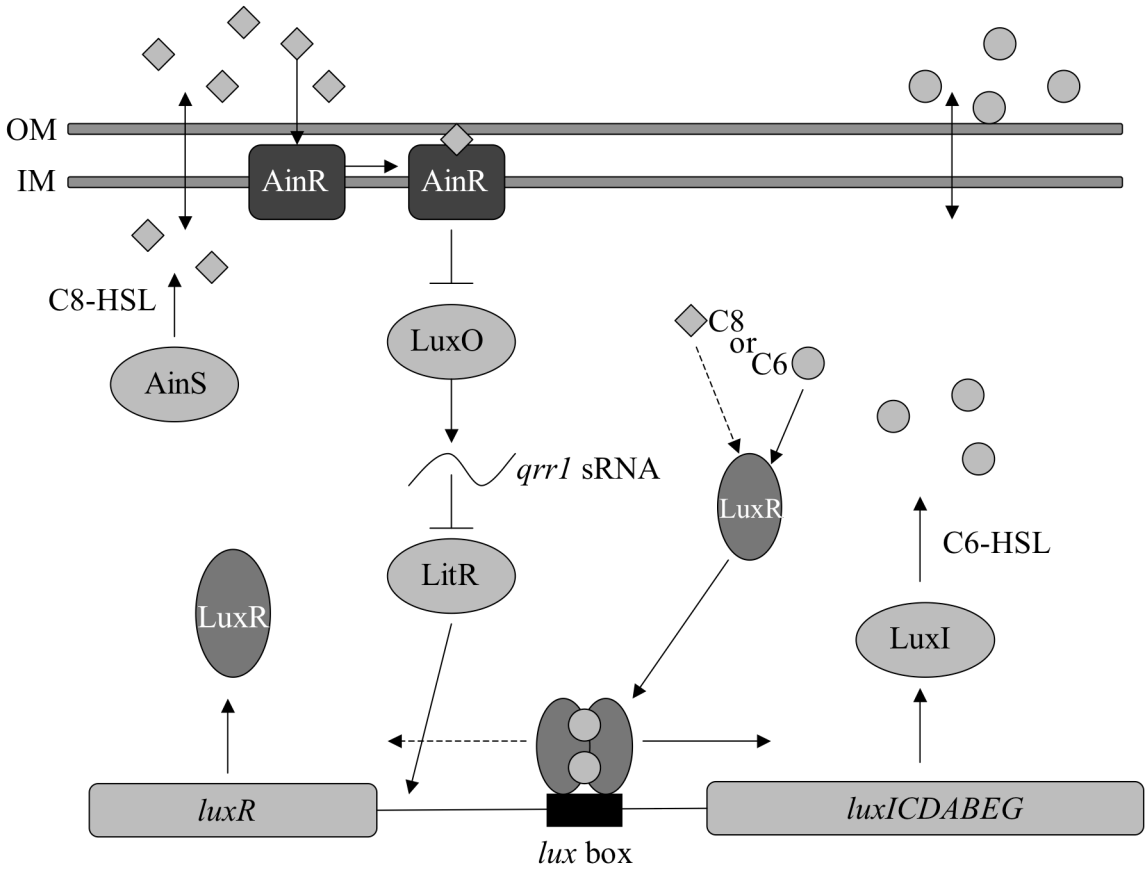

Figure 1.2: The quorum-sensing system of *Vibrio fischeri* (See text for details)

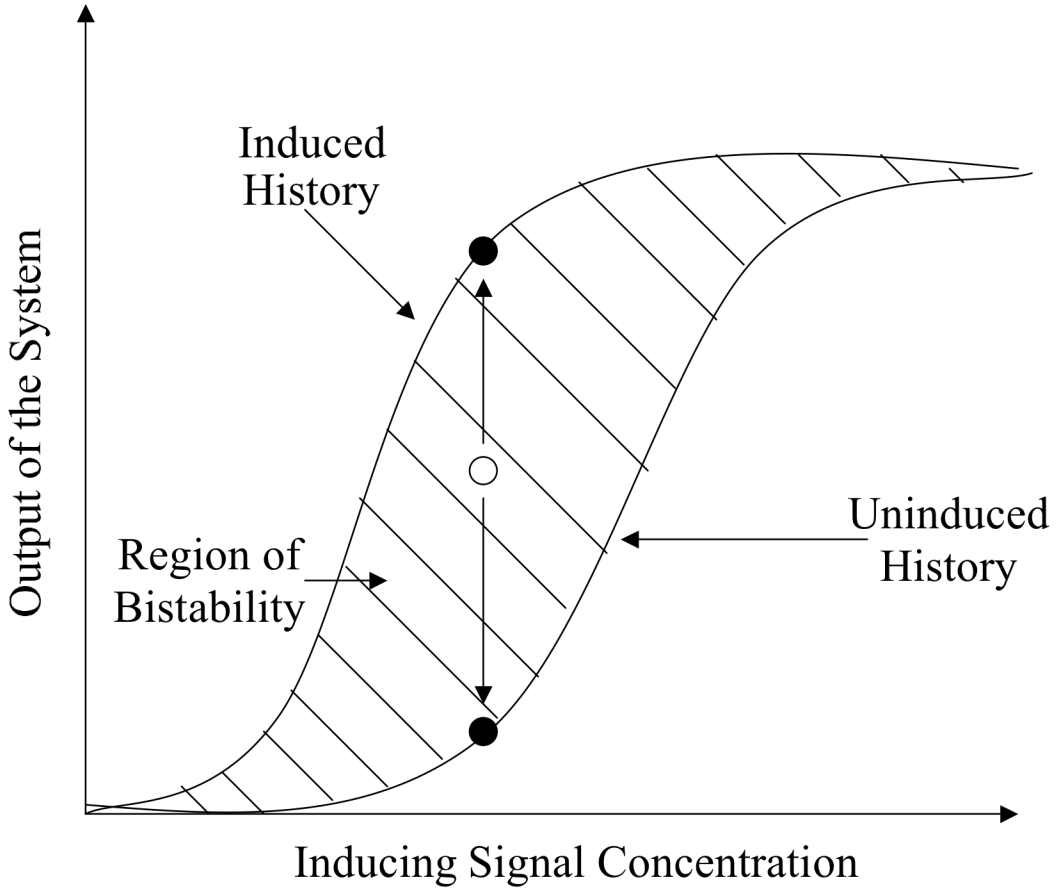

Figure 1.3: Diagram of a hysteretic response. As the concentration of an inducing signal increases, a system follows an induction curve leading to increased output with increasing signal concentration (uninduced history). A fully induced system may experience loss of inducing signal (viewed as moving from right to left on the upper curve), which will gradually lead to loss of the response, but may cause a different level of output for the system at the same concentration of inducing signal, than when the system increased from low to high inducing signal (induced history). This difference in expression value is separated by a region of bistability which is unstable. A small change in inducing signal will cause the system to move to one of the two expression curves, depending on the history of exposure to the inducer. The two possible stable states for one [AI] are indicated as black circles, whereas the unstable state is represented by a white circle. The transition to one state or the other from the unstable state is shown with vertical arrows moving away from the white circle.

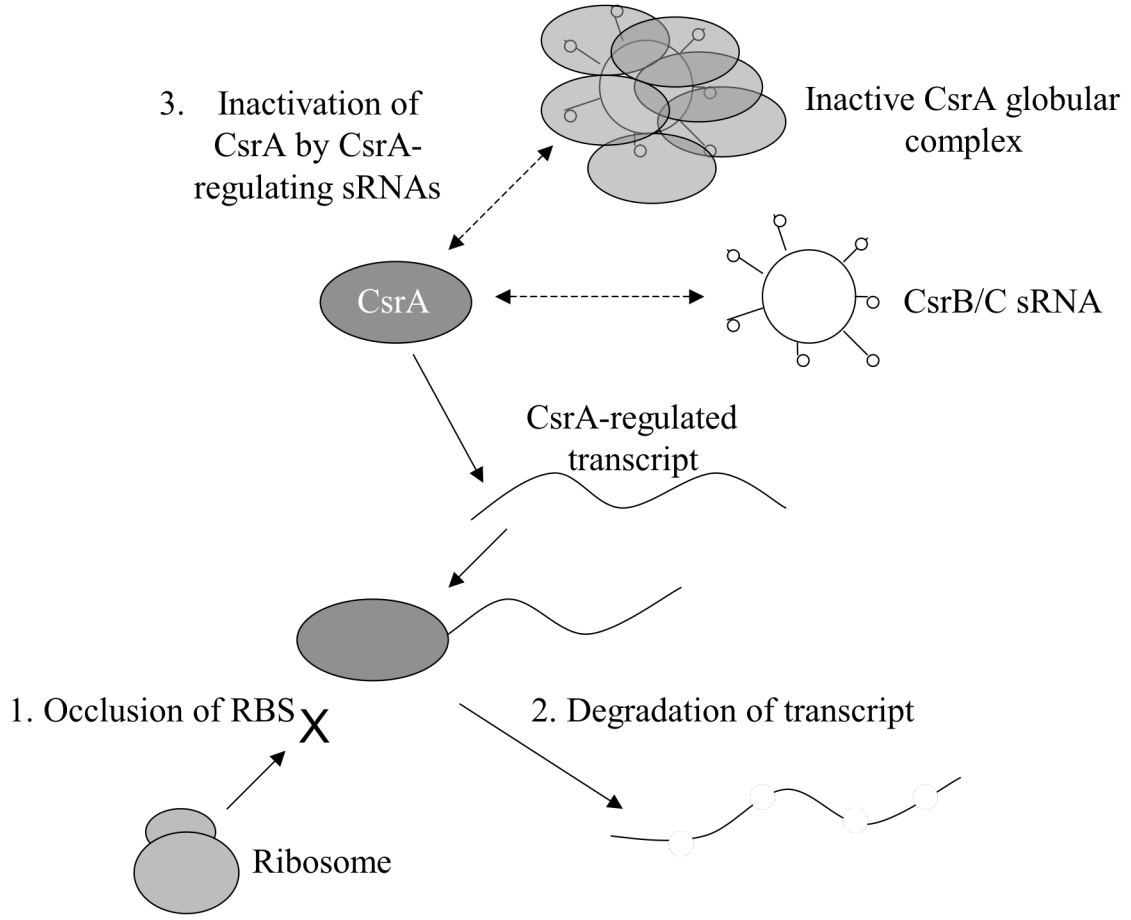

Figure 1.4: Regulatory mechanism of CsrA. The post-transcriptional regulatory protein CsrA functions by binding specific regions of an mRNA and either blocking the ribosome binding site, thus preventing translation of the transcript (1), or destabilizing the transcript so that it is more rapidly degraded by RNases (2). CsrA activity is itself controlled by small non-coding RNAs for which the protein has very high affinity. This affinity is due to the presence of multiple CsrA-binding sites on the sRNA, which leads to multiple CsrA proteins binding a single Csr sRNA and becoming inactive (3).

Chapter 2

Robust and sensitive control of a quorum-sensing circuit by two interlocked feedback loops

Joshua W. Williams, Xiaohui Cui, Andre Levchenko, and Ann M. Stevens. (2008). Robust and sensitive control of a quorum-sensing circuit by two interlocked feedback loops. Molecular Systems Biology 4:234

Abstract

The quorum-sensing (QS) response of *Vibrio fischeri* involves a rapid switch between low and high induction states of the *lux* operon over a narrow concentration range of the autoinducer (AI) 3-oxo-hexanoyl-L-homoserine lactone. In this system, LuxR is an AI-dependent positive regulator of the *lux* operon, which encodes the AI synthase. This creates a positive feedback loop common in many bacterial species that exhibit QS controlled gene expression. Applying a combination of modeling and experimental analyses, we provide evidence for a LuxR autoregulatory feedback loop that allows LuxR to increase its concentration in the cell during the switch to full *lux* activation. Using synthetic *lux* gene fragments, with or without the AI synthase gene, we show that the buildup of LuxR provides more sensitivity to increasing AI, and promotes the induction process. Elevated LuxR levels buffer against spurious variations in AI levels ensuring a robust response that endows the system with enhanced hysteresis. LuxR autoregulation also allows for two distinct responses within the same cell population.

Introduction

Quorum sensing (QS) is an example of cell-cell communication in bacteria, allowing an assemblage of closely positioned cells to alter its behavior in a coordinated manner, if the cell density exceeds a specific threshold. QS regulates a plethora of critically important phenotypes, including antibiotic production, release of exoenzymes, production of virulence factors, induction of genetic competency, conjugative plasmid transfer, biofilm formation and bioluminescence (15, 34, 42). In addition to understanding the role of these bacterial phenotypes to pathogenic and symbiotic states, analysis of the mechanisms underlying QS might shed light on how the behavior of a single cell can be tightly and robustly coordinated with the behavior of the cell group.

The QS response of *Vibrio fischeri* is a model system for many other QS systems which share networks similar to the LuxR/I network (39). LuxR is an autoinducer (AI)-dependent positive regulator of the *lux* operon, and LuxI produces the AI molecule, 3-oxo-hexanoyl-L-homoserine lactone. Much is known about how the LuxR/I system achieves activation of the *lux* operon leading to bioluminescence. A number of factors, including the activator complex cAMP-CRP, regulate expression of *luxR* (9, 10, 14). LuxR then activates expression of the *lux* operon when the concentration of LuxR-AI complexes reaches a critical threshold. This leads to higher levels of AI, generating a positive feedback loop (7, 10, 26, 38). It has been proposed that LuxR not only regulates the *lux* operon, but that it might positively or negatively autoregulate the QS response through modulating its own expression (6, 11, 36, 37), although the precise molecular basis for this autoregulation remains unknown.

The presence of one or more feedback interactions in the molecular networks underlying QS in *V. fischeri* and other bacterial systems might lead to such emergent properties as hysteretic responses and the associated 'memory' of the previous network states. Such memory-like properties have been suggested for other systems containing positive feedback interactions, based both on mathematical modeling and experimental investigation (2, 13, 25, 30, 31, 35). Some mathematical models of *V. fischeri* QS signaling have suggested the existence of hysteresis in response to extracellular AI concentration ([AI]), based on AI-induced *luxI* expression leading to a further increase in AI production (8, 18, 22, 29). This positive feedback is reliant on retention and accumulation of AI in the cell milieu. However, since the AI can freely diffuse across the cell membrane (23) this can make the system vulnerable to potentially rapid changes in [AI]. In a classical hysteresis analysis, the [AI] is exogenously fixed at various levels. This can mask the feedback-based increase of [AI], and hence complicate the experimental and theoretical analysis of the effects of the positive LuxI-based feedback.

Because the mechanism of LuxR autoregulation in *V. fischeri* is unknown, the analysis of the onset of QS has been based on various assumptions (28, 36, 37). If this autoregulation is indeed present, its role in the QS response is presently not clear. In this report, through a combination of modeling and experiments, we provide further evidence for the existence of this second feedback circuit in the *luxR/I* QS network. Moreover, we demonstrate the presence of hysteresis in a reduced *lux* network lacking LuxI-based feedback. In the network containing both feedback interactions, *luxR*-positive autoregulation can enhance response diversification and endow it with higher robustness to AI perturbation, thereby increasing the fidelity of the QS switch.

Results

Decoupling LuxI-mediated positive feedback

A convenient way to computationally and experimentally analyze feedback loops is to decouple them. For the example of *lux* operon regulation, the [AI] can be held at a fixed value, and the resulting expression of the system determined. This analysis can be repeated for different [AI] values, yielding curves showing dependencies of *luxI* expression on AI ([LuxI] = f([AI])) or AI production on LuxI ([AI] = g([LuxI])). These curves, known as null-clines of the underlying dynamical system, can intersect when plotted in the same coordinate system (e.g., by co-plotting f and g^{-1}), revealing points corresponding to the steady state concentrations of AI and LuxI in the reconstituted feedback system (Fig. 2.1A). Depending on how nonlinear the functions f and g^{-1} are, they can intersect in various ways, yielding a different number of steady states, which can be either stable, (i.e., resistant to small concentration changes due to molecular noise or other random perturbations) or unstable (2). Multiple steady states signal that the response can stably display different values, depending on the initial conditions of the systems (e.g., whether the initial [AI] is high or low). In the presence of many AI-secreting cells, the [AI] experienced by individual cells would be the sum of endogenously produced LuxI-mediated AI (AI_{in}) and AI diffusing from other cells (AI_{ex}). Additionally, AI_{ex} can be controlled experimentally, by supplying synthetic AI. The presence of AI_{ex} can further lead to a shift of the g nullcline by uniform addition of AI_{ex}: $g' = g + [AI_{ex}]$. This shift can lead to a change in the number of the steady states, allowing for a fast transition from low to high values of the response. For the complete

lux operon this would imply the frequently assumed hysteretic (history dependent) behavior, and a rapid onset of QS beyond a critical cell density.

Previous analyses suggested that at least one of the null-clines f or g^{-1} should be sufficiently non-linear for multiple steady states to occur (2, 13, 41). To determine the properties of the f null-cline, an *Escherichia coli* strain was created with a chromosomal insertion of a synthetic *lux01* genetic circuit capable of expressing LuxR, but with a truncated divergently transcribed *lux* operon, so that all of the transcripts normally downstream of the promoter are replaced with *gfp*. Thus exogenous AI is required for GFP expression (Fig. AI.1). This allowed decoupling of the AI-LuxI feedback and experimental measurement the f null-cline under different conditions. Using the *lux*01 circuit, the steady-state GFP expression values for various [AI] was determined by increasing AI from 0 up to 100 nM (Fig. 2.1B). The resulting nonlinear steady-state response curves provided an estimate of the true f null cline (referred to henceforth as f_L). This experiment also established that the *lux*01 circuit became maximally induced after about 6 h under the conditions used. When AI was diluted from the media of the cells in a highly induced state (7 h incubation at 100 nM AI), either instantaneously to lower [AI] or through hourly 25% dilutions, the resulting, virtually identical response curves were distinct from f_L in the 0-50 nM AI range when compared to cultures that were induced but not diluted (this higher response curve, referred to as f_H,, was identical with f_L in the 50-100 nM AI range; Fig. 2.1C). Furthermore, when AI_{ex} was gradually diluted at an hourly rate of 25% from cells stimulated to less than the maximally induced state (2 h incubation at 30, 50 or 100 nM), cellular GFP concentration transiently increased over time in all three cases, converging to and closely following the upper response curve f_H (Fig. 2.1C).

This suggests that the cells remained in the higher state of induction while undergoing continual loss of AI_{ex}, until a critical threshold was met, at which point the cells began to return to the lower induction state. In combination, these results suggested that the response could stably converge to different response curves, f_L and f_H, following different types of *lux01*circuit induction, and thus that the particular shape of the *f* nullcline was dependent on the initial induction state of the cells.

LuxR-mediated positive feedback is supported by experimentation and modeling

It has been proposed earlier that LuxR can transcriptionally regulate its own expression (6, 11, 36, 37). To determine the dependence of *luxR* transcription on $[AI_{ex}]$, qRT-PCR analysis was performed on RNA samples extracted from cells with steady-state GFP expression corresponding to the lower branch of the hysteresis graph (i.e., induced from 0 to maximum with 100 nM AI); Fig. 2.1C). In the range of 0-30 nM AI, *luxR* transcription varied as a function of exogenous AI, and there was an increase in *luxR* mRNA that reached a maximum level at exogenous [AI] above 10 nM (Fig. 2.2). These findings are consistent with the proposed AI-dependent LuxR controlled hysteretic autoregulation of *luxR* and support the hypothesis that the second feedback loop suggested by the data could be due to positive LuxR transcriptional autoregulation.

To further bolster this hypothesis and explore the underlying putative regulatory mechanism, a simple mathematical model of LuxR autoregulation in the *lux01* circuit was developed. This model investigated two distinct possibilities: the presence and absence of LuxR-positive autoregulation encoded in this simplified *lux* network using two corresponding systems of ordinary differential equations. In both cases, plus or minus LuxR-positive autoregulation, the corresponding models could be treated

analytically, allowing us to derive a number of conclusions without explicit definition of the model parameter values, many of which are still unknown. The model postulating a positive feedback was based on the following assumptions, for which there is some experimental basis: (1) expression of LuxR is regulated by both LuxR-AI complexes and cAMP-CRP; (2) the stoichiometry of the LuxR·AI complex is such that two molecules of LuxR are coupled to two molecules of AI; (3) there is a non-zero, basal, AI-independent synthesis of LuxR. In the model analysis we have examined the influence of these assumptions on the properties of the output using the following system of differential equations:

$$\begin{cases} \dfrac{dR}{dt} = c_0 + \dfrac{k_1 C}{C + K_D} - k_2 R - k_5 R \cdot A + k_6 (RA), \\ \dfrac{dC}{dt} = k_3 (RA)^2 - k_4 C, \\ \dfrac{d(RA)}{dt} = k_5 R \cdot A - k_6 (RA) - 2k_3 (RA)^2 + 2k_4 C. \end{cases} \qquad [1]$$

In this system, the first equation describes the rate of change of the concentration of LuxR (denoted as R), which positively depends on the sum of the basal (c_0) and auto-induced synthesis rates and negatively depends on constitutive degradation and dilution due to cell division. The inducible synthesis rate, described by the second term of the first equation, is assumed to be proportional to the probability of transcriptional initiation controlled by the $(\text{LuxR·AI})_2$ complex (C) binding to the corresponding binding site in the regulatory sequence of the operon with the dissociation constant K_D. The second and third equations describe the formation of the LuxR·AI complex through formation of the intermediate bi-molecular LuxR·AI complex (RA), which can either dissociate or form a more stable ternary molecular complex C. The [AI] is denoted as A. In the model [1], we

assume constant glucose concentration, leading to no regulatory role of cAMP-CRP. CRP-mediated regulation is explored in an expanded model below. For this analysis, it is important that LuxR dimerizes to form the complex C, whereas the exact stoichiometry of the complex with respect to the number of AI molecules is not consequential. The same results would be valid if *C* was tri-molecular, with one molecule of AI and two molecules of LuxR.

At steady state, all derivatives in the systems [1] are equal to zero, which converts both systems into the same system of algebraic equations, which in turn can be reduced, with $\gamma = k_1/k_2$, $\delta = c_0/k_2$ and $\beta = K_D/\alpha A^2$, to the following form:

$$-R^3 + (\delta + \gamma) R^2 - \beta R + \delta\beta = 0 \qquad [2]$$

The steady state levels of *luxR* expression are obtained by solution of equation [2], which has 3 roots. One can further show that two of the steady states are stable and one is unstable, further implying that the system is indeed bistable.

To determine the bifurcation diagram defined by [2], the method used by Ozbudak *et al* (31) was applied. At the boundary between the monostable and bistable regimes, two of the three solutions to [2] coincide. Denoting them as *a* and denoting the third, distinct, solution as θa, one has $(y-a)(y-a)(y-\theta a)$, or

$$y^3 - (2+\theta) a y^2 + (1+2\theta) a^2 y - \theta a^3 = 0 \qquad [3]$$

Comparing the coefficients in this equation with those in [2], one can obtain the following system of parametric equations for the parameters γ, δ and β:

$$\begin{cases} \dfrac{(\delta+\gamma)^2}{\beta} = \dfrac{(2+\theta)^2}{1+2\theta} \\ \dfrac{\gamma}{\delta} = \dfrac{2(1+\theta)^2}{\theta}. \end{cases}, \qquad [4]$$

Both parameters, $(\gamma+\delta)^2/\beta$ and $\mu = \gamma/\delta$ are non-dimensional. Using [4] one can create the bifurcation diagram in Fig. 2.3A It is apparent from this diagram that, for certain combinations of parameters, two steady states can coexist for the expression levels of *luxR*, and by extension, those of GFP expression in the *lux01* strain. Raising the concentration of the exogenous [AI] is equivalent to 'moving' on this diagram parallel to the *X* axis from the far left uninduced state to the far right induced state with a transition through a bistable regime (dashed line with arrows). Importantly, for this type of transition, the ratio $\mu = \gamma/\delta = k_1/c_0$ (i.e. the ratio of the strengths of inducible and constitutive transcription) has to be greater than approximately 8.

The strength of inducible transcription is regulated, in part, by the occupancy of the CRP-binding site, and thus by the level of glucose, as absence of glucose activates CRP. As the concentration of glucose increases, the occupancy of the CRP site decreases, and the bistability regime may exist in a progressively narrower range of $[AI_{ex}]$. To account for this, the system [1] must be modified to explicitly include the effect of cAMP-CRP binding. Following the example of Buehler *et al* (5), we can write for the equivalent of equation [3]:

$$c_0 + \frac{k_1 \alpha R^2 A^2 k_7 P}{\alpha R^2 A^2 + K_D + k_7 P K_D + k_7 P \alpha R^2 A^2} - k_2 R = 0 \qquad [5]$$

Here, *P* denotes the concentration of active CRP and k_7 is the equilibrium association constant of cAMP-CRP binding to its cognate binding site. Making the substitution: $\eta = k_7 P$, present in equation [5], leads to:

$$R^3 - (\gamma w + \delta) R^2 + \beta R - \delta\beta = 0 \qquad [6]$$

where the weight $w = \eta/(1+\eta)$ varies between zero and unity, as CRP varies from zero to maximal values. Variation of the contribution of γ to equation [5] is equivalent to raising or lowering along the *Y* axis the 'trajectory' describing the response to AI variation in the bifurcation diagram above, with the trajectory itself being parallel to the *X* axis. In particular, increasing glucose levels would be equivalent to moving the trajectory lower. Ultimately, when $w\gamma/\delta$ levels become less than approximately 8, bistability is lost.

In an alternative model, no positive autoregulation of *luxR* expression is assumed. This corresponds to equating k_1 to zero in [1], thus the value of $\gamma = 0$. As seen above, this implies no bistability in the response. Therefore, positive LuxR autoregulation is required for a bistable response in the framework of our model.

Validating model predictions: dependence of *lux01* output on glucose

In addition to positive autoregulation, bistability is predicted to be critically dependent on the existence of basal constitutive *luxR* expression, as bistability is lost when $c_0 = 0$ and thus $\delta = 0$. The model also predicted that the range of $[AI_{ex}]$ spanning the region of bistability would expand with increasing ratio of the rates of inducible to constitutive *luxR* transcription, γ/δ. Owing to the fact that the rate of *luxR* transcription is regulated in part by occupancy of the cAMP-CRP binding site, the range of $[AI_{ex}]$ in which LuxR bistability could occur was predicted to expand as the concentration of glucose decreased. This effect can be seen both in the bifurcation histogram in Fig. 2.3A and in a more direct representation of bistability of *R* (= [LuxR]) expression as a function of $1/\sqrt{\beta}$, which in turn is proportional to *A* (= [AI]) (Fig. 2.3B). The maximum *luxR* expression was predicted to rapidly diminish with increasing glucose and

correspondingly decreasing [cAMP-CRP], whereas the bistability range was expected to shift to higher [AI] under the same conditions.

To test the model predictions, the *lux01* circuit response was analyzed at different glucose levels. Analysis of the response using the aforementioned dilution techniques in media with different glucose concentrations (0, 1.5 and 2.5 mM) confirmed the model predictions (Fig. 2.3C). As discussed above, in RM minimal medium supplemented with succinate, hysteresis occurred in the range of 0-50 nM AI. In agreement with the model, smaller [AI_{ex}] ranges yielding bistable responses were seen when glucose concentration was increased. Moreover, the bistability ranges progressively shifted to higher [AI_{ex}] with increasing glucose and the maximal response decreased, as was also predicted by the model (Fig. 2.3B). Hence, these experimental results support the model that is consistent with positive LuxR autoregulation leading to a hysteretic dependence on fixed [AI_{ex}].

It would be informative to show more directly that LuxR-positive transcriptional autoregulation plays a key role during the hysteretic response, e.g., if *luxR* expression could be controlled by an inducible promoter other than its native promoter. However, when this was attempted, it was found to be extremely difficult to maintain the levels of LuxR production in a physiologically relevant range. Specifically, a *luxR* deletion was generated in the *lux*01 circuit construct and *luxR* was expressed from a plasmid under the control of P_{tac} or P_{gcvR}. LuxR production from a pEXT22-based vector (1-1.5 copies per cell (12)) with the P_{tac} promoter was so high that it nearly saturated the response with as little as 1 nM AI (data not shown). A pPROBE'gfp tagless (27) construct with a low level constitutive promoter P_{gcvR} from the *E. coli gcvR* gene (17) yielded GFP levels at less than 10% the normal maximum steady-state response even in the presence of 500 nM

AI (data not shown). These findings further illustrate the importance of LuxR levels to the precise control of the QS response. Although using glucose levels in the medium to manipulate LuxR levels does not eliminate LuxR-positive feedback, it does allow for an analysis of the effect of different expression levels of LuxR, in a physiologically relevant manner. The observation that decreasing the levels of LuxR production in this manner also leads to a decrease in the degree of hysteresis implies that elimination of LuxR-mediated positive feedback would completely eliminate this behavior from the system. Indeed, a recent analysis of different synthetic LuxR-LuxI based genetic circuits strongly suggested absence of hysteresis in the response of a plasmid-based circuit analogous to the *lux01* circuit, when investigated in glucose-rich medium (20).

Response bistability on a single cell level

Population-level measurements can hide the details of the distribution of single cell responses. To investigate the *lux01* response on the single-cell level, cell samples from the induction and 25% hourly dilution experiments were analyzed using flow cytometry (Fig. 2.3D and Figs. AI.2-AI.5). For all $[AI_{ex}]$ values, the cellular populations were well described by bimodal distributions. The lower fluorescence peaks for $[AI_{ex}] = 5$ and 10 nM had peak fluorescence intensities virtually indistinguishable from that of the unimodal distribution of the uninduced cell population ($[AI_{ex}] = 0$). As $[AI_{ex}]$ increased to 100 nM, both peaks of the bimodal distributions gradually shifted to higher fluorescence intensity values, with the maximum increase of the lower peak being about three-fold versus uninduced control. The peak fluorescence intensity of the higher response sub-population, which at $[AI_{ex}] = 10$ nM was approximately 70-fold higher than the peak fluorescence of the lower response sub-population, also shifted with $[AI_{ex}]$.

As a result, at $[AI_{ex}]$ = 50 or 100 nM, the position of the higher peak exceeded that of the lower peak by almost two orders of magnitude. As $[AI_{ex}]$ increased, the relative amplitude of the second peak also progressively increased, and that of the first peak decreased. There was no noticeable difference between the distributions corresponding to 7 and 14 h of induction, further suggesting that at 7 h post-induction the response is close to being maximally induced (data not shown).

When AI was diluted from the media of the cells in a highly induced state (7 h in $[AI_{ex}]$ = 100 nM) and assayed at various final $[AI_{ex}]$, the response distributions were also bimodal. However, although the positions of the response peaks coincided with those found in the induction experiment (induction of the response from low initial $[AI_{ex}]$), the relative amplitudes of the peaks were distinct, with the amplitude of the lower response peak considerably diminished. By plotting the ratio of the high to low maxima as a function of $[AI_{ex}]$, a hysteretic bistable response is clearly demonstrated for these coinciding peaks (Fig. 2.4). There is approximately an 80-fold difference between the two steady states of expression that the response can achieve within the 0-50 nM range of $[AI_{ex}]$. These results suggested that each point used to obtain different null clines in Fig. 2.1C was an average of two modes of response, and the hysteresis was a consequence of different weights placed on these modes by the history of the response induction. The results are consistent with the notion that response bimodality is a reflection of underlying response bistability coupled with the effects of molecular noise over prolonged periods of time, as recently shown in other well-characterized signaling and genetic systems (16, 31, 32). Bistability is commonly a reflection of underlying positive feedback, further implying that hysteresis and bimodality in the response of the *lux*01

circuit depends on the presence of a second, LuxI-independent feedback loop in the system.

Noise reduction due to LuxR upregulation

Occupancy of LuxR by AI can be viewed for each individual LuxR molecule as a binary variable (i.e., either LuxR is occupied or not). Thus occupancy of many LuxR molecules could be represented as a series of Bernoulli trials, with the average and standard deviation given by the binomial distribution. The probability that an individual receptor is occupied is given by:

$$p = \frac{A}{A + \tilde{K}_D}, \qquad [7]$$

where A = [AI] and $\tilde{K}_D$ is the affinity of AI to LuxR. Correspondingly, the probability that a LuxR molecule is not occupied by AI is:

$$q = \frac{\tilde{K}_D}{A + \tilde{K}_D}. \qquad [8]$$

Therefore, for the binomial distribution of occupancy levels, we have the mean:

$$\mu = np = \frac{nA}{A + \tilde{K}_D}, \qquad [9]$$

where n is the number of LuxR molecules. For the ratio of the standard deviation to the mean (the coefficient of variation), a frequently used metric of molecular noise, we have:

$$\eta = \frac{\sigma}{\mu} = \frac{\sqrt{np(1-p)}}{np} = \sqrt{\frac{1-p}{np}} = \sqrt{\frac{\tilde{K}_D}{nA}}. \qquad [10]$$

Thus the molecular noise characterizing LuxR-AI binding events scales as the inverse of the square root of the total number of LuxR molecules, making the response more robust

if [LuxR] is upregulated. To evaluate η using the flow cytometry experiments (Fig. 2.3D and Figs. AI.3-AI.5), we fitted the curves with a sum of two Gaussian distributions, corresponding to the constituent distributions, and estimated their mean and standard deviation values. The analysis suggested that the molecular noise, η, in the expression of *luxI* can decrease from 0.93 to 0.29 for [AI] = 5 nM, and from 0.47 to 0.19 for [AI] =10 nM, confirming that an increase in expression of *luxR* can indeed decrease the molecular noise in the QS response.

Examination of the *luxR/I* circuit

As explained above, the steady-state responses of the full *lux* operon can be obtained by considering the intersections of the null clines f and g^{-1}. Alternatively, the intersections of the related null clines: $[LuxR] = [R] = \tilde{f}([AI])$ and $[AI] = \tilde{g}([LuxR]) \propto 1/\sqrt{\beta}$, describing mutual dependencies between *luxR* expression and [AI] can be considered. The simulated null cline $\tilde{f}$, plotted in Fig. 2.3B and reproduced in Fig. 2.5A, describes bistability of the *lux01* circuit. Unfortunately, determination of the other null cline, $\tilde{g}$, is less straightforward for several reasons. First, although it is clear from our (data not shown) and other analyses that *luxR* overexpression positively regulates *luxI* expression, the details of *luxI* expression and AI synthesis as a function of LuxR autoregulation are poorly known. Secondly, as AI can diffuse into the space surrounding the cells, the effect of *luxR* expression on [AI] experienced by cells can depend on cell density, the rate of removal of AI from extracellular spaces, the geometry of extracellular spaces, etc. We therefore, simplified the analysis to assume that

the [AI] experienced by cells depends on *luxR* expression as follows:

$$[AI] = \frac{\sigma[LuxR]}{[LuxR] + K_{QS}} + [AI_{Ex}]$$

Thus [AI] is assumed to have a saturable dependence on the expression of *luxR* (reaching the maximal value σ for very high LuxR levels), with the sensitivity to LuxR defined by the constant K_{QS}. In addition, [AI] can also be augmented by addition of exogenous AI experimentally. This equation describes a series of the null clines $\tilde{g}$, discussed above, which can be used to obtain the steady-state solutions for the whole QS circuit. Note that one reduces the problem to the case of the *lux01* circuit by putting $\sigma = 0$, which would correspond to the null clines being perpendicular to the [AI] axis. This was implicitly done in our previous analysis of Fig. 2.3B. Any $\sigma \neq 0$ implies therefore that the corresponding null clines would intersect the higher stable branch of $\tilde{f}$ at values of $[AI_{ex}]$ higher than those of the *lux01* case, due to sloping of the $\tilde{g}$ null clines (see Fig. 2.5A). In addition, as shown in Fig. 2.5A, null clines for a larger range of $[AI_{ex}]$ can intersect with both stable branches of $\tilde{f}$, thus extending the hysteresis range. Therefore, generally speaking, if AI can be produced endogenously by the cells, one would expect increased values of LuxR for the higher steady-state response versus the *lux01* circuit case, for the same $[AI_{ex}]$. The hysteresis range would also be expected to increase.

To validate these predictions, we investigated the *lux02* circuit, which differs from the *lux01* circuit by having the capacity to express *luxI* and thereby synthesize AI (Fig. AI.1). Cells carrying the *lux02* circuit were grown in the presence of different [AI] in the range of 0-100 nM, in order to compare the response to that of the *lux*01 circuit. The response increased over the first 6 h, stabilizing at 7-8 h (Fig. AI.6). Consistent with

model predictions, the single cell response displayed bistability, with the higher steady-state distributions substantially exceeding (for $[AI_{ex}]$ = 0-10 nM) or closely coinciding (for $[AI_{ex}]$ = 10-100 nM) with those of the highest steady-state response distributions (for $[AI_{ex}]$ = 50 and 100 nM) of the *lux01* single cell responses. These results suggested that the coexistence of two coupled feedback loops can increase the degree to which the response can be induced at lower $[AI_{ex}]$.

The predicted expansion of the hysteresis range implied that the higher response steady state can exist at very low $[AI_{ex}]$, possibly even zero. One strategy to test this involved inducing the cell response by addition of AI at specific values, followed by continuous cell and AI dilution. This insured dilution of exogenously added AI to values close to zero, which may or may not be compensated by AI secretion and cell induction to the higher response steady state. When 25% hourly dilutions of AI were performed with *lux02* circuit-expressing cells that had been weakly induced (2 h induction) at different initial $[AI_{ex}]$, not only did the population achieve its higher state of induction, it remained in that state throughout the experiment in spite of continuous removal of AI and cells (Fig. 2.5D). The 25% per hour dilution rate appeared to match cell division and AI production rates by *lux02*-carrying cells, as at higher dilution rates, both the response was lost and cells were diluted out (data not shown). Overall, these results suggested that in a situation modeling the QS response in the context of a biofilm or a light organ, when the number of cells is relatively constant, the QS response can be induced and stably maintained even in the face of constant removal of AI.

Discussion

Using a combination of mathematical modeling and experimental analysis, we have shown that the regulation of expression of *luxI* during the *V. fischeri* QS response exhibits complex hysteretic dependency on the $[AI_{ex}]$, due to AI-dependent autoregulation of *luxR* expression. In particular, *luxI* expression can assume two distinct levels in response to fixed $[AI_{ex}]$ within the 0-50 nM range. The chosen response value depends on whether there is a recent history of cell exposure to high [AI]. Thus in the full *lux* operon, two nested feedback loops can control the onset and maintenance of the collective cell responses. This combination of feedback responses adds to a growing list of the functionally important nested feedback systems, including multiple feedbacks regulating galactose utilization in yeast (1) and a combination of positive and negative feedback loops in many other natural and synthetic circuits (40).

A number of important advantages can be gained from this type of feedback loop architecture. One important consideration for this circuit is that LuxI-mediated feedback is distinct from a classical cell-autonomous type of feedback in that AI does not remain within or around a single cell, but rather is shared among the cells within a population, thus coupling their responses. Therefore the extent to which this feedback occurs depends on the local cell microenviroment, including cell density, geometric constraints and the rate of AI removal (21). This uncertainty in the feedback circuit regulation has the potential of making the circuit performance less robust and more subject to perturbations in the environment. Hence an additional level of response control, provided by *luxR* transcriptional autoregulation, can facilitate establishment of a cell sub-population, that once induced, continues to stably display QS, even if the local [AI] undergoes transient or

persistent reduction. The memory of QS induction is maintained in the population due to a high level of LuxR, and thus a relatively high level of LuxR-AI complexes, even if [AI] is decreased.

A complementary advantage is response diversification. Although response diversification can arise in many bistable systems with substantial amounts of molecular noise, the range of concentrations under which bistability can occur can be substantially augmented in the presence of two coupled feedback loops (Fig. 2.5). This further implies that, under a wide range of extracellular conditions, two sub-populations may emerge, the responses of which can exist at two distinct stable states. The higher stable response state, in which most cells would predominantly reside, would mediate the QS response. At the same time, the less abundant lower response state would represent a reservoir of cells that can quickly displace the higher response state cells, due to a decreased metabolic load associated with lower levels of *luxR* and *luxI* expression. Should the conditions dramatically change (e.g., due to removal of most of the population), a fast replenishment of the uninduced population would ensue in a manner not dependent on the gradual decrease of LuxR and LuxI levels by degradation and cell growth-related dilution. This small cell reservoir, capable of replenishing the population following a major alteration of the surrounding medium, is not unlike the reservoir of persister cells resistant to the level of antibiotics capable of killing most of a population in a situation such as a biofilm (3). Thus the QS circuit appears to combine two distinct strategies previously proposed for how a cell population can best respond to a changing environment (24). It can both adapt to an increased cell population by progressive upregulation of the QS response, and

diversify the response as a means of coping with catastrophic changes in cell numbers and [AI].

The concentration of glucose is also a key parameter to consider, since cAMP-CRP levels control the levels of *luxR* transcriptional regulation, which determines whether or not full QS induction can be achieved and robustly maintained over a wide range of [AI_{ex}]. Interestingly, Freidrich and Greenberg (14) also saw evidence that *V. fischeri* cells grown in chemostats had a memory of their previous exposure to glucose during QS. Importantly, the corresponding dependence of luminescence on active CRP may facilitate the establishment and maintenance of the symbiosis between *V. fischeri* and its squid host. The host may be capable of controlling the onset of QS by providing lower levels of glucose at a lower cell density, which would trigger induction earlier than a dense population under higher initial nutrient levels. This bacterial-host interaction thus represents yet another potential feedback system, stabilizing the level of luminescence output.

In addition to cAMP-CRP regulation of *luxR*, LuxR autoregulation affords a mechanism to increase the precision of AI sensing by the cells. Indeed, cells can mount a significant response to [AI] as low as 5 nM. This concentration, for the typical *E. coli* and *V. fischeri* cell volumes of a few femptoliters, translates into less than 10 molecules of AI per cell. This is a very small number, likely subject to significant variation, or molecular noise within a cell, which could lead to pronounced noise in signaling output. This study has shown both analytically and experimentally, that upregulation of *luxR* expression could considerably reduce this noise, with as much as a three-fold reduction in the variability of LuxR-AI binding and ensuing transcriptional regulation for [AI_{ex}] = 5 nM.

Upregulation of LuxR can also serve to control regulation of other genes in the *lux* regulon. At least three other members of the *lux* regulon, *qsrP, acf* and *ribB* have lower affinities for LuxR-AI complexes compared to that of the *luxI* promoter (33). Upregulation of *luxR* expression may increase the expression of these genes following the onset of QS, while maintaining them at a low level during the initial stages of the response.

In the native host, *V. fischeri,* additional upstream signal-transduction pathways and regulators might also have an influence on *luxR* expression rates. However, utilizing a simplified genetic circuit in recombinant *E. coli* has enabled an analysis of how the available pools of LuxR and AI ultimately modulate the response. Development of a quantitative understanding of this isolated genetic circuit can both help elucidate the more complex behavior of the native QS response, and assist in synthetic biology efforts where such interspecies transfer of parts of genetic networks, including the *lux* operon, is very common (i.e. (5)).

In conclusion, these results provide a comprehensive picture of the ability of the basic LuxR/I genetic system, which is a common motif of many QS circuits, to favor and maintain a high level of expression of its target genes once a certain threshold of expression is reached. It would seem logical that the hindrance of this activation would be the most effective way to prevent high level expression of QS-controlled genes, because shutting down an activated system would be difficult in natural settings, such as during tissue infections, symbiosis, or biofilm formation.

Materials and methods

Strains and growth conditions

To create *E. coli* MG1655-01S (*lux*01 circuit; *luxR* divergently transcribed from P_{luxI} fused to *gfp*) and MG1655-02S (*lux*02 circuit; *luxR* divergently transcribed from *luxI* fused to *gfp*) (Fig. AI.1), *lux* operon fragments were removed via *Eco*RI-*Kpn*I, and *Eco*RI-*Bam*HI restriction digestions from pLVA01 and pLVA02 respectively (19) and placed into the multiple cloning site (MCS) of pPROBE`-GFP-Tagless which encodes a stable GFP (27) as a transcriptional reporter. These reporter fragments were then removed through *Eco*RI-*Not*I digestion and ligated into the λInCh vector, a modified pDHB60 (4). The pDHB60 vector had been modified by (1) removal of the P_{tac} promoter via *Eco*RI-*Bam*HI digestion, (2) ligation with an *Eco*RI-*Bam*HI fragment of pPROBE`-GFP (LAA) containing its MCS and (3) adding a *Not*I site between the *Eco*RI and *Xba*I sites. This modified pDHB60 was ligated with the *lux-gfp* reporter cassettes and used in the λInCh insertion protocol to place the expression cassettes into the *E. coli* MG1655 chromosome, generating stable, single-copy expression systems (4). During cloning stages, strains were grown shaking at 250 r.p.m. and 37°C in Luria-Bertani broth (containing 100 μg/ml ampicillin (Ap) and 50 μg/ml kanamycin (Kn), as necessary). During the analyses for hysteresis, strains were grown shaking at 250 r.p.m in RM minimal medium (RM) (2% Casamino Acids, 1x M9 salts [12.8 g Na_2HPO_4 $7H_2O$, 3 g KH_2PO_4, 0.5 g NaCl, and 1 g NH_4Cl per liter], 1 mM $MgCl_2$) with 0.4% succinate and 25 μg/ml Ap at 30°C unless otherwise indicated.

Gradual hourly dilution of AI from induced cultures

E. coli MG1655-01S or -02S were grown overnight at 37°C in RM minimal medium with succinate and 25 μg/ml Ap. The overnight culture was subcultured into the same medium to an OD_{590} of 0.15. Prior to subculturing, samples were centrifuged, the supernatant was discarded, and the pellet was resuspended in fresh medium twice to eliminate any AI carry over. The culture was incubated at 30°C with shaking until an OD_{590} of 0.25 was reached. At this point, 5 ml aliquots of culture were added to tubes that contained known amounts of dried AI. These induced cultures were incubated for various times, up to 7 h (depending on the type of analysis) at 30°C with shaking.

Here, 25% dilutions were performed by adding 3.75 ml of the induced culture to 1.25 ml of pre-warmed fresh RM minimal medium without AI. Prior to dilution, 200 μl of culture was placed in a 96-well optical bottom microtiter plate for analysis of both fluorescence output (excitation and emission wavelengths of 485 nm and 535 nm respectively) and OD_{590} on a Tecan SpectraFluor Plus plate-reader (Tecan, Mannedorf/Zurich, Switzerland). Fluorescence values were corrected for background by subtracting the RFU obtained from an uninduced culture of MG1655-01S at comparable cell density, and the per cell output was determined by dividing the corrected RFU by the OD. The procedure was repeated hourly to achieve a gradual dilution of the AI in the medium and maintain the culture in the mid-exponential phase of growth. Assays were performed as two independent triplicate sets. A major concern for the analysis of hysteresis was that any differences observed between diluted cultures and undiluted controls, allowed to grow to high steady-state expression, could be caused by changes in cell physiology due to the controls reaching stationary phase. To ensure that this did not

occur, control cultures were not allowed to reach an OD_{590} higher than 1.0. The manner in which the dilution assays were performed maintained all of the diluted cultures between an OD_{590} 0.4 and 0.7. Hence, the cells were maintained in the exponential phase over extended periods beyond that of normal batch culture.

Instantaneous serial dilution of AI from induced cultures

A more conventional method for testing hysteresis is to induce to a maximum steady state, and then dilute the AI from the system. To perform this type of assay, cultures were induced as described above, for 7 h prior to dilution, which corresponds to near maximum levels of QS induction for the system. Induced cultures were serially diluted 25% by combining and mixing two 5 ml induced cultures (induced at the same [AI]) and adding 9 ml of this culture to 3 ml of pre-warmed RM minimal medium; 9 ml of the first dilution was used to make the second dilution. This was repeated for a total of 7 dilutions. At 1 and 2 h post-dilution, 200-μl samples were taken and analyzed as described above. Assays were performed as three independent trials.

Modulation of the QS response by glucose addition

E. coli MG1655-01S cultures grown in RM minimal medium with succinate were supplemented with glucose concentrations up to 10 mM. A 25% gradual hourly dilution of AI assay was performed as above, using dilution medium containing the same concentration of glucose as the original culture. If the induction period was longer than 2 h, 1 ml of culture was replaced with 1 ml of fresh medium containing the same concentration of glucose and AI every hour starting at hour 4. This ensured that the culture was maintained in mid-exponential phase until the dilution assay began at either 6

or 8 hrs induction, and that the glucose in the medium did not become depleted. Culture density and fluorescence were measured as described above.

qRT-PCR analysis of *luxR* transcript levels

When undiluted cultures had been induced for 6 h, 500 μl was added to 1 ml of Qiagen RNAprotect Bacteria Reagent (Qiagen, Valencia, CA). Samples were stored at -70°C until the RNA was extracted according to the Qiagen RNA spin mini kit and stored at -70°C. RNA was analyzed for quality and concentration, converted to cDNA via the Applied Biosystems High-Capacity cDNA Reverse Transcription Kit protocol (Applied Biosystems, Foster City, CA) and stored at -20°C. The cDNA samples were then used as templates in an Applied Biosystems 7300 Real-Time PCR system. The primers used during the PCR reaction to amplify a region of *luxR* were 5' TGGCAGCGGTTAGTTGTATTG 3' and 5'TAGCGTGGGCGAGTGAAG 3'. Here, 50 ng of cDNA was used as template, with primer concentrations at 250 μM. 2x SYBR Green master mix (2x) (Applied Biosystems) and dH_2O were added to a final reaction volume of 50 μl per well in a MicroAmp Optical 96-well Reaction Plate (Applied Biosystems). The thermal cycler settings were programmed for 52°C for 2 min., 95°C for 10 min., then 45 cycles of the following: 95°C for 15 s, 52°C for 15 s, and 60°C for 1 min., which was also set as the data collection point. Three independent samples were analyzed in triplicate.

Flow cytometry analysis

Cultures of *E. coli* MG1655-01S or *E. coli* MG1655-02S were grown and induced with AI as stated previously. At 7 h induction, samples were diluted as per the 25% hourly dilution of AI protocol listed above. Here, 500-μl samples were taken at each

hourly time point and pelleted via centrifugation at 14,000 r.p.m. for 2 min at 4°C. Cells were then resuspended in cold PBS (0.2 M potassium phosphate monobasic, 0.2 M sodium chloride, pH 7) containing 100 μg/ml chloramphenicol, and placed on ice overnight. The following day, samples were analyzed at the flow cytometry lab at the Virginia-Maryland Regional College of Veterinary Medicine on a BD (Becton Dickinson) FACS Aria flow cytometer. Data for two independent sets was collected using the software FlowJo version 7 (Tree Star). All cells producing a fluorescent signal were counted in the gating so that an accurate distribution of expression across the entire population would be achieved.

Acknowledgements

We thank Joan Kalnitsky and Melissa Makris for assistance in performing flow cytometry and Steven Lindow for providing the *gfp* transcriptional fusion vectors. This research was supported by NIH R01 GM066786, NSF IGERT DGE-0504196 and the Virginia Tech Graduate Research Development Program.

References

1. **Acar, M., A. Becskei, and A. van Oudenaarden.** 2005. Enhancement of cellular memory by reducing stochastic transitions. Nature **435:**228-32.
2. **Angeli, D., J. E. Ferrell, Jr., and E. D. Sontag.** 2004. Detection of multistability, bifurcations, and hysteresis in a large class of biological positive-feedback systems. Proc Natl Acad Sci U S A **101:**1822-7.
3. **Balaban, N. Q., J. Merrin, R. Chait, L. Kowalik, and S. Leibler.** 2004. Bacterial persistence as a phenotypic switch. Science **305:**1622-5.
4. **Boyd, D., Weiss, S.D., Chen, J.C., and Beckwith, J.** 2000. Towards single copy gene expression systems making gene cloning physiologically relevant: lambda InCh, a simple *Escherichia coli* plasmid-chromosome shuttle system. J. Bacteriol. **182:**842-847.
5. **Buchler, N. E., U. Gerland, and T. Hwa.** 2003. On schemes of combinatorial transcription logic. Proc Natl Acad Sci U S A **100:**5136-41.
6. **Chatterjee, J., C. M. Miyamoto, and E. A. Meighen.** 1996. Autoregulation of *luxR*: the *Vibrio harveyi lux*-operon activator functions as a repressor. Mol Microbiol **20:**415-25.
7. **Choi, S. H., and E. P. Greenberg.** 1992. Genetic dissection of DNA binding and luminescence gene activation by the *Vibrio fischeri* LuxR protein. J Bacteriol **174:**4064-9.
8. **Cox, C. D., G. D. Peterson, M. S. Allen, J. M. Lancaster, J. M. McCollum, D. Austin, L. Yan, G. S. Sayler, and M. L. Simpson.** 2003. Analysis of noise in quorum sensing. Omics **7:**317-34.
9. **Dunlap, P. V., Greenberg, E.P.** 1985. Control of *Vibrio fischeri* luminescence gene expression in *Escherichia coli* by cyclic AMP and cyclic AMP receptor protein. J. Bacteriol. **164:**45-50.
10. **Dunlap, P. V., Greenberg, E.P.** 1988. Control of *Vibrio fischeri lux* gene transcription by a cyclic AMP receptor protein-LuxR protein regulatory circuit. J. Bacteriol. **170:**4040-4046.
11. **Dunlap, P. V., and J. M. Ray.** 1989. Requirement for autoinducer in transcriptional negative autoregulation of the *Vibrio fischeri luxR* gene in *Escherichia coli*. J Bacteriol **171:**3549-52.
12. **Dykxhoorn, D. M., St. Pierre, R., Linn, T.** 1996. A set of compatible *tac* promoter expression vectors. Gene **177:**133-136.
13. **Ferrell, J. E., Jr.** 2002. Self-perpetuating states in signal transduction: positive feedback, double-negative feedback and bistability. Curr Opin Cell Biol **14:**140-8.
14. **Friedrich, W. F., Greenberg, E.P.** 1983. Glucose Repression of Luminescence and Luciferase in *Vibrio fischeri*. Archives of Microbiology **134:**87-91.
15. **Fuqua, C., Parsek, M.R., Greenberg, E.P.** 2001. Regulation of gene expression by cell-to-cell communication: acyl-homoserine lactone quorum sensing. Annu. Rev. Genet. **35:**439-468.
16. **Gardner, T. S., C. R. Cantor, and J. J. Collins.** 2000. Construction of a genetic toggle switch in *Escherichia coli*. Nature **403:**339-42.

17. **Ghrist, A. C., and G. V. Stauffer.** 1998. Promoter characterization and constitutive expression of the *Escherichia coli gcvR* gene. J Bacteriol **180:**1803-7.
18. **Goryachev, A. B., D. J. Toh, and T. Lee.** 2006. Systems analysis of a quorum sensing network: design constraints imposed by the functional requirements, network topology and kinetic constants. Biosystems **83:**178-87.
19. **Groisman, A., C. Lobo, H. Cho, J. K. Campbell, Y. S. Dufour, A. M. Stevens, and A. Levchenko.** 2005. A microfluidic chemostat for experiments with bacterial and yeast cells. Nat Methods **2:**685-9.
20. **Haseltine, E. L., and F. H. Arnold.** 2008. Implications of rewiring bacterial quorum sensing. Appl Environ Microbiol **74:**437-45.
21. **Hense, B. A., C. Kuttler, J. Muller, M. Rothballer, A. Hartmann, and J. U. Kreft.** 2007. Does efficiency sensing unify diffusion and quorum sensing? Nat Rev Microbiol **5:**230-9.
22. **James, S., P. Nilsson, G. James, S. Kjelleberg, and T. Fagerstrom.** 2000. Luminescence control in the marine bacterium *Vibrio fischeri*: An analysis of the dynamics of *lux* regulation. J Mol Biol **296:**1127-37.
23. **Kaplan, H. B., Greenberg, E.P.** 1985. Diffusion of autoinducer is involved in regulation of the *Vibrio fischeri* luminescence system. J. Bacteriol. **163:**1210-1214.
24. **Kussell, E., and S. Leibler.** 2005. Phenotypic diversity, population growth, and information in fluctuating environments. Science **309:**2075-8.
25. **Levchenko, A.** 2003. Dynamical and integrative cell signaling: challenges for the new biology. Biotechnol Bioeng **84:**773-82.
26. **Lupp, C., M. Urbanowski, E. P. Greenberg, and E. G. Ruby.** 2003. The *Vibrio fischeri* quorum-sensing systems *ain* and *lux* sequentially induce luminescence gene expression and are important for persistence in the squid host. Mol Microbiol **50:**319-31.
27. **Miller, W. G., Leveau, J.H.J., Lindow, S.E.** 2000. Imporved *gfp* and *inaZ* broad-host-range promoter-probe vectors. Molec. Plant-Microbe Interactions **13:**1243-1250.
28. **Minogue, T. D., M. Wehland-von Trebra, F. Bernhard, and S. B. von Bodman.** 2002. The autoregulatory role of EsaR, a quorum-sensing regulator in *Pantoea stewartii* ssp. *stewartii*: evidence for a repressor function. Mol Microbiol **44:**1625-35.
29. **Muller, J., C. Kuttler, B. A. Hense, M. Rothballer, and A. Hartmann.** 2006. Cell-cell communication by quorum sensing and dimension-reduction. J Math Biol **53:**672-702.
30. **Ninfa, A. J., and A. E. Mayo.** 2004. Hysteresis vs. graded responses: the connections make all the difference. Sci STKE **2004:**pe20.
31. **Ozbudak, E. M., Thattai, M., Lim, H.N., Shraiman, B.I., von Oudenaarden, A.V.** 2004. Multistability in the lactose utilization network of *Escherichia coli*. Nature **427:**737-740.
32. **Paliwal, S., P. A. Iglesias, K. Campbell, Z. Hilioti, A. Groisman, and A. Levchenko.** 2007. MAPK-mediated bimodal gene expression and adaptive gradient sensing in yeast. Nature **446:**46-51.

33. **Qin, N., S. M. Callahan, P. V. Dunlap, and A. M. Stevens.** 2007. Analysis of LuxR regulon gene expression during quorum sensing in *Vibrio fischeri*. J Bacteriol **189:**4127-34.
34. **Reading, N. C., and V. Sperandio.** 2006. Quorum sensing: the many languages of bacteria. FEMS Microbiol Lett **254:**1-11.
35. **Sha, W., Moore, J., Chen, K., Lassaletta, A.D., Yi, C., Tyson, J.J., Sible, J.C.** 2003. Hysteresis drives cell-cycle transitions in *Xenopus laevis* egg extracts. Proc. Natl. Acad. Sci., USA **100:**975-980.
36. **Shadel, G. S., and T. O. Baldwin.** 1992. Positive autoregulation of the *Vibrio fischeri luxR* gene. LuxR and autoinducer activate cAMP-catabolite gene activator protein complex-independent and -dependent *luxR* transcription. J Biol Chem **267:**7696-702.
37. **Shadel, G. S., Baldwin, T.O.** 1991. The *Vibrio fischeri* LuxR protein is capable of bidirectional stimulation of transcription and both positive and negative regulation of the *luxR* gene. J. Bacteriol. **173:**568-574.
38. **Stevens, A. M., Greenberg, E.P.** 1999. Transcriptional activation by LuxR: Cell-cell signaling in bacteria. Presented at the ASM conference, Washington, D.C.
39. **Taga, M. E., Bassler, B.L.** 2003. Chemical communication among bacteria. Proc. Natl. Acad. Sci., USA **100:**14549-14554.
40. **Tsai, T. Y., Y. S. Choi, W. Ma, J. R. Pomerening, C. Tang, and J. E. Ferrell, Jr.** 2008. Robust, tunable biological oscillations from interlinked positive and negative feedback loops. Science **321:**126-9.
41. **Tyson, J. J., K. C. Chen, and B. Novak.** 2003. Sniffers, buzzers, toggles and blinkers: dynamics of regulatory and signaling pathways in the cell. Curr Opin Cell Biol **15:**221-31.
42. **Waters, C. M., and B. L. Bassler.** 2005. Quorum sensing: cell-to-cell communication in bacteria. Annu Rev Cell Dev Biol **21:**319-46.

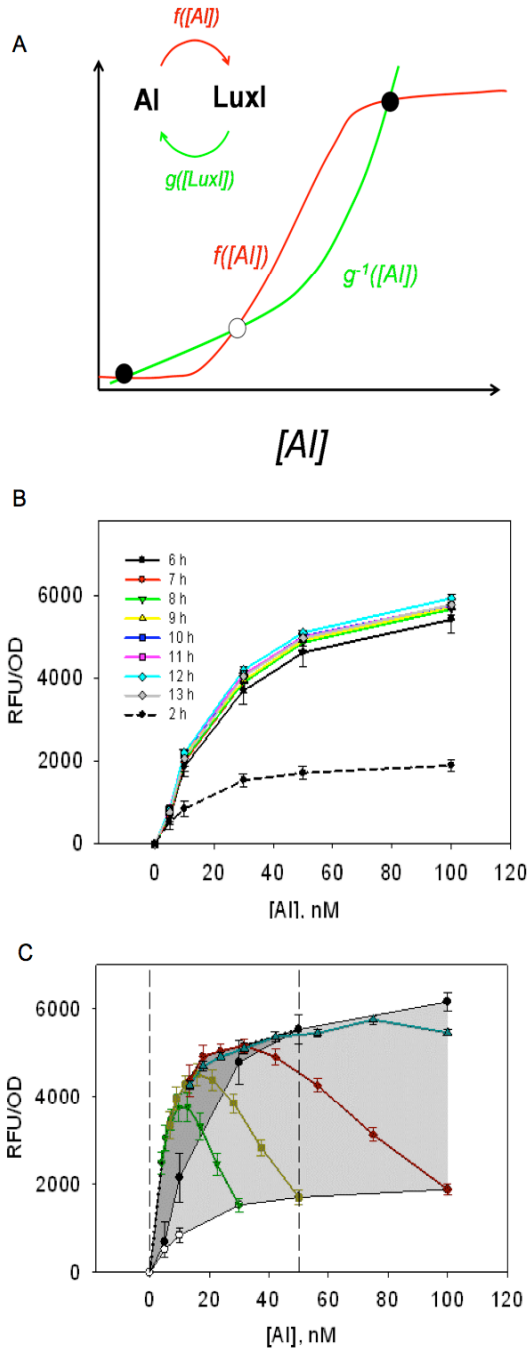

Figure 2.1. Analysis of GFP expression in the *lux01* circuit in response to different AI concentrations. (A) An illustrative cartoon of a decoupled LuxI-AI positive feedback system. One can find possible stable-steady state responses in a positive feedback circuit by separately analyzing how AI regulates LuxI and how LuxI regulates AI. The resulting dependencies, or null clines: *f([AI])* and *g([LuxI])*, can be plotted together, with the intersection points yielding the steady states, which can be stable (closed circles) or not (open circle); (B) Analysis of the *f([AI])* null-cline by allowing the response of the *lux01* circuit to reach steady states after addition of different exogenously added [AI], for different amounts of time. The data are expressed as relative fluorescence units /optical density of the culture. Error bars represent the standard deviation between two independent triplicate data sets; (C) Analysis of the *f([AI])* null cline by allowing the response of the *lux01* circuit to reach steady state after dilution from high initial induction values (reached at 8 h after instantaneous 25% serial dilution from 6 h incubation in 100 nM [AI]) (blue triangles). This response is overlaid with the results of the 6 h incubation obtained in (B) (closed circles) and the area between the curves is shaded dark grey. The area between the 2 h and 6 h induction curves in (C) is shaded light grey. The results of the 25% hourly dilution experiments from cultures initially induced for 2 h at different exogenous [AI] (30 nM, inverted triangles; 50 nM, squares; 100 nM, rhombi) prior to dilution are also shown. Error bars represent the standard deviation between two independent triplicate data sets.

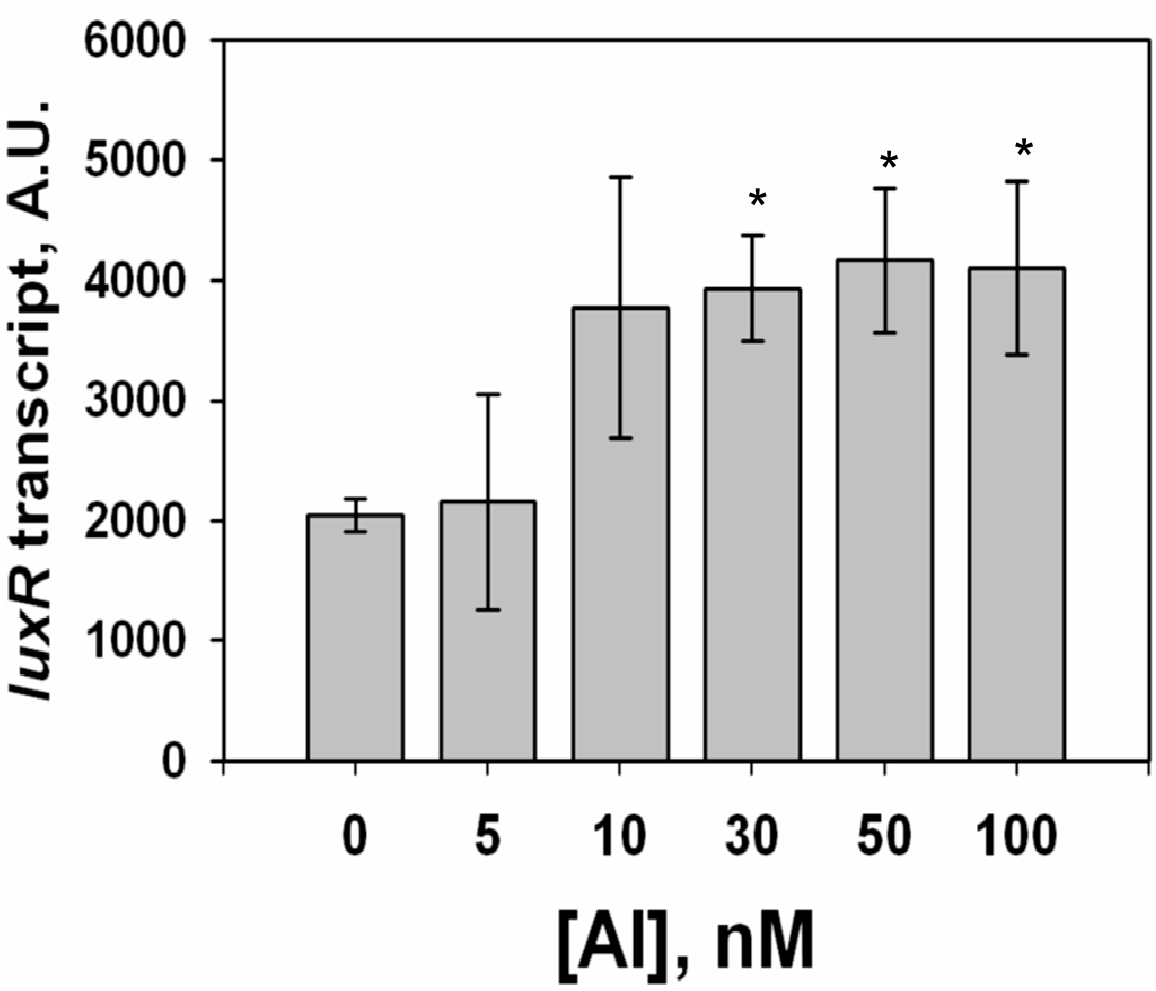

Figure 2.2. Validation of induced *luxR* expression by qRT-PCR analysis of *luxR* transcript levels in the *lux01* circuit. qRT-PCR analysis of *luxR* transcript quantity was performed on undiluted MG1655-01S induced for 6 h at [AI] of 5, 10, 30, 50 and 100 nM. Error bars represent the standard deviation between three independent triplicate data sets. Asterisks indicate data values that are significantly higher than that of the 5 nM data with a $P<0.025$ (standard t-test).

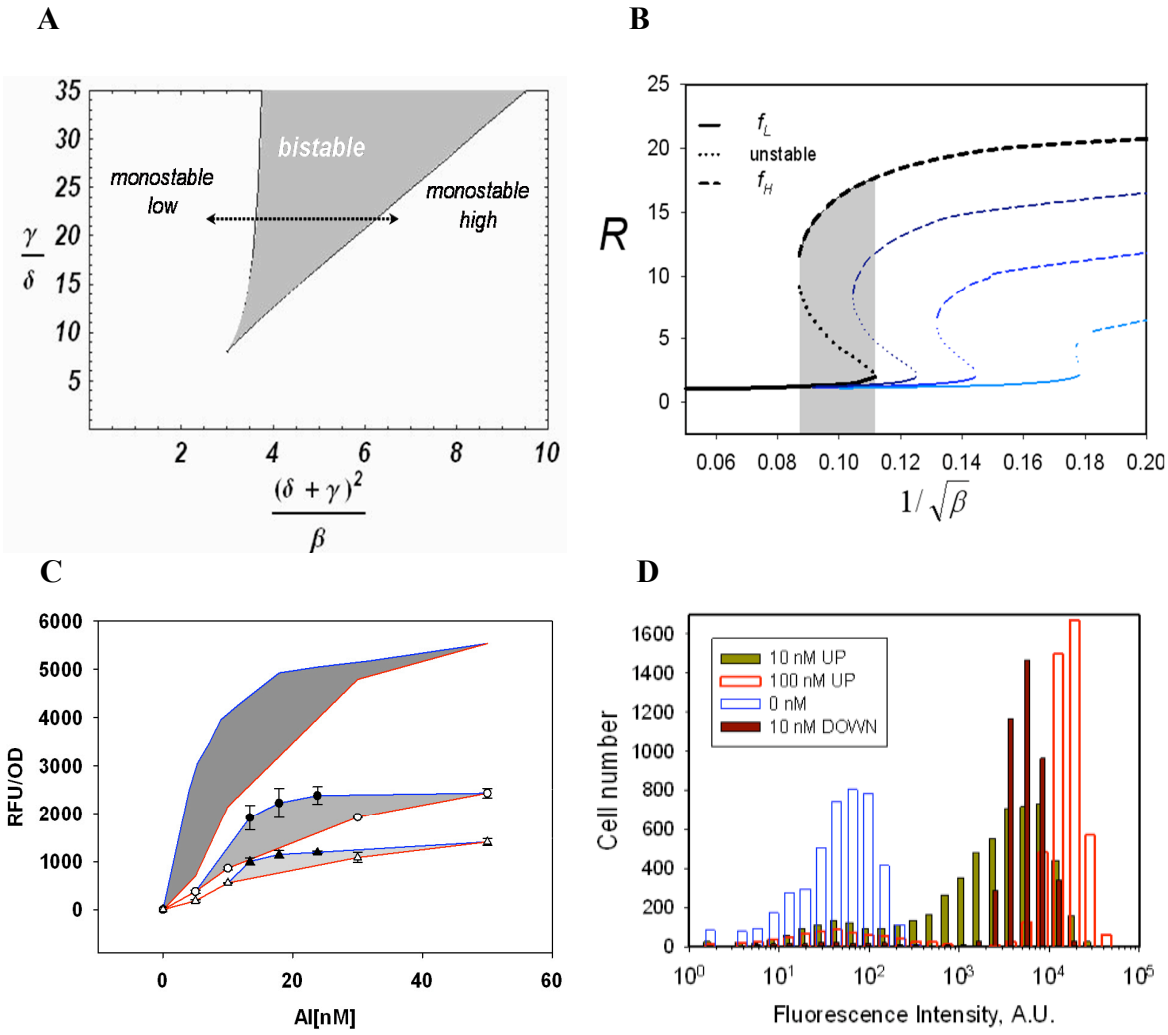

Figure 2.3. Mathematical modeling and experimental analysis of the *lux01* circuit response. (A) The model analysis predicts the existence of a domain of non-dimensional parameters characterizing the influence of AI and cAMP-CRP (see the text for the parameter description) on the number and stability of the steady states. The variation of [AI] is equivalent to moving on this graph parallel to the *X* axis. The bistability curve describing the expression of *luxR* as a function of [AI] corresponding to the dashed line with arrows is shown in black in (B); (B) The predicted dependencies of *luxR* expression (*R*) on [AI] (proportional to $1/\sqrt{\beta}$) for δ=1 and γ = 20 (black), 16, 12, 8 (smaller curves moving left to right). The bistability region corresponding to the overlap of two stable response branches f_L and f_H is shaded in grey. Note the progressive decrease in both the magnitude of responses and the location and the extent of the bistability regions; (C) Experimental analysis of the regions of hysteresis for glucose concentrations of 2.5 (light grey), 1.5 (medium grey) and 0 mM (dark grey, copied from Fig. 1C for comparison). Red lines for each shaded area indicate induction from low [AI_{ex}] and blue lines indicate dilution from high [AI_{ex}]. Note the reduction of the bistability ranges and the decrease in the response amplitudes with increasing glucose, in agreement with the predictions in (B). Error bars represent the standard deviation of two independent triplicate sets. (D) Flow cytometry analysis of the hysteresis in *lux01* single cell response. The results are given as histograms corresponding to different modes of response induction: 'UP' for the induction for 7 h from the initial [AI_{ex}] = 0 nM to [AI_{ex}] =10 nM, and 'DOWN' for the dilution experiment from the initial [AI_{ex}] = 100 nM to [AI_{ex}] =10 nM. The histograms of the 'UP' induction experiments for the final [AI] = 100 nM and the uninduced control (0 nM) are shown for comparison.

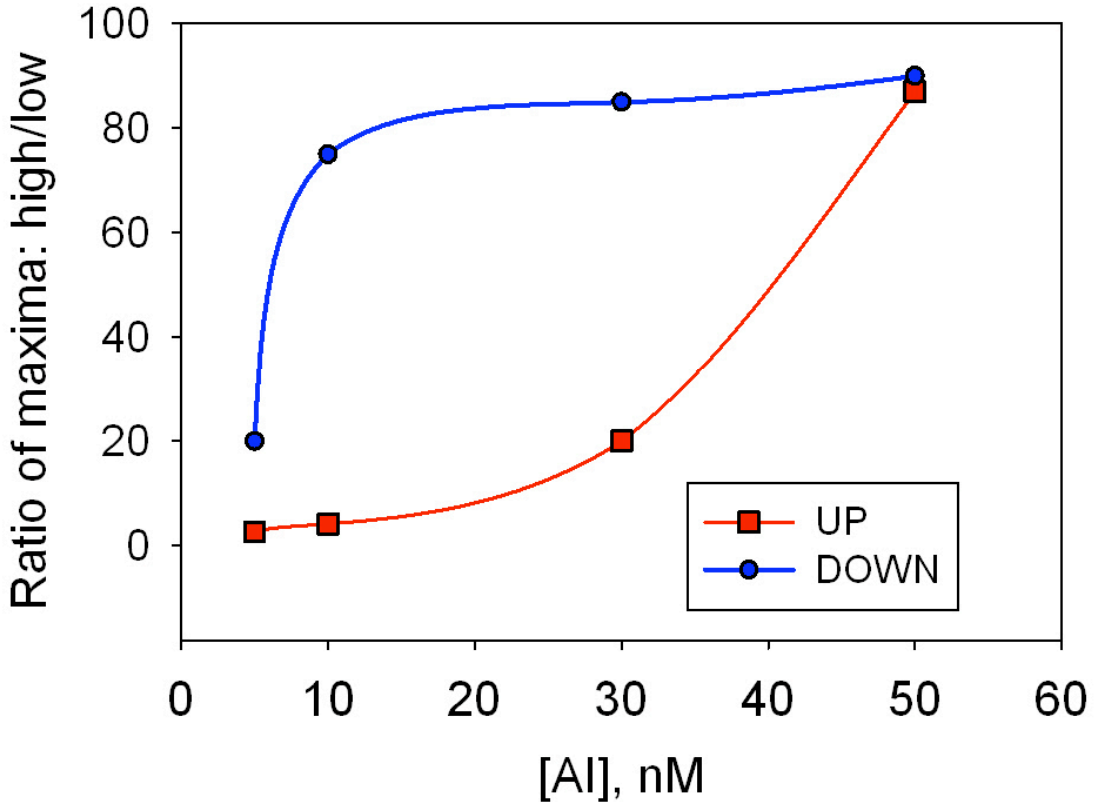

Figure 2.4. Comparison of the response peak maxima obtained from flow cytometry analysis of the *lux01* circuit induced to, and diluted from 100 nM AI_{ex}. The amplitude ratios of coinciding fluorescence peak values obtained from flow cytometry analysis of the *lux01* circuit induced from 0 to 100 nM AI_{ex} (UP), and diluted from a high state of induction obtained after 7 h induction at 100 nM AI_{ex} (DOWN) are shown for several concentrations of AI_{ex}. The data are represented as the ratio of fluorescence values for UP and DOWN experiments as a function of [AI_{ex}]. Data are representative of two independent triplicate sets.

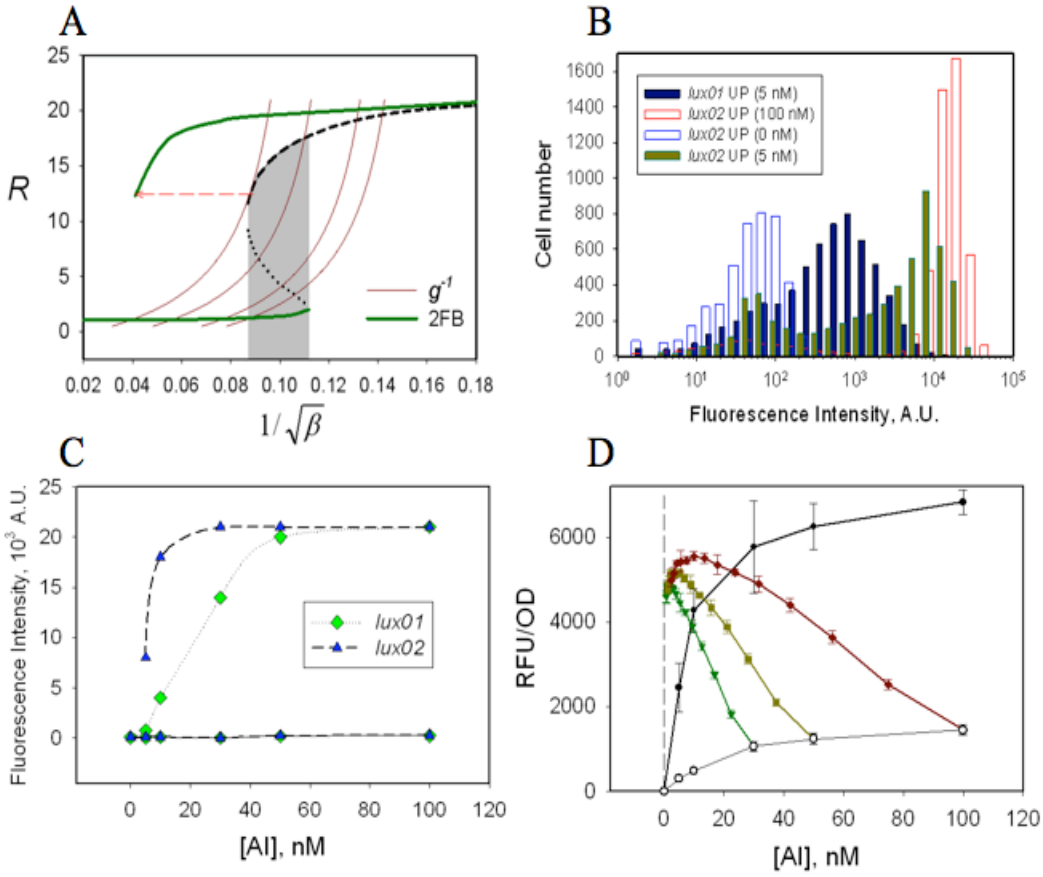

Figure 2.5. Mathematical modeling and experimental analysis of the *lux02* circuit response. (A) Graphical analysis of bistability in the presence of AI synthesis in the *lux02* circuit in the form of intersection of the bistable curve, $\tilde{f}([AI])$ from Fig. 2.1A (black) and the assumed series of curves representing the dependence of [AI] on the expression of *luxR* (as a proxy for *luxI* expression). These $\tilde{g}^{-1}([AI])$ null clines are assumed to be of the form $\tilde{g}^{-1}([AI]) = \frac{G \cdot [AI]}{K + [AI]} + [AI_{ex}]$, where K = 5; $[AI_{ex}]$ = 0.02; 0.04; 0.06; 0.07 and G = 0.09. The curves resulting from the intersection of $\tilde{f}([AI])$ and $\tilde{g}^{-1}([AI])$ as a function of $[AI_{ex}]$ are shown in red, and the extension of the bistability range is indicated by the red arrow; (B) Flow cytometry analysis of the single cell responses of the *lux02* circuit exposed to $[AI_{ex}]$ = 5 nM contrasted with the responses of this circuit to $[AI_{ex}]$ = 0 and 100 nM, and with the response of the *lux01* circuit to $[AI_{ex}]$ = 5 nM; (C) The peak values of the fluorescence intensity distributions obtained from two cell response sub-populations of the *lux01* and *lux02* exposed to different $[AI_{ex}]$ values, obtained using flow cytometry experiments; (D) The 2 h (open circles) and 8 h (closed circles) induction curves are overlaid with 25% hourly AI dilution from the medium of cells expressing *lux02* from 30 (inverted triangles), 50 (squares), or 100 nM (diamonds) $[AI_{ex}]$, with the output converging to a constant level in spite of multiple rounds of cell and AI dilution from the medium. Error bars represent the standard deviation of two independent triplicate assays.

Chapter 3

Prediction of CsrA-regulating sRNAs in bacteria and their experimental verification in *Vibrio fischeri*

Selected portions relevant to the experimental work from:

Kulkarni, P. R., X. Cui, J. W. Williams, A. M. Stevens, and R. V. Kulkarni. 2006. Prediction of CsrA-regulating small RNAs in bacteria and their experimental verification in *Vibrio fischeri*. Nucleic Acids Res **34:**3361-9.

Abstract

The role of small RNAs as critical components of global regulatory networks has been highlighted by several recent studies. An important class of such small RNAs is represented by CsrB and CsrC of *Escherichia coli*, which control the activity of the global regulator CsrA. Given the critical role played by CsrA in several bacterial species, an important problem is the identification of CsrA-regulating small RNAs. We have verified experimentally our predictions for two CsrA-regulating small RNAs in *Vibrio fischeri*. These small RNAs in *V. fischeri* were shown by northern blot analysis to be expressed at relatively constant level during exponential growth, and were also shown to functionally regulate CsrA in recombinant *E. coli*. As more genomes are sequenced, the approach used in this paper may be used to locate the sRNAs that regulate CsrA homologues. This work thus opens up several avenues of research in understanding the mode of CsrA regulation through small RNAs in bacteria.

Introduction

Recent studies combining bioinformatics and experimental approaches have led to the discovery of numerous small non-coding RNAs (sRNAs) in bacteria (4, 11, 19, 32, 33, 37). Although the functions for a majority of these sRNAs are yet to be determined, an emerging trend is that they play crucial regulatory roles in bacterial adaptation to changing environments (26). In particular, sRNAs have been shown to be critical components of global regulatory networks that coordinate large-scale changes in gene expression (16, 23). Further identification and analysis of sRNAs as components of such regulatory networks will aid efforts to elucidate their roles in mediating the global response to changing conditions.

In *Escherichia coli*, the RNA-binding protein CsrA is a key component of one such global regulatory network that is involved in the transition from exponential to stationary growth phase (22, 27). The activity of CsrA is modulated by two small RNAs, CsrB and CsrC, which control CsrA levels by binding to multiple copies of the protein (17, 34). Recent work has further demonstrated that these sRNAs are activated by the BarA-UvrY two-component system in *E. coli* in a CsrA-dependent manner (28). Homologs of CsrA (e.g. RsmA in *Pseudomonas aeruginosa*) are highly conserved and are found in diverse bacteria where they play key roles in biofilm formation and dispersal (13), and in regulating virulence factors of animal and plant pathogens (2, 12, 15, 21). It is interesting to note that, in the proteobacteria, most of the bacterial species having CsrA homologs also contain homologs of BarA and/or UvrY (e.g. the GacA-GacS two-component system in *P. aeruginosa*) and the interaction network between these proteins has been studied in several bacteria (5, 10, 14, 15, 28-30).

The presence of both CsrA and BarA-UvrY homologues in several bacterial species naturally leads to the question: Is the method of CsrA regulation via small RNAs also conserved in these species? Indeed, sRNA-encoding genes that regulate CsrA homologs have been identified already in several bacterial species, e.g. *rsmX*, *rsmY*, and *rsmZ* in *Pseudomonas fluorescens* (1, 10, 14, 30), *rsmB* in *Erwinia carotovora* (18), and *csrB*, *csrC* and *csrD* in *Vibrio cholerae* (15) to name a few. However, there are many bacterial species in which homologs of CsrA and BarA-UvrY are known to be important global regulators [e.g. in *Vibrio fischeri* (35) and in *Legionella pneumophila* (24)] for which the corresponding sRNAs, if they exist, have not been identified to date. The discovery of such sRNAs is complicated by the fact that they cannot all be identified by homology searches alone. Identifying potential CsrA-regulating sRNAs is therefore an important challenge in the field.

In this paper, we develop a procedure to discover potential CsrA-regulating sRNAs in bacteria. Recent experiments have shown that a repeated GGA motif in loop regions is a crucial element in the small RNAs that regulate CsrA and its homologues (7, 31). This suggests that the occurrence of a large number of such sequence motifs in a small genomic region could be a signature of CsrA-binding small RNAs. Building on this basic observation, we have developed a computer program (CSRA_FIND) to search intergenic regions of the bacteria for potential CsrA-regulating sRNAs. The identification of multiple AGGA/ARGGA (where R stands for [T,C,G]) motifs within an intergenic region, especially within a stem-loop structure, was the first step in identifying these CsrA-regulating sRNAs. Once a potential sRNA was located, the sequence was examined for rho-independent terminators, and UvrY binding sites to establish the 5' and

3' ends of the gene. The output of the program, in combination with secondary structure predictions using the program MFOLD (38), identifies all the experimentally known CsrA-regulating sRNAs and also leads to novel predictions for such sRNAs in several bacterial species. These predictions have been confirmed in *V. fischeri* through experiments that demonstrate the transcription of the predicted sRNAs in *V. fischeri*, as well as their ability to control CsrA levels in *E. coli*. As more genomes are sequenced and further experimental details regarding the binding motifs become available, this approach can be used to locate potential CsrA-regulating sRNAs in these genomes.

Experimental results

Transcription of *csrB1* and *csrB2* in *V. fischeri*

The presence of two *V. fischeri* sRNAs, *csrB1* and *csrB2*, was confirmed. *csrB1* is located between VF0602 and VF0603 and *csrB2* is located between VF0051 and VF0052 on the chromosome. First, the existence of functional promoters for these two genes was measured via transcriptional fusions to *lacZ* in recombinant *E. coli* (Figure 3.1A). Second, the expression of *csrB1* and *csrB2* in *V. fischeri* were analyzed over time via northern blots. The total amount of the pool of CsrB1 and CsrB2 appears to remain steady between an OD_{600} of 0.25 and 2.0 as identical results were obtained using probes against either sRNA. Given that CsrB1 and CsrB2 are only 4 bp different in size and 88% identical, a single band of the appropriate size and thought to be representative of both sRNAs was observed (Fig. 3.1B and data not shown). These experiments were performed by Dr. Xiaohui Cui.

Activity of CsrA, CsrB1 and CsrB2 in recombinant *E. coli*

A qualitative iodine-staining assay (34) was used to visualize glycogen production in recombinant *E. coli* strains overexpressing *V. fischeri* CsrA, CsrB1, and CsrB2 (Fig. 3.2). Cells overexpressing CsrA had a noticeably lighter yellow-brown appearance than cells containing only the pKK223-3 vector. Overexpression of CsrA leads to decreased glycogen accumulation, which causes the lighter staining to be seen. Cells over-expressing CsrB1 or CsrB2 showed a much darker brown color than the other strains, which indicates that they overproduce glycogen as a result of the inactivation of CsrA. Hence, the genes predicted to encode CsrA, CsrB1 and CsrB2 from *V. fischeri* are able to function in *E. coli* and interact with the glycogen regulatory network in a manner consistent with that of their *E. coli* homologues.

Discussion

Recent work has shown that there is a close connection between the quorum-sensing regulatory network and the CsrA regulon in *V. cholerae* (15). Studying the genome context of the predicted sRNAs also suggests further connections between the CsrA regulon and global regulatory networks such as the quorum-sensing regulon. For example, one of the flanking genes for *csrB4* in *Photobacterium profundum* is *PBPRB1151*. The orthologue of this gene in *V. fischeri* (VFA1016) was shown recently to be part of a regulatory locus that is differentially regulated by quorum sensing (20). Furthermore, *csrC* is always found in the genome neighborhood of the gene *yihA* which has been shown to be essential for normal cell division (6). This suggests a hypothesis linking the CsrA regulon with the regulation of cell division. The suggested connection is further strengthened by the observation that in *E. coli*, the protein SdiA (which is a

homolog of the quorum-sensing regulator LuxR of *V. fischeri*) has been shown to regulate both transcription of *csrB* and *csrC* (28) as well as the transcription of *ftsZ* (a gene that is essential for cell division) (9). It would be of interest to explore these connections further in *V. fischeri* to study the integration of these global regulatory networks.

In conclusion, we have developed an algorithm for the discovery of CsrA-regulating sRNAs in bacteria. Our analysis recovers all experimentally known sRNAs and makes novel predictions for such sRNAs in important species such as *Legionella pneumophila*, *Vibrio parahaemolyticus*, *Shewanella oneidensis*, and *Pseudoalteromonas haloplanktis* to name a few. Our experimental results have verified the predictions in *V. fischeri* and also provide the groundwork for future studies exploring the connections between the CsrA regulon and other global regulatory networks. It should be noted that while predictions have been made for some species, there are many more bacterial species with CsrA homologs for which our program could not find a definitive signature of CsrA-regulating sRNAs. This may be because the mode of regulation of CsrA (via sRNAs) is not conserved in other species. Alternatively, in the species with distant CsrA homologs, the mode of regulation (via sRNAs) is retained but the binding motifs for CsrA have changed to the extent that these sRNAs cannot be identified using our present scheme. It is hoped that future experimental studies in combination with similar bioinformatics approaches will be instrumental in unraveling the mode of CsrA regulation in additional bacterial species.

Materials and methods

Bacterial strains and growth conditions

E. coli DH5α or MG1655 were grown at 30 or 37ºC in Luria-Bertani (LB) medium with ampicillin (100 μg/ml) when necessary. *V. fischeri* ES114 was grown in LBS medium (8) at 30ºC. Kornberg agar plates (1.1% K_2HPO_4, 0.85% KH_2PO_4, 0.6% yeast extract containing 1% glucose) with 1 mM isopropyl-β-D-thiogalactopyranoside (IPTG) and 100 μg/ml ampicillin were used to grow recombinant *E. coli* cultures for the glycogen iodine-staining assay.

DNA manipulation

Standard DNA manipulation procedures were used for all cloning steps. PCR purification, gel extraction and plasmid purification kits were obtained from Qiagen. High-fidelity Deep Vent DNA Polymerase from New England Biolabs (Beverly, MA) was used to generate PCR products for cloning.

β-galactosidase assays

The transcriptional fusions containing the promoter and part of the 5' transcribed regions of *csrB1* and *csrB2* were separately amplified from *V. fischeri* ES114 chromosomal DNA by PCR with primers 5`GTGACTTCCTATATTTCAGCTTTGC3` and 5`CGCGGATCCGTGAGCGGTGTCCCTTACAT3` for *csrB1* and 5`TGAGAATTCGTTGATGATTATCAGCGCTTT3` and 5`CGCGGATCCTTGAGCGGTGTCCTTTAC3` for *csrB2*. *Eco*RI-*Bam*HI fragments from these PCR products were then subcloned into a *lacZ* expression vector pSP417 (25) and the integrity of their nucleotide sequence was confirmed (Virginia Bioinformatics Institute Core Laboratories). The resulting constructs were used to perform β-

galactosidase assays from cells grown to mid-log phase (OD_{600}= 0.5) in LB medium. Cell extracts were prepared from cells diluted 1:200 in Z buffer and permeabilized via chloroform and SDS. Assays were performed on 20 μl of cell extract using the Tropix Galacto-Light Plus Kit as per the manufacturer's recommendations. Triplicate assays were performed for each culture and the experiment was repeated three times.

Northern hybridization

V. fischeri cells harvested at four different OD_{600} values were treated with RNAprotect Bacteria Reagent (Qiagen) to stabilize the RNA prior to the RNA isolation. The RNA was isolated using the RNeasy Mini Kit (Qiagen). ^{32}P labeled *csrB1* and *csrB2* riboprobes were produced by using a random primer DNA labeling kit as described by the manufacturer (Roche). 16 μg of total cellular RNA was separated on a 1% agarose formaldehyde gel and transferred overnight onto a Nytran supercharge membrane (Turboblotter Gel Transfer Kit, Schleicher & Schuell) in 20x SSC transfer buffer. The RNA was immobilized on the membrane by an UV cross-linker (SpectroLinker, Spectronics Corporation). The membrane was pre-hybridized and hybridized in 10 ml of QuickHyb solution (Stratagene) at 65°C, for 30 min. and 2-4 h, respectively, with a probe concentration of 2 x 10^6 c.p.m./ml and then washed twice for 15 min each in 2 x SSC, 0.1% SDS at room temperature and once for 30 min in 0.2 x SSC, 0.1% SDS at 60°C. The membrane was air-dried and then exposed to a phosphorimager screen (Molecular Dynamics).

Assays for glycogen production

The gene coding for CsrA was PCR amplified from *V. fischeri* chromosomal DNA with the primers 5`CCCGGGATGCTAATTTTGACTCGCCGTGTAGG3` and 5`AAGCTTTTAGTGGTGGTGGTGGTGGTGAAAGTTACCTTGCGAAGCCGCAGG TG3`.

The resulting PCR product encoded CsrA with a C-terminal His_6 tag, flanked by *Sma*I and *Hind*III restriction sites. The PCR product was ligated into pGEM (Promega, Madison, WI) and sequenced. A *Sma*I-*Hind*III fragment from this vector was subsequently ligated into pKK223-3 (3). The primers 5`CACGGTACCTGGTGTCGGAAGGATACTGA` and 5`GTTCTGCAGAAAAACCCCACCAAGCTCTC` for *csrB1* and 5`GTAGGTACCTATTGGTGTCGGAAGGATGC3`

and 5`GTTCTGCAGAAAAGCCCCACTAGATTTTCA3`

for *csrB2* were used to amplify these genes from *V. fischeri* chromosomal DNA. *Kpn*I-*Pst*I fragments from these PCR products were ligated into pUC19 (36) and the integrity of the nucleotide sequences was confirmed. *Eco*RI-*Pst*I fragments from the *csrB1*- and *csrB2*-pUC19 constructs were then subsequently ligated into the expression vector pKK223-3. *E. coli* MG1655 encoding CsrB1, CsrB2, or CsrA under the control of the IPTG-inducible P_{tac} promoter in pKK223-3, as well as the empty vector, were individually streaked onto Kornberg agar plates. Plates were incubated at 30°C overnight, then inverted over iodine crystals until a noticeable change in color could be detected.

Acknowledgements

The authors thank Andre Levchenko for his support of this project, Jill Sible for assistance with northern blotting procedures, and Tony Romeo for helpful suggestions. Work in the Stevens lab was funded by the National Institutes of Health (GM066786). Funding to pay the Open Access publication charge for this article was provided by a research grant from the Jeffress Memorial Trust.

References

1. **Aarons, S., A. Abbas, C. Adams, A. Fenton, and F. O'Gara.** 2000. A regulatory RNA (PrrB RNA) modulates expression of secondary metabolite genes in *Pseudomonas fluorescens* F113. J Bacteriol **182:**3913-9.
2. **Altier, C., M. Suyemoto, A. I. Ruiz, K. D. Burnham, and R. Maurer.** 2000. Characterization of two novel regulatory genes affecting *Salmonella* invasion gene expression. Mol Microbiol **35:**635-46.
3. **Amann, E., J. Brosius, and M. Ptashne.** 1983. Vectors bearing a hybrid *trp-lac* promoter useful for regulated expression of cloned genes in *Escherichia coli*. Gene **25:**167-78.
4. **Argaman, L., R. Hershberg, J. Vogel, G. Bejerano, E. G. Wagner, H. Margalit, and S. Altuvia.** 2001. Novel small RNA-encoding genes in the intergenic regions of *Escherichia coli*. Curr Biol **11:**941-50.
5. **Cui, Y., A. Chatterjee, and A. K. Chatterjee.** 2001. Effects of the two-component system comprising GacA and GacS of *Erwinia carotovora* subsp. *carotovora* on the production of global regulatory *rsmB* RNA, extracellular enzymes, and harpinEcc. Mol Plant Microbe Interact **14:**516-26.
6. **Dassain, M., A. Leroy, L. Colosetti, S. Carole, and J. P. Bouche.** 1999. A new essential gene of the 'minimal genome' affecting cell division. Biochimie **81:**889-95.
7. **Dubey, A. K., C. S. Baker, T. Romeo, and P. Babitzke.** 2005. RNA sequence and secondary structure participate in high-affinity CsrA-RNA interaction. Rna **11:**1579-87.
8. **Dunlap, P. V.** 1989. Regulation of luminescence by cyclic AMP in *cya*-like and *crp*-like mutants of *Vibrio fischeri*. J Bacteriol **171:**1199-202.
9. **Garcia-Lara, J., L. H. Shang, and L. I. Rothfield.** 1996. An extracellular factor regulates expression of *sdiA*, a transcriptional activator of cell division genes in *Escherichia coli*. J Bacteriol **178:**2742-8.
10. **Heeb, S., C. Blumer, and D. Haas.** 2002. Regulatory RNA as mediator in GacA/RsmA-dependent global control of exoproduct formation in *Pseudomonas fluorescens* CHA0. J Bacteriol **184:**1046-56.
11. **Hershberg, R., S. Altuvia, and H. Margalit.** 2003. A survey of small RNA-encoding genes in *Escherichia coli*. Nucleic Acids Res **31:**1813-20.
12. **Heurlier, K., F. Williams, S. Heeb, C. Dormond, G. Pessi, D. Singer, M. Camara, P. Williams, and D. Haas.** 2004. Positive control of swarming, rhamnolipid synthesis, and lipase production by the posttranscriptional RsmA/RsmZ system in *Pseudomonas aeruginosa* PAO1. J Bacteriol **186:**2936-45.
13. **Jackson, D. W., K. Suzuki, L. Oakford, J. W. Simecka, M. E. Hart, and T. Romeo.** 2002. Biofilm formation and dispersal under the influence of the global regulator CsrA of *Escherichia coli*. J Bacteriol **184:**290-301.
14. **Kay, E., C. Dubuis, and D. Haas.** 2005. Three small RNAs jointly ensure secondary metabolism and biocontrol in *Pseudomonas fluorescens* CHA0. Proc Natl Acad Sci U S A **102:**17136-41.

15. **Lenz, D. H., M. B. Miller, J. Zhu, R. V. Kulkarni, and B. L. Bassler.** 2005. CsrA and three redundant small RNAs regulate quorum sensing in *Vibrio cholerae*. Mol Microbiol **58:**1186-202.
16. **Lenz, D. H., K. C. Mok, B. N. Lilley, R. V. Kulkarni, N. S. Wingreen, and B. L. Bassler.** 2004. The small RNA chaperone Hfq and multiple small RNAs control quorum sensing in *Vibrio harveyi* and *Vibrio cholerae*. Cell **118:**69-82.
17. **Liu, M. Y., G. Gui, B. Wei, J. F. Preston, 3rd, L. Oakford, U. Yuksel, D. P. Giedroc, and T. Romeo.** 1997. The RNA molecule CsrB binds to the global regulatory protein CsrA and antagonizes its activity in *Escherichia coli*. J Biol Chem **272:**17502-10.
18. **Liu, Y., Y. Cui, A. Mukherjee, and A. K. Chatterjee.** 1998. Characterization of a novel RNA regulator of *Erwinia carotovora* ssp. *carotovora* that controls production of extracellular enzymes and secondary metabolites. Mol Microbiol **29:**219-34.
19. **Livny, J., M. A. Fogel, B. M. Davis, and M. K. Waldor.** 2005. sRNAPredict: an integrative computational approach to identify sRNAs in bacterial genomes. Nucleic Acids Res **33:**4096-105.
20. **Lupp, C., and E. G. Ruby.** 2005. *Vibrio fischeri* uses two quorum-sensing systems for the regulation of early and late colonization factors. J Bacteriol **187:**3620-9.
21. **Ma, W., Y. Cui, Y. Liu, C. K. Dumenyo, A. Mukherjee, and A. K. Chatterjee.** 2001. Molecular characterization of global regulatory RNA species that control pathogenicity factors in *Erwinia amylovora* and *Erwinia herbicola* pv. *gypsophilae*. J Bacteriol **183:**1870-80.
22. **Majdalani, N., C. K. Vanderpool, and S. Gottesman.** 2005. Bacterial small RNA regulators. Crit Rev Biochem Mol Biol **40:**93-113.
23. **Masse, E., C. K. Vanderpool, and S. Gottesman.** 2005. Effect of RyhB small RNA on global iron use in *Escherichia coli*. J Bacteriol **187:**6962-71.
24. **Molofsky, A. B., and M. S. Swanson.** 2003. *Legionella pneumophila* CsrA is a pivotal repressor of transmission traits and activator of replication. Mol Microbiol **50:**445-61.
25. **Podkovyrov, S. M., and T. J. Larson.** 1995. A new vector-host system for construction of *lacZ* transcriptional fusions where only low-level gene expression is desirable. Gene **156:**151-2.
26. **Repoila, F., N. Majdalani, and S. Gottesman.** 2003. Small non-coding RNAs, co-ordinators of adaptation processes in *Escherichia coli*: the RpoS paradigm. Mol Microbiol **48:**855-61.
27. **Romeo, T.** 1998. Global regulation by the small RNA-binding protein CsrA and the non-coding RNA molecule CsrB. Mol Microbiol **29:**1321-30.
28. **Suzuki, K., X. Wang, T. Weilbacher, A. K. Pernestig, O. Melefors, D. Georgellis, P. Babitzke, and T. Romeo.** 2002. Regulatory circuitry of the CsrA/CsrB and BarA/UvrY systems of *Escherichia coli*. J Bacteriol **184:**5130-40.
29. **Teplitski, M., R. I. Goodier, and B. M. Ahmer.** 2003. Pathways leading from BarA/SirA to motility and virulence gene expression in *Salmonella*. J Bacteriol **185:**7257-65.

30. **Valverde, C., Heeb, S., Keel, C., and Haas, D.** 2003. RsmY, a small regulatory RNA, is required in concert with RsmZ for GacA-dependent expression of biocontrol traits in *Pseudomonas fluorescens* CHA0. Molec. Microbiol. **50:**1361-1379.
31. **Valverde, C., M. Lindell, E. G. Wagner, and D. Haas.** 2004. A repeated GGA motif is critical for the activity and stability of the riboregulator RsmY of *Pseudomonas fluorescens*. J Biol Chem **279:**25066-74.
32. **Vogel, J., V. Bartels, T. H. Tang, G. Churakov, J. G. Slagter-Jager, A. Huttenhofer, and E. G. Wagner.** 2003. RNomics in *Escherichia coli* detects new sRNA species and indicates parallel transcriptional output in bacteria. Nucleic Acids Res **31:**6435-43.
33. **Wassarman, K. M., F. Repoila, C. Rosenow, G. Storz, and S. Gottesman.** 2001. Identification of novel small RNAs using comparative genomics and microarrays. Genes Dev **15:**1637-51.
34. **Weilbacher, T., Kazushi, S., Dubey, A.K., Wang, X., Gudapaty, S., Morozov, I., Baker, C.S., Georgellis, D., Babitzke, P., Romeo, T.** 2003. A novel sRNA component of the carbon storage regulatory system of *Escherichia coli*. Molec. Microbiol. **43:**657-670.
35. **Whistler, C. A., and E. G. Ruby.** 2003. GacA regulates symbiotic colonization traits of *Vibrio fischeri* and facilitates a beneficial association with an animal host. J Bacteriol **185:**7202-12.
36. **Yanisch-Perron, C., J. Vieira, and J. Messing.** 1985. Improved M13 phage cloning vectors and host strains: nucleotide sequences of the M13mp18 and pUC19 vectors. Gene **33:**103-19.
37. **Zhang, A., K. M. Wassarman, C. Rosenow, B. C. Tjaden, G. Storz, and S. Gottesman.** 2003. Global analysis of small RNA and mRNA targets of Hfq. Mol Microbiol **50:**1111-24.
38. **Zuker, M.** 2003. Mfold web server for nucleic acid folding and hybridization prediction. Nucleic Acids Res **31:**3406-15.

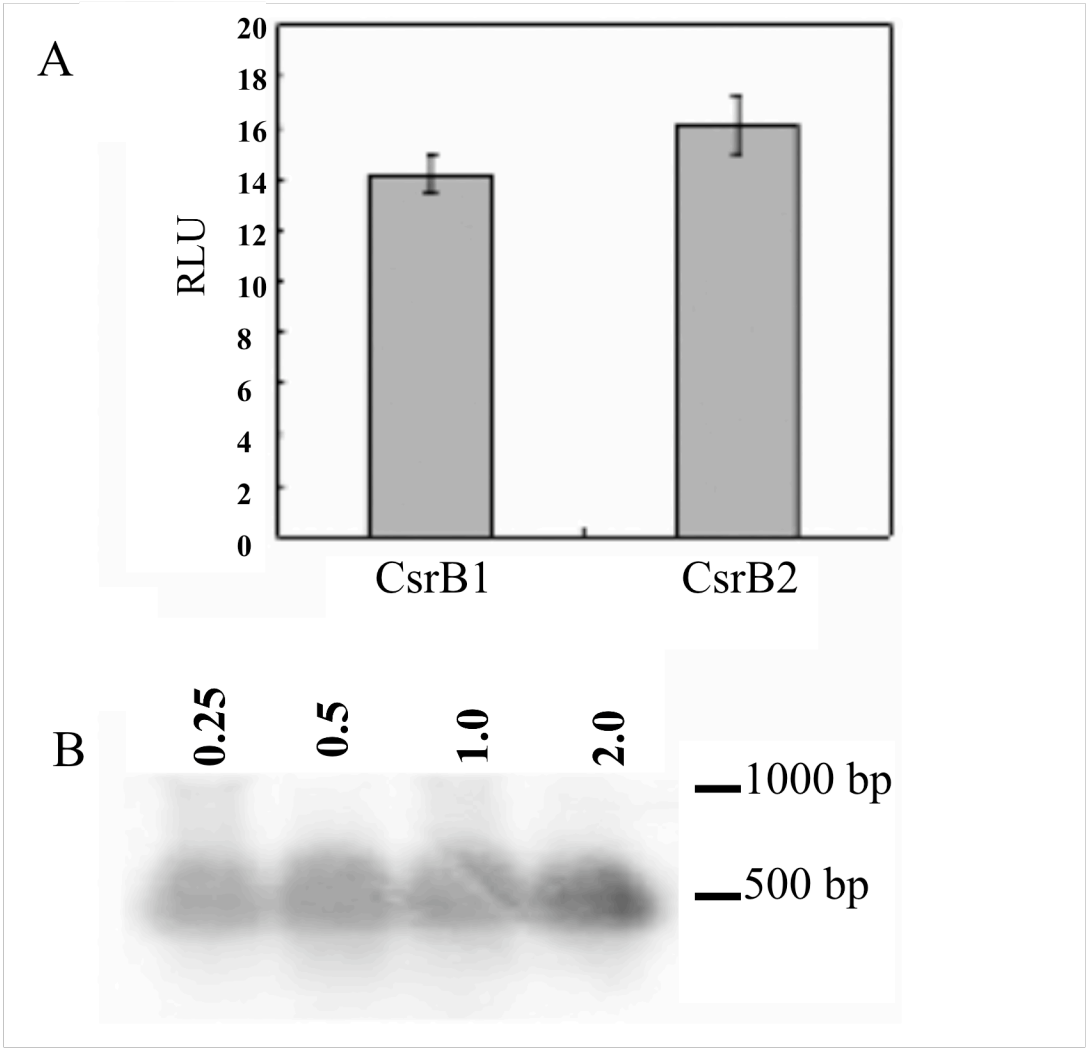

Figure 3.1. **Transcription of *csrB1* and *csrB2*.** (A) β-galactosidase activity levels of recombinant *E. coli* DH5α strains encoding *csrB1- or csrB2-lacZ* transcriptional fusions in pSP417. Background levels of β-galactosidase produced from the negative control pSP417 were 0.063 +/- 0.004 RLU. Error bars represent the standard deviation of assays performed in triplicate from three independent samples. (B) Northern blot analysis of the amount of *csrB1* and *csrB2* transcript in *V. fischeri* ES114 grown to different OD values as indicated using *csrB2* sequences as a probe (data not shown). The blot shown is representative of two independent experiments. The migration of RNA size standards is indicated on the right.

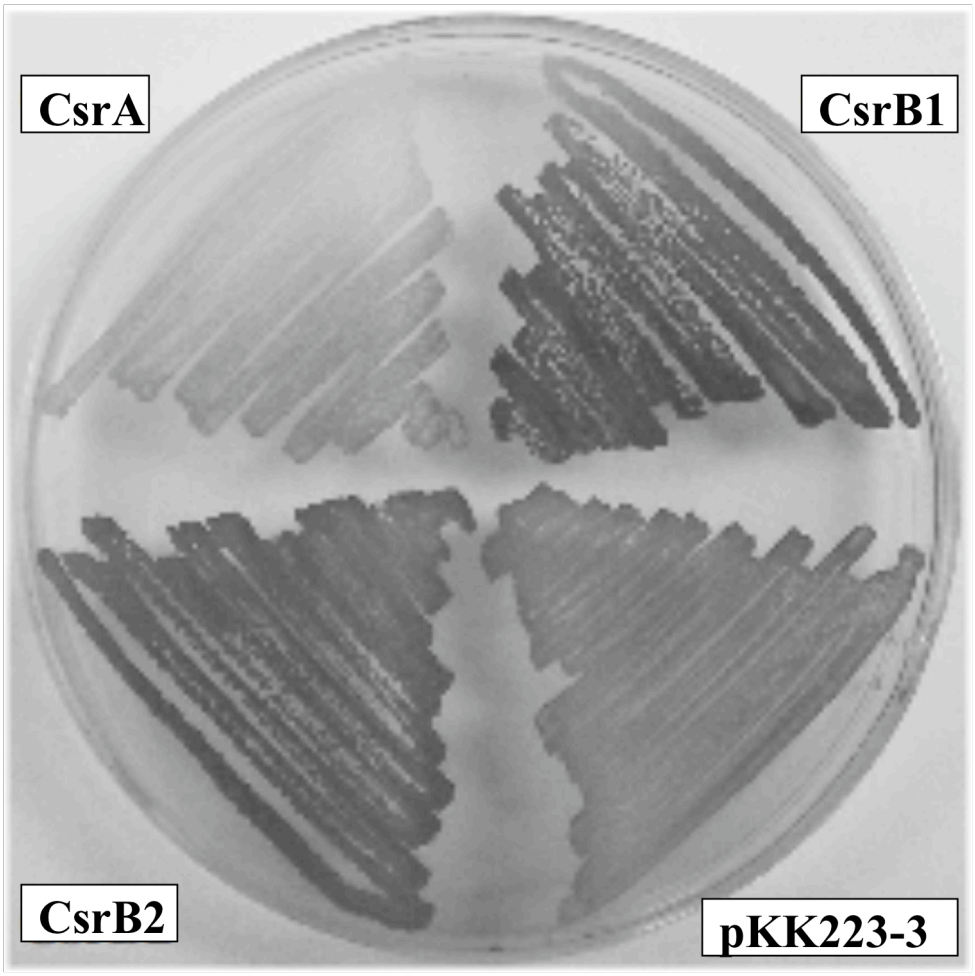

Figure 3.2. **Effects of *V. fischeri* CsrA, CsrB1, and CsrB2 on glycogen regulation.** Recombinant *E. coli* MG1655 overexpressing *V. fischeri* CsrA, CsrB1, CsrB2 or no protein (pKK223-3) were grown on Kornberg agar plates supplemented with 1 mM IPTG and 100 μg/ml ampicillin and qualitatively assayed for levels of glycogen production.

Chapter 4

Evidence of interactions between the CsrA and quorum-sensing regulons of *Vibrio fischeri*

Manuscript in preparation

Joshua W. Williams[1], A.L. Ritter[2], and Ann M. Stevens[1]*

[1]Dept. of Biological Sciences, Virginia Tech, Blacksburg, VA 24061
[2]Dept. of Physics, Virginia Tech, Blacksburg, VA 24061

*Corresponding author information:
Life Sciences I
Washington St.
Virginia Tech
Blacksburg, VA 24061

Abstract

The quorum sensing and CsrA regulons of *Vibrio fischeri* control overlapping cellular functions during the exponential and stationary phases of growth. Hence, the potential exists for regulatory network interactions between the CsrA and quorum-sensing pathways that enable them to be coordinately regulated. Using an experimental approach combined with statistical analysis of variance methods, it was demonstrated that CsrA is capable of causing an increase in transcription of the quorum-sensing regulatory gene *luxR*. The increase in *luxR* transcription caused by CsrA does not depend on cAMP-CRP or any of the known upstream regulatory circuitry of the quorum-sensing pathway, including the *luxR* transcriptional activator LitR. Instead, CsrA appears to exert some negative effect on the activity of the quorum-sensing repressor ArcA.

Introduction

The quorum-sensing response of *Vibrio fischeri* involves a complex signal transduction pathway that is responsible for regulating many processes in the cell, including bioluminescence, host-association, certain metabolic functions, and motility (9, 15, 21, 22). Many of the major regulatory genes in the quorum-sensing regulon have been identified and thoroughly characterized through mutagenesis in *V. fischeri* or analysis of function studies in recombinant *Escherichia coli* (5, 8, 15). However much of the work on this system has focused on understanding interactions that lead to drastic changes in gene expression, such as a hyper-luminescent response, or a completely dark response. These types of all-or-nothing observations established the critical genes in the regulon, but there are potentially important interactions that do not show up as well in standard statistical analyses. In a complicated regulatory network, where there are many downstream components and multiple pathways functioning coordinately, even a small change in the expression of one component can lead to much larger differences in others.

Because the quorum-sensing response of *V. fischeri* leads to activation of luminescence, which consumes a large amount of oxygen and ATP (4), it is likely that there are mechanisms in place that regulate the response based on the metabolic state of the cell. It has been shown in previous work that the secondary metabolism regulator CRP can activate transcription of *luxR* (5, 6). This may be important in linking metabolism and quorum sensing, but it may not be the only point of convergent regulation. We hypothesized that the global regulatory RNA-binding protein CsrA may have some role in controlling the quorum-sensing response at the post-transcriptional level in relation to the metabolic state of the cell. CsrA is an important component in

regulating carbon storage and utilization in the cell during exponential-growth phase (1, 14, 16), which is the point where the quorum-sensing response begins to become induced. CsrA has also been shown to play a regulatory role in the quorum-sensing response of other *Vibrio* species (11, 13). An approach employing modulation of CsrA levels via overexpression of *csrA* itself, or its regulatory sRNA CsrB1, was chosen to examine how CsrA levels influence the amount of luminescence output during the quorum-sensing response. This was done using several strains of *V. fischeri* ES114 containing mutations in critical components of the quorum-sensing system.

In addition to examining potential interactions between CsrA and the quorum-sensing pathway, two other important *luxR* transcriptional regulators, cAMP-CRP (5, 6) and ArcA (3), were examined for possible interactions with CsrA that would cause changes in luminescence output. cAMP-CRP is important in secondary metabolism, and was considered a possible candidate to link the CsrA and quorum-sensing regulons. ArcA is important in regulating cellular processes in relation to redox state, which is important during the transition into stationary growth phase as oxygen tension decreases. Because the production of luminescence also consumes a large amount of oxygen, ArcA regulation of the quorum-sensing response needed to be considered in our examination of the influence of CsrA on luminescence production.

Analyzing the interconnections between major regulator networks is challenging both because of their extreme complexity and because of the influence of environmental factors on their response. The analysis of these networks can be facilitated by a statistical technique, called factorial design, which is based on analysis of variance (ANOVA) and which is widely used in agricultural and industrial research and development. The

primary advantage of applying factorial design, versus the standard approach of changing one variable at-a-time, is the significant enhancement of statistical power that it provides. For example, a standard experiment looking for epistasis between two genes *A* and *B* requires 12 experiments (WT, *A* mutant, *B* mutant, and the double mutant *AB* each replicated 3 times). The power of such an experiment for a 10% alpha effect at one standard deviation is 20%. In one of our factorial experiments, we looked for epistasis between 3 genes (*litR*, *arcA*, and the expression level of CsrA) and also looked for the influence of two external factors (exogenous autoinducer and exogenous cAMP) at 3 levels of each external factor. Each measurement was replicated twice giving a total of 80 measurements (that were broken down into 2 blocks of 40 experiments each). We could test 9 hypotheses with this experiment; that is, whether epistasis existed between any pair of the 3 genes (3 hypotheses) plus the environmental influences of exogenous autoinducer and cAMP on each epistasis (6 hypotheses). The power of our experiment for a 10% alpha effect at one standard deviation was 99%. Thus, for 6.7 times as many experiments (80/12), we obtained 9 times as much information with 5 times as much statistical power.

Using the statistical technique of factorial design, we have demonstrated that CsrA, through epistasis with *litR*, increases the amount of *luxR* transcript in the cell. This increase in *luxR* transcription is not caused by CsrA-dependent changes in cAMP or CRP levels, nor is it dependent on any of the known components of the upstream quorum-sensing pathway. Our data also suggests that CsrA may exert some repressive effect on the redox-responsive regulator ArcA, which is known to repress both *luxR* and the *lux* operon (3).

Results and discussion

Epistasis experiments between CsrA and the quorum-sensing pathway upstream of *luxR*

When *V. fischeri* strains containing *ainS*, *luxO*, or *ainS-luxO* mutations (15) were examined in relation to the same strains overexpressing *csrA*, no statistically significant change in luminescence output was observed. These strains were also compared at two different [AI]s (20 nM and 100 nM), but there was still no significant changes in luminescence in relation to CsrA level (Fig. 4.1). This indicates that CsrA has no regulatory role in modulating luminescence output through the *ainS* signaling cascade or the proposed LuxO-mediated repression of LitR via activation of the sRNA *qrr1*. This is an important point in the quorum-sensing network to examine, due to the fact that this signaling cascade results in derepression of *litR*. LitR not only activates *luxR* transcription, but also other processes in the cell that are important for host-colonization, motility, and metabolism (9, 20). In particular, LitR is known to be important in regulating acetate metabolism (20), which may be part of the reason that CsrA does not affect LitR or its upstream regulatory components. Therefore, regulation of luminescence may not necessarily always occur upstream of LitR, but may instead occur directly on *luxR* or the *lux* operon so that the two regulators (LitR and LuxR) can be differentially regulated depending on environmental or metabolic conditions.

Next, a Δ*litR* strain of *V. fischeri* (PMF8) was examined using this type of analysis to determine if CsrA could affect luminescence downstream of LitR. Even though overexpression of CsrA is sufficient to generate a physiological difference in the cell, it was better for our statistical analysis to use a ternary system in which the

expression state of *csrA* could be considered "-1" or "1", which corresponds to either a very low or very high state of expression respectively. The normal state of expression is considered a "0". To obtain this range of expression of *csrA*, strains carried plasmids that allowed for overexpression of the sRNA CsrB1 or the CsrA protein, or the empty vector (pVSV104) for the wild-type level of CsrA when a mid-point analysis was desired. In this case, there was a significant effect seen when CsrA levels were altered. A Δ*litR* strain of *V. fischeri* produces low levels of luminescence, even with the addition of exogenous AI. PMF8 (pJW4), which has depressed CsrA activity, produced less luminescence than when *csrA* was overexpressed in PMF8 (pJW3), and CsrA overexpression caused a large increase in luminescence values that was statistically equal to the expression level of the wild-type strain *V. fischeri* ES114 (Fig. 4.2). This effect was stronger (3.5-fold increase) at lower [AI] (20 nM; Fig. 4.2A) than at higher [AI] (2-fold increase) (100 nM; Fig. 4.2B), indicating that LuxR levels may be altered in some way by CsrA. *V. fischeri* ES114 either underexpressing or overexpressing *csrA* showed no statistically significant change in luminescence values when the level of CsrA was altered (Fig. 4.2).

These results indicated that CsrA was capable of modulating the luminescence response at a regulatory point downstream of *litR*, which would place its interaction outside the known quorum-sensing cascade that leads to the activation of *luxR*. Because LitR is a transcriptional activator of *luxR*, its disruption leads to lower levels of *luxR* transcription, and therefore lower levels of luminescence expression, which requires activation by the LuxR-AI complex. Since *csrA* expression in a Δ*litR* strain restored near wild-type levels of luminescence, but had no effect on ES114 luminescence, we

hypothesized that CsrA must in some way cause activation of *luxR* in a LitR-independent manner. This effect is most likely masked in the wild-type strain due to *luxR* transcription already being fully activated.

Effect of altering CsrA levels on *crp* and *luxR* transcription

Other than LitR, the only known positive regulators of *luxR* are the cAMP-CRP complex (6), and AI-dependent LuxR positive autoregulation (17, 18, 23). Because LuxR levels are very low in a Δ*litR* strain, it is unlikely that the effect seen in a *csrA* overexpression strain was due to LuxR autoregulation, leaving CRP as the most likely cause. In order to determine if CsrA was influencing *crp* expression, and to verify that the increase in luminescence observed in PMF8 (pJW3) was in fact due to an increase in *luxR* expression, quantitative RT-PCR was performed on cDNA samples obtained from ES114 (wild-type) and PMF8 (Δ*litR*) strains (from the previous experiment which generated the data for Figure 4.2) that were either underexpressing or overexpressing *csrA*, in 20 nM or 100 nM AI.

As a control, *csrA* transcript was measured to ensure that there were significantly different levels of *csrA* expression between the strains containing pJW3 and pJW4. As anticipated, there was lower level transcription of *csrA* in strains overexpressing CsrB1 (pJW4), whereas there were much higher levels of *csrA* transcription in cells overexpressing *csrA* (pJW3) (Fig. 4.3). Because CsrA is post-transcriptionally repressed by CsrB1, the actual decrease in activity of CsrA is much stronger than what is observed by simply measuring differences in *csrA* transcript. The 16S rRNA was used as an internal control to normalize the data.

As expected, there was a significant increase in the quantity of *luxR* transcript in PMF8 (Δ*litR*) as CsrA level was increased. This effect was more dramatic at 20 nM AI than at 100 nM AI (Fig. 4.4), which is consistent with the luminescence data shown previously (Fig. 4.2). This is most likely due to LuxR positive transcriptional autoregulation occurring at higher [AI], and masking the influence of CsrA on *luxR* transcription. Interestingly, in addition to the increase in *luxR* transcript in PMF8 caused by increased *csrA* expression, there was a decrease in ES114 *luxR* transcript that correlated with increased *csrA* expression. This effect was only seen at 20 nM AI, and was not evident at 100 nM AI. This may simply be due to variation in the amount of *luxR* positive transcriptional autoregulation at lower [AI], as there is no difference in ES114 *luxR* transcript as AI is increased. Also, because 20 nM AI is within the [AI] range where *V. fischeri* switches from low to high quorum-sensing induction states, it is a highly variable physiological condition at which to measure luminescence values or transcript levels of the key quorum-sensing genes.

The quantity of *crp* transcript also increased when *csrA* was overexpressed in PMF8 in the presence of 20 nM AI, but this effect was not seen when [AI] was increased to 100 nM (Fig. 4.5). Even if CsrA in some way influences *crp* expression when [AI] is low, this does not explain the differences in luminescence values obtained at high [AI] when CsrA levels are varied, but *crp* transcript quantity is statistically equal. It is more likely that the difference in *crp* transcript seen at low [AI] is due to some other effect caused at low [AI], or simply a result of experimental error. These results indicate that increased CsrA levels do in fact lead to increased *luxR* transcription, and that the effect is most likely not caused by increased levels of CRP.

Interaction of CsrA with the ArcA redox-responsive regulatory system

Another possible reason for the increase in *luxR* transcription could be due to the repression of a *luxR* repressor by CsrA, rather than the activation of an activator. One such known *luxR* repressor is ArcA, which has been shown to have a moderate repressive effect on *luxR* transcription, as well as a stronger repressive effect on *luxICDABEG* transcription (3). The ArcA binding site lies in the intergenic region between *luxR* and *luxICDABEG*, and overlaps the CRP binding site that is important for activation of *luxR* transcription. If ArcA binding were diminished in some way, it could potentially allow better access by cAMP-CRP to the *luxR* promoter, as well as allow LuxR positive transcriptional autoregulation to have a more significant role in the response.

When *arcA* is deleted in *V. fischeri* there is higher luminescence production than in wild-type ES114, which is caused by lack of repression of the *lux* genes (3). When *arcA* is deleted in a Δ*litR* strain, there is also a very high level of luminescence, which is independent of CsrA level (Fig. 4.6). This result is consistent with our prediction that CsrA increases *luxR* transcription by exerting a repressive effect on the repressor ArcA. This repressive effect does not create the same effect as an *arcA* mutation, but is significant enough to allow increased transcription of *luxR* and the *lux* operon.

In a Δ*litR* background, there should be significantly lower levels of luminescence due to lack of *luxR* activation, which was seen in the previous data (Fig. 4.2). By removing repression by ArcA, the level of LuxR in the cell increases enough to mount a significant quorum-sensing response that is indistinguishable from the *arcA* single mutant. Because a mutation in *litR* leads to low activation of *luxR*, it is unlikely that the large luminescence values seen in a Δ*litR*-Δ*arcA* strain are the sole result of derepression

of the *lux* operon, but are more likely a combination of this derepression combined with increased *luxR* transcription. This is consistent with previous findings by Bose *et al* (3), showing that Δ*arcA* strains of *V. fischeri* have increased *luxR* transcription in addition to derepression of the *lux* operon.

Effects of altered cAMP levels on the CsrA-dependent luminescence increase observed in PMF8 (Δ*litR*)

Finally, in an effort to rule out any influence of cAMP levels on the increase in luminescence seen in PMF8 (pJW3), cAMP was added at a concentration of 5 mM and the previous experiment involving *litR*, *arcA*, and *litR*-*arcA* mutants was repeated. If *cya* were in some way being positively affected by CsrA, then addition of high levels of cAMP would abolish the effect, much as deletion of *arcA* did in the previous experiment. If the cAMP-CRP complex were playing a role in causing this CsrA-dependent phenotype in the Δ*litR* strain (in addition to the effect that was previously demonstrated in the *arcA* mutants) cAMP addition could cause PMF8 (pJW4) luminescence expression to increase much as *csrA* overexpression causes an increase in luminescence in PMF8 (pJW3). 5 mM cAMP was chosen to be added exogenously for this experiment due to the fact that *V. fischeri* is capable of metabolizing cAMP, and it therefore needed to be provided in excess in order to ensure that there was enough to generate a response.

When *V. fischeri* ES114, PMF8 (Δ*litR*), JB21 (Δ*litR*-Δ*arcA*), and AMJ2 (Δ*arcA*) luminescence was analyzed in the presence or absence of 5 mM cAMP, and with *csrA* either under- or overexpressed, there was no statistically significant change caused by the addition of cAMP in relation to CsrA level (Fig. 4.7). Overall, the addition of cAMP caused an increase in luminescence for each strain, due to cAMP-CRP activation of *luxR*

transcription, but this was an across-the-board effect. These results also indicate that the increase in the quantity of *crp* transcript seen in the Δ*litR* strain at 20 nM AI when CsrA levels are increased (Fig. 4.5A), is either the result of experimental error, or not caused directly by CsrA. If CsrA were in fact causing increased transcription (or transcript stability) of *crp*, then addition of cAMP in those conditions would lead to a higher luminescence output, which was not observed in this experiment.

Conclusions

By analyzing luminescence expression in various *V. fischeri* mutant backgrounds expressing different levels of *csrA*, we have demonstrated that CsrA increases the amount of *luxR* transcript in the cell, which in turn elevates luminescence output. The mechanism by which this occurs is not yet known, but our results indicate that CsrA does not act on any of the known quorum-sensing network components upstream of *luxR*, nor does it influence the level of *crp* transcription or adenylate cyclase activity (Fig. 4.8). There does appear to be a CsrA-mediated effect on ArcA activity, which could occur by indirectly repressing transcription of *arcA* or *arcB*, directly binding the *arcA* or *arcB* transcript, or affecting the phosphorylation state of ArcA. It is unclear whether the increase in *luxR* transcript levels caused by CsrA is mediated solely through ArcA, or if there are additional regulatory inputs that have not yet been identified.

The ability of CsrA to increase *luxR* transcription is independent of LitR, but dependent on AinS. An *ainS* mutation results in lower LitR levels in the cell, which would mimic a *litR* mutation, but more importantly, an *ainS* mutant fails to produce the C8-HSL autoinducer that is important in the initial activation of the luminescence response. Although overexpression of CsrA in a Δ*litR* strain of *V. fischeri* restored wild-

type levels of luminescence, its overexpression in an *ainS* mutant had no effect (i.e. the dark phenotype was observed). Without C8-HSL, LuxR cannot increase the expression of the *lux* operon, nor autoregulate its own transcription. This leads to a very low level of C6-HSL production, which is not sufficient to induce the *lux* operon. Even with the addition of exogenous C6-HSL, the level of luminescence in an *ainS* mutant remains low, most likely because of the very low levels of *luxR* transcription as a result of the lack of LitR activation as well as the lack of C8-HSL.

These results indicate that there is some degree of CsrA-mediated regulation of the quorum-sensing system of *V. fischeri*. The fact that the only phenotype generated by altered CsrA levels occurs in a Δ*litR* strain indicates that the regulation may occur prior to activation of the quorum-sensing network, and that it may be important in generating an increase in *luxR* levels that is independent of the quorum-sensing regulatory pathway. This could occur in response to certain environmental cues or metabolic changes, and could be an important factor in the timing of the quorum-sensing response in relation to metabolic state. In physiological context, CsrA is most active when cells are in exponential growth phase, and its levels become lower as the cell enters into late log and early stationary phase. The opposite is true of the quorum-sensing system, which becomes increasingly active as the cells transition from exponential growth to a high cell density stationary phase. This again indicates that the interactions between these two regulatory networks may be important in determining when the quorum-sensing system begins to become induced.

Acknowledgements

We would like to thank Eric Stabb for providing the *arcA* mutant strains used in this study, and for his helpful comments and suggestions. We would also like to thank Edward Ruby and Cheryl Whistler for providing the *ainS*, *luxO*, and *ainS-luxO* mutants used in the study. We thank Andre Levchenko and Rahul Kulkarni for their support of this work. This work has been funded by NIH R01 GM066786, NSF IGERT DGE-0504196 and the Institute for Critical Technology and Applied Science at Virginia Tech.

Materials and methods

Strains and growth conditions

Strains of *E. coli* were grown with aeration at 37°C in Luria-Bertani broth (5 g NaCl, 10 g tryptone, 5 g yeast extract per liter), unless otherwise indicated. Strains of *V. fischeri* were grown with aeration at 30°C in RMS minimal medium (2% casamino acids, 1X M9 salts [128 g $Na_2HPO_4*7H_2O$, 30 g KH_2PO_4, 5 g NaCl, 10 g NH_4Cl per liter for 10X stock], 0.4% carbon source, 0.1% $MgCl_2$, 15 g NaCl per liter) with glucose as the main carbon source, unless otherwise indicated. Ampicillin and/or kanamycin were added to the medium at concentrations of 100 μg/ml and 50 μg/ml respectively, when necessary. cAMP was added to the medium at 5 mM where specified.

DNA manipulation

Standard molecular biology techniques for DNA cloning and manipulation were used for all cloning steps. PCR purification, gel extraction, and plasmid miniprep kits were obtained from Qiagen.

Creation of CsrA and CsrB1 overexpression plasmids for use in *V. fischeri*

In order to increase CsrA levels in *V. fischeri*, the P_{tac}-*csrA* expression cassette from plasmid pKK223-3-CsrA (12) was removed via an *Eco*RI-*Bam*HI restriction digest, and the single-stranded overhangs generated by the digestion were enzymatically removed via T4 DNA polymerase, leaving blunt ends. The plasmid pVSV104, which is stably maintained in *V. fischeri* was digested with *Hpa*I, and treated with CIP to generated a blunt-ended linear fragment lacking 5' phosphates in order to prevent self-ligation in subsequent cloning steps. The P_{tac}-*csrA* expression cassette fragment was then ligated with the *Hpa*I-digested pVSV104 vector with T4 DNA ligase, to create pJW3. In order to decrease CsrA levels in *V. fischeri*, the P_{tac}-*csrB1* expression cassette from pKK223-3-*csrB1* (12) was PCR amplified with Deep Vent DNA polymerase using the following primers:

PtacUP1 5' GGTACCGGAGCTTATCGACTGCACG 3' and PstcsrB1right 5' GTTCTGCAGAAAAACCCCACCAAGCTCTC 3'. Adenine was added to the end of the PCR product using *Taq* polymerase, and it was then ligated into the pGEM-T TA-cloning vector using T4 DNA ligase. The ligation product was used to transform *E. coli* Top10. The P_{tac}-*csrB1* expression cassette was then removed from pGEM via *Sal*I-*Sph*I digestion, and ligated into pVSV104 which had be digested in the same way to create pJW4. pJW3 or pJW4 were used to transform *E. coli* DH5αλ*pir* via heat shock transformation. pJW3 or pJW4 were introduced into *V. fischeri* ES114, or various mutant strains of ES114 via tri-parental conjugation using the helper strain *E. coli* (pEVS104) (19).

Factorial design and statistical analyses

The experiments reported in this paper are summarized in Table AIII.1 and AIII.2. Note that the experiment measuring the effect of CsrA levels in a *litR*- strain versus wild-type, which corresponds to the data presented in Figure 4.2, was repeated within the experiment whose data is depicted in Figure 4.7. Because of this, only the factorial design for the data shown in Figure 4.7 is listed as experiment number two. The measured response was the specific luminescence (RLU/OD) in these experiments. The factors (two levels of the factors) in the first experiment were *ainS* (categorical: off and on), *luxO* (categorical: off and on), CsrA (categorical: normal expression (NE) and overexpression (OE)), and exogenous C6 autoinducer (numerical: 20 and 100 nM). There are two levels of autoinducer and two replications for each of the 8 categorical treatments (the statistical term for the factor settings such as [AI], mutant versus wild-type gene, or CsrA expression level for a given experiment) giving a total of 32 treatments for this experiment. The treatments are done in random order to minimize systematic error from uncontrolled factors such as drift in measurement instruments.

The factors (two levels of the factors) in the second experiment were *litR* (categorical: off and on), *arcA* (categorical: off and on), CsrA (numerical: underexpression (UE) and overexpression (OE)), exogenous cAMP (numerical: 0 and 5 mM) and exogenous C6 autoinducer (numerical: 20 and 100 nM). There are two levels of cAMP, two levels of autoinducer and two replications for each of the listed 8 categorical treatments giving a total of 64 factorial treatments. In this experiment we added treatments with the levels of the numerical factors midway between their low and high values (normal expression of CsrA, concentration of cAMP = 2.5 mM and

concentration of autoinducer = 60 nM). These midpoints were replicated four times for each of the 4 categorical treatments giving 16 center points and a total of 80 treatments. These 80 treatments were split into two blocks of 40 treatments each. The treatments within blocks were done in random order.

The 32 measurements from experiment 1 were analyzed by analysis of variance (ANOVA) and the results are given in Table AIII.3. The mean square variability from all contributions other than residual error (model mean square) is significantly larger than the residual mean square ($F = 123.05$, p-value < 0.0001) and, therefore, we infer that there are contributions to the total sum of squares than cannot be attributed to random variability. The 31 degrees of freedom (df) are broken down into 16 pure error df and 15 model df. The model df are broken down into main effects (4 df), second order interactions (6 df), third order interactions (4 df) and a fourth order interaction (1 df). Of these terms, only the main effects of *ainS* (p-value < 0.0001), *luxO* (p-value < 0.0001) and autoinducer (p-value $= 0.0001$) plus the second order interaction of *ainS* and *luxO* ($p > 0.0001$) are statistically significant. The second order interactions of CsrA expression with *ainS* and *luxO* are not statistically significant (p-values = 0.464 and 0.491, respectively).

The results of ANOVA for the 80 measurements from experiment 2 are given in Table AIII.4. The mean square variability from all contributions other than residual error (model mean square) is significantly larger than the residual mean square ($F = 81.73$, p-value < 0.0001) and, therefore, we infer that there are contributions to the total sum of squares that cannot be attributed to random variability. The 79 degrees of freedom are broken down into 63 factorial df and 16 center point df. The 63 factorial df break down

into 32 error df and 31 model df. The model df are broken down into main effects (5 df), second order interactions (10 df), third order interactions (10 df), fourth order interactions (5 df) and fifth order interactions (1 df). The statistically significant model terms are the main effects of *arcA* (p-value < 0.0001), expression of CsrA (p-value < 0.015), autoinducer (p-value < 0.0001) and cAMP (p-value < 0.0001); plus the second order interactions of *litR* and *arcA* (p-value < 0.0001), *litR* and cAMP (p-value = 0.0051), *litR* and expression of CsrA (p-value < 0.001), *arcA* and cAMP (p-value = 0.0013) and *arcA* and expression of CsrA (p-value < 0.001); plus the third order interaction of *litR*, *arcA* and expression of CsrA. Note that the second order interaction between cAMP and expression of CsrA (p-value = 0.1774) is not statistically significant.

After identifying the statistically significant model terms in an experiment, the model is fit to the experimental data by multivariable regression. The residuals are then computed between the model and terms not used in the model and terms from the center points. The mean squares of these residuals are compared to the pure error mean square by an F-test to obtain the "curvature" and the "lack of fit". If the model fit is good, then both curvature and lack of fit will not be significant (p-value > 0.05). We see that in both experiment 1 (Table AIII.3) and 2 (Table AIII.4), the lack of fit is not significant. The curvature is not significant in experiment 2.

The column data in Figures 4.1, 4.2, 4.6, and 4.7 are obtained from the model fits to the data. The error bars (95% confidence intervals) are proportional to the square root of the residual errors listed in the ANOVA tables.

Assays for *V. fischeri* luminescence

V. fischeri strains were grown to an $OD_{600\ nm}$ of 0.6. Once this OD was reached, 200 μl samples were taken and added in triplicate to a white 96-well microtiter plate for luminescence readings. Data was collected on a Beckman-Coulter LD400 luminometer, with an integration time of 1 sec per well, and with the photometer wavelength set to 492 nm. Luminescence data is shown as the square root of RLU/OD in order to normalize error as part of the statistical methods used in this study.

Quantitative RT-PCR analysis

V. fischeri was grown and luminescence was measured as stated above, and 500 μl cell samples were collected. 1 ml of Qiagen RNAprotect Bacteria Reagent was added to each sample to stabilize the RNA. Samples were vortexed and incubated at room temperature for 5 minutes, and then centrifuged for 10 minutes at 5000 x g. The supernatant was discarded, and the stabilized cell pellets were stored at -70°C. Total RNA was extracted using a Qiagen RNeasy mini kit according to the manufacturer's directions, and stored at -70°C. RNA was then analyzed for integrity and concentration at the Virginia Bioinformatics Institute core lab facility using a Biorad Bioanalyzer, and converted to cDNA using a High-Capacity cDNA Reverse Transcription Kit (Applied Biosystems, Foster City, CA). The cDNA samples were stored at -20°C until they were used as templates in an Applied Biosystems 7300 Real-Time PCR system. The primers used in the analysis of *luxR*, *crp*, *csrA*, and the *V. fischeri* 16S rRNA transcript are listed in Table 4.2. 50 ng of cDNA was used as template for the RT-PCR reaction, with primer concentrations of 250 μM. 2x SYBR Green master mix (Applied Biosystems) and dH_2O

were added to a final reaction volume of 50 μl/well in a MicroAmp Optical 96-well reaction plate (Applied Biosystems). The thermal cycler settings were programmed for 52°C for 2 min., 95°C for 10 min., then 45 cycles of the following: 95°C for 15s, 51°C for 15s, and 60°C for 1 min. which was also set as the data collection point. Two independent samples were analyzed in triplicate. 16S rRNA was analyzed in the same manner and used as in internal control.

References

1. **Baker, C. S., I. Morozov, K. Suzuki, T. Romeo, and P. Babitzke.** 2002. CsrA regulates glycogen biosynthesis by preventing translation of *glgC* in *Escherichia coli*. Mol Microbiol **44:**1599-610.
2. **Boettcher, K. J., and Ruby, E.G.** 1990. Depressed light emission by symbiotic *Vibrio fischeri* of the sepiloid squid *Euprymna scolopes*. J. Bacteriol. **172:**3701-3706.
3. **Bose, J. L., U. Kim, W. Bartkowski, R. P. Gunsalus, A. M. Overley, N. L. Lyell, K. L. Visick, and E. V. Stabb.** 2007. Bioluminescence in *Vibrio fischeri* is controlled by the redox-responsive regulator ArcA. Mol Microbiol **65:**538-53.
4. **Bose, J. L., C. S. Rosenberg, and E. V. Stabb.** 2008. Effects of *luxCDABEG* induction in *Vibrio fischeri*: enhancement of symbiotic colonization and conditional attenuation of growth in culture. Arch Microbiol **190:**169-83.
5. **Dunlap, P. V., Greenberg, E.P.** 1985. Control of *Vibrio fischeri* luminescence gene expression in *Escherichia coli* by cyclic AMP and cyclic AMP receptor protein. J. Bacteriol. **164:**45-50.
6. **Dunlap, P. V., Greenberg, E.P.** 1988. Control of *Vibrio fischeri lux* gene transcription by a cyclic AMP receptor protein-LuxR protein regulatory circuit. J. Bacteriol. **170:**4040-4046.
7. **Dunn, A. K., D. S. Millikan, D. M. Adin, J. L. Bose, and E. V. Stabb.** 2006. New *rfp*- and pES213-derived tools for analyzing symbiotic *Vibrio fischeri* reveal patterns of infection and *lux* expression *in situ*. Appl Environ Microbiol **72:**802-10.
8. **Engebrecht, J., Silverman, M.** 1984. Identification of genes and gene products necessary for bacterial bioluminescence. Proc. Natl. Acad. Sci., USA **81:**4154-4158.
9. **Fidopiastis, P., Miyamato, C., Jobling, M., Meighan, E., Ruby, G.** 2002. LitR, a new transcriptional activator in *Vibrio fischeri* regulates luminescence and symbiotic light organ colonization. Molec. Microbiol. **45:**131-143.
10. **Hanahan, D.** 1983. Studies on the transformation of *Escherichia coli* with plasmids. . J. Mol. Biol. **166:**557-580.
11. **Jones, M. K., E. B. Warner, and J. D. Oliver.** 2008. *csrA* inhibits the formation of biofilms by *Vibrio vulnificus*. Appl Environ Microbiol **74:**7064-6.
12. **Kulkarni, P. R., X. Cui, J. W. Williams, A. M. Stevens, and R. V. Kulkarni.** 2006. Prediction of CsrA-regulating small RNAs in bacteria and their experimental verification in *Vibrio fischeri*. Nucleic Acids Res **34:**3361-9.
13. **Lenz, D. H., M. B. Miller, J. Zhu, R. V. Kulkarni, and B. L. Bassler.** 2005. CsrA and three redundant small RNAs regulate quorum sensing in *Vibrio cholerae*. Mol Microbiol **58:**1186-202.
14. **Liu, M. Y., H. Yang, and T. Romeo.** 1995. The product of the pleiotropic *Escherichia coli* gene *csrA* modulates glycogen biosynthesis via effects on mRNA stability. J Bacteriol **177:**2663-72.

15. **Lupp, C., M. Urbanowski, E. P. Greenberg, and E. G. Ruby.** 2003. The *Vibrio fischeri* quorum-sensing systems *ain* and *lux* sequentially induce luminescence gene expression and are important for persistence in the squid host. Mol Microbiol **50:**319-31.
16. **Romeo, T.** 1998. Global regulation by the small RNA-binding protein CsrA and the non-coding RNA molecule CsrB. Mol Microbiol **29:**1321-30.
17. **Shadel, G. S., and T. O. Baldwin.** 1992. Positive autoregulation of the *Vibrio fischeri luxR* gene. LuxR and autoinducer activate cAMP-catabolite gene activator protein complex-independent and -dependent *luxR* transcription. J Biol Chem **267:**7696-702.
18. **Shadel, G. S., Baldwin, T.O.** 1991. The *Vibrio fischeri* LuxR protein is capable of bidirectional stimulation of transcription and both positive and negative regulation of the *luxR* gene. J. Bacteriol. **173:**568-574.
19. **Stabb, E. V., and E. G. Ruby.** 2002. RP4-based plasmids for conjugation between *Escherichia coli* and members of the *Vibrionaceae*. Methods Enzymol **358:**413-26.
20. **Studer, S. V., M. J. Mandel, and E. G. Ruby.** 2008. AinS quorum sensing regulates the *Vibrio fischeri* acetate switch. J Bacteriol **190:**5915-23.
21. **Visick, K. L.** 2005. Layers of signaling in a bacterium-host association. J Bacteriol **187:**3603-6.
22. **Waters, C. M., and B. L. Bassler.** 2005. Quorum sensing: cell-to-cell communication in bacteria. Annu Rev Cell Dev Biol **21:**319-46.
23. **Williams, J. W., X. Cui, A. Levchenko, and A. M. Stevens.** 2008. Robust and sensitive control of a quorum-sensing circuit by two interlocked feedback loops. Mol Syst Biol **4:**234.

Table 4.1. Bacterial strains and plasmids used in this study

Strain	Relevant Description	Reference
V. fischeri		
ES114	Wild-type strain of *V. fischeri*	(2)
PMF8	ES114Δ*litR*, Km^r	(9)
CL21	ES114Δ*ainS*, Cm^r	(15)
CL42	ES114Δ*luxO*, Km^r	(15)
CL64	ES114Δ*ainS*-Δ*luxO*, Cm^r,Km^r	(15)
E. coli		
DH5αλ*pir*	F- endA1 *glnV44 thi-1 recA1 relA1 gyrA96 deoR nupG* Φ80*dlacZ*ΔM15 Δ(*lacZYA-argF*)U169, *hsdR17*(rK^- mK^+), λ*pir*	(10)
Top10	F- *mcrA* Δ(*mrr-hsdRMS-mcrBC*) φ80*lacZ*ΔM15 Δ*lacX74 nupG recA1 araD139* Δ(*ara-leu*)7697 *galE*15 *galK*16 rpsL(StrR) endA1 λ^-	(Invitrogen)
Plasmids:		
pVSV104	$R6K_\gamma$ *ori*, pES213 *ori*, RP4 *oriT*, Km^r *lacZα*-(SphI-AvrII-HpaI-SalI-NcoI-Kpn-SacI)	(7)
pEVS104	RP4-based conjugal helper plasmid	(19)
pGEM-T	Ap^r, *lacZ*-MCS, used in TA-cloning	(Promega)
pJW3	P_{tac}-*csrA* expression cassette from pKK223-3-CsrA cloned into pVSV104	This study
pJW4	P_{tac}-*csrB1* expression cassette from pKK223-3-CsrB1 clonged into pVSV104	This study

Table 4.2. Primers used in RT-PCR analysis

Primer Name	Sequence	Reference
RT-luxRF	5'TGGCAGCGGTTAGTTGTATTG3'	(23)
RT-luxRR	5'TAGCGTGGGCGAGTGAAG3'	(23)
RT-crpF	5'TTTCTTATTGATGGGTTTTGTCATTC3'	This study
RT-crpR	5'AACCCAATCTCCTTTCCAATAAAAT3'	This study
RT-Vf16SF	5'GGGTTAAGTCCCGCAACGA3'	This study
RT-Vf16SR	5'CCATTACGTGCTGGCAAACA3'	This study
RT-CsrAF	5'ATGCTAATTTTGACTCGCCGTGTAG3'	This study
RT-CsrAR	5'GGTGTACCTTTTTCCGCTTGAATGC3'	This study

A

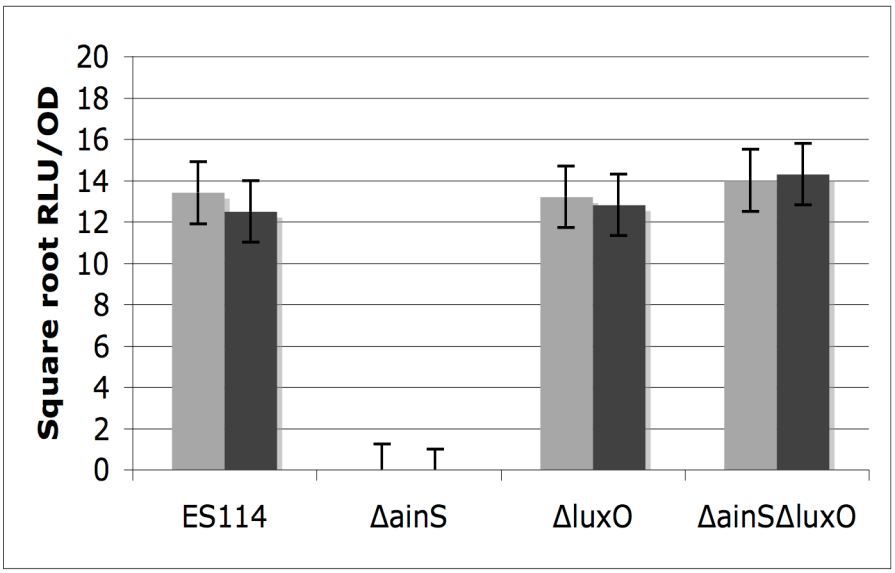

B

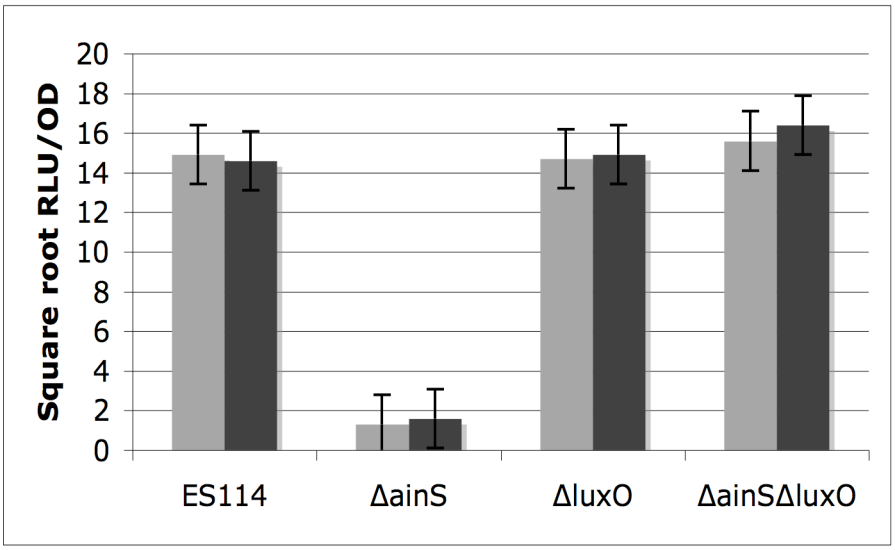

Figure 4.1. Luminescence expression in *V. fischeri* quorum-sensing network mutants with or without CsrA overexpression. When wild-type or mutant strain luminescence (light grey) is compared to its counterpart strain overexpressing CsrA (dark grey), no statistically significant difference in RLU/OD value is seen. This result is seen at both 20 nM AI (panel A) and 100 nM AI (panel B). Data are represented as the square root of RLU/OD. Error bars represent the 95% confidence interval for the mean value. Data was obtained as two independent samples with luminescence readings taken in triplicate.

A

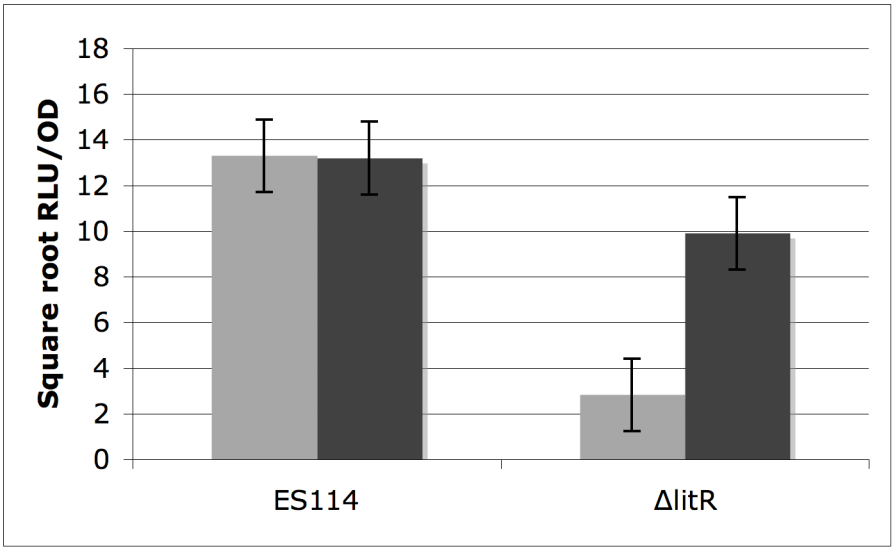

B

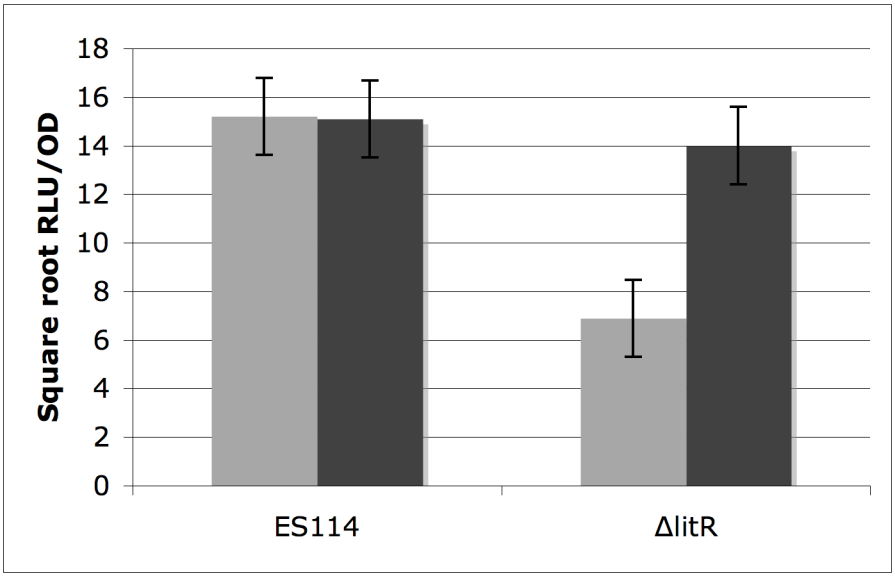

Figure 4.2. Comparison of luminescence values in *V. fischeri* ES114 and PMF8 (Δ*litR)* when CsrA levels are altered. When CsrA level is changed from underexpression (light grey) to overexpression (dark grey) in 20 nM (A) or 100 nM (B) AI, there is a significant increase seen in a Δ*litR* strain that is not seen in ES114. Data is represented as the square root of RLU/OD. Error bars represent the 95% confidence interval for the mean value. Data was obtained as two independent samples with luminescence readings taken in triplicate.

A

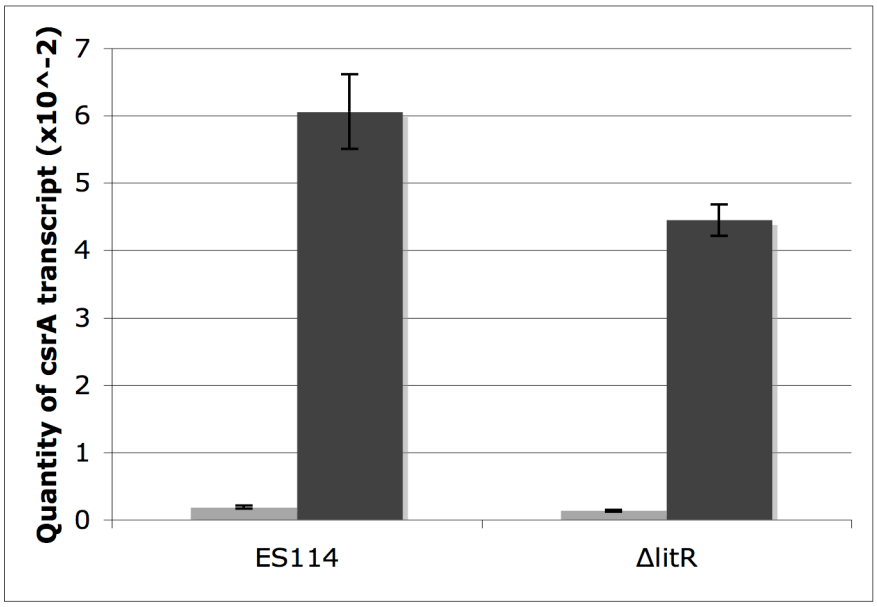

B

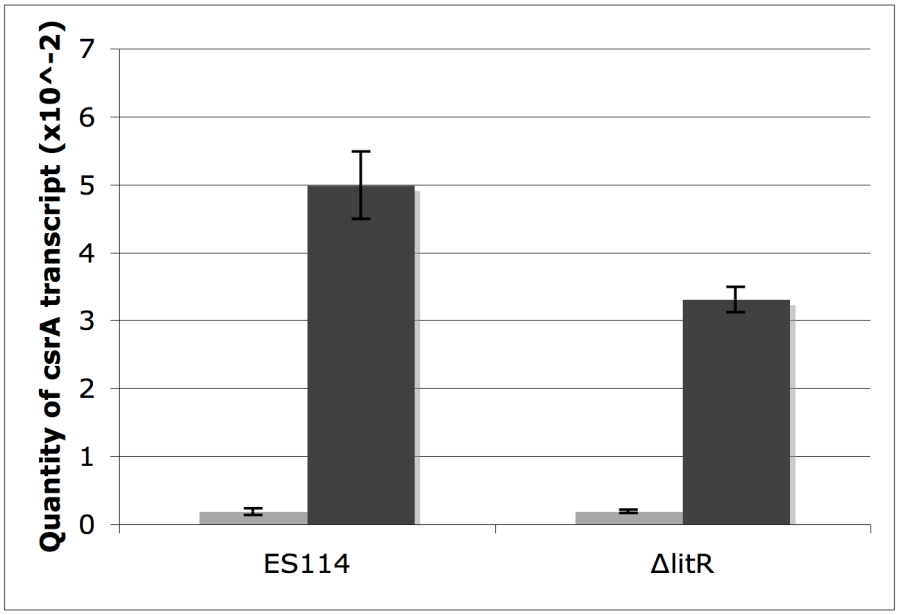

Figure 4.3. **Quantitative RT-PCR analysis of *csrA* transcript**. When *csrA* level is changed from underexpression (light grey) to overexpression (dark grey) in the indicated strains, there is a significantly higher amount of *csrA* transcript generated, which is demonstrated at both 20 nM AI (panel A) and 100 nM AI (panel B). Data was obtained from two independent triplicate sets, and *csrA* transcript was normalized relative to the 16S rRNA transcript data as an internal control. Error bars represent the standard deviation from the mean.

A

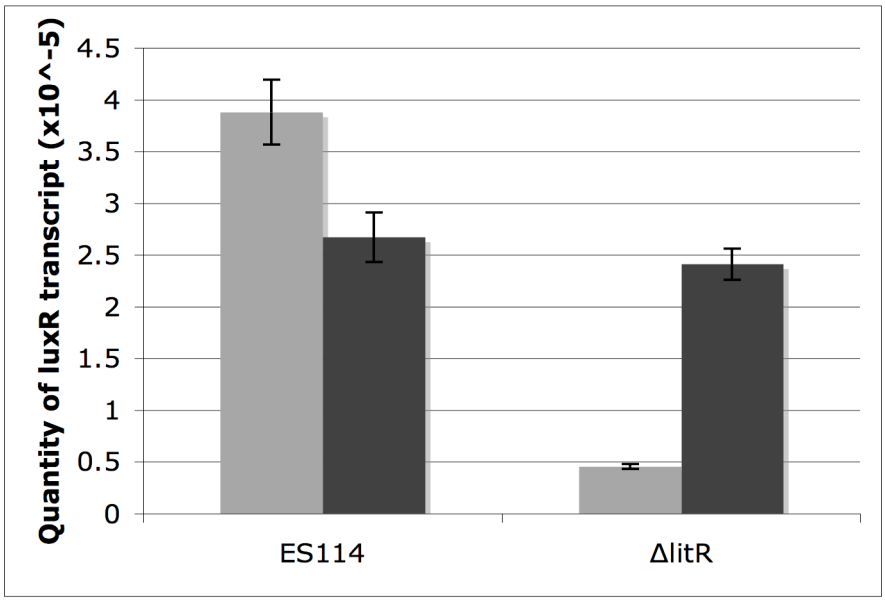

B

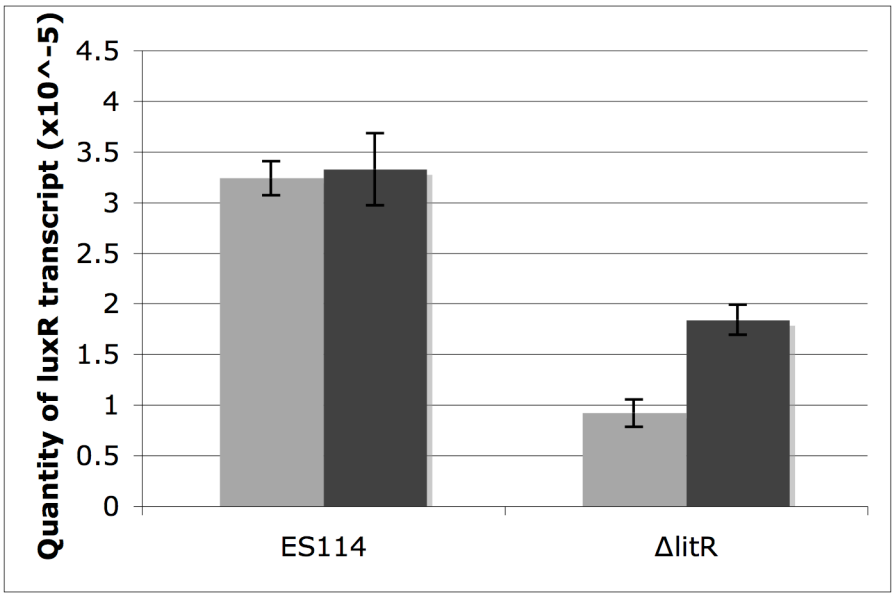

Figure 4.4. **Quantitative RT-PCR analysis of *luxR* transcript**. As *csrA* level is changed from underexpression (light grey) to overexpression (dark grey) the amount of *luxR* transcript increases in a Δ*litR* strain. In ES114, there is a decrease in the number of *luxR* transcripts as *csrA* expression increases at 20 nM AI (panel A) that is not apparent at 100 nM AI (panel B). Data was obtained from two independent triplicate sets, and *luxR* transcript was normalized relative to the 16S rRNA transcript data as an internal control. Error bars represent the standard deviation from the mean.

A

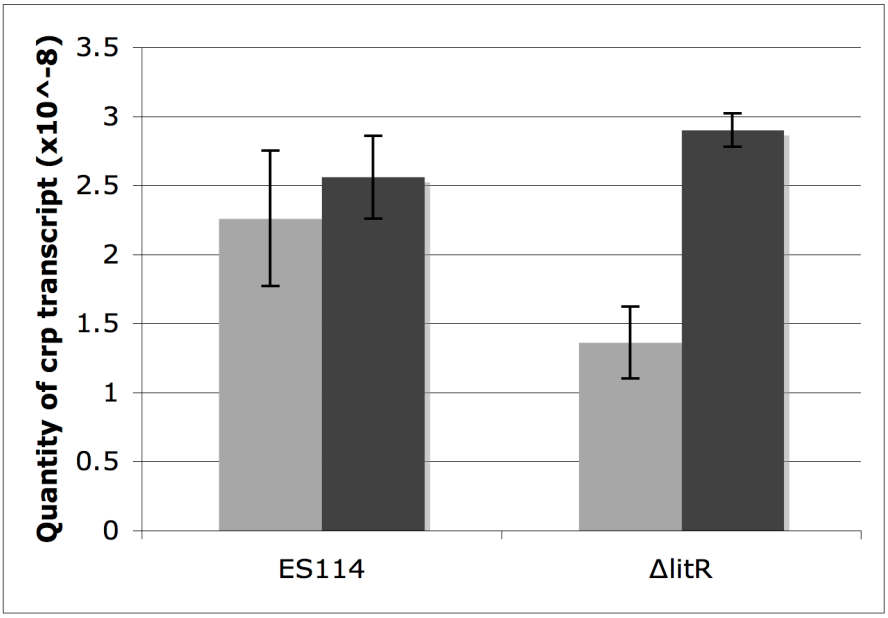

B

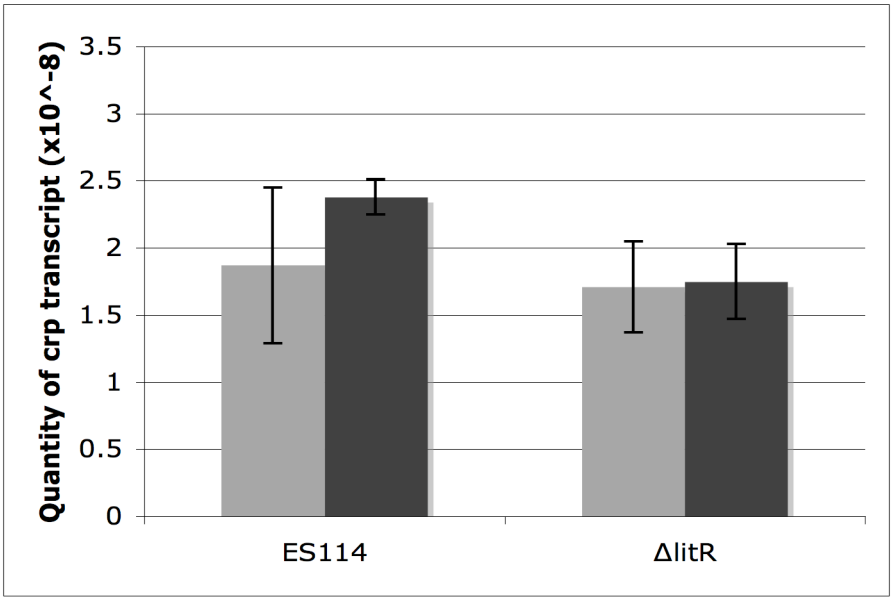

Figure 4.5. **Quantitative RT-PCR analysis of *crp* transcript**. As *csrA* level is changed from underexpression (light grey) to overexpression (dark grey) there is an increase in *crp* transcript at 20 nM AI (panel A), that is not apparent at 100 nM AI (panel B) for the Δ*litR* strain. There is no affect of altering *csrA* expression on ES114 in either [AI]. Data was obtained from two independent triplicate sets, and *crp* transcript was normalized relative to the 16S rRNA transcript data as an internal control. Error bars represent the standard deviation from the mean.

A

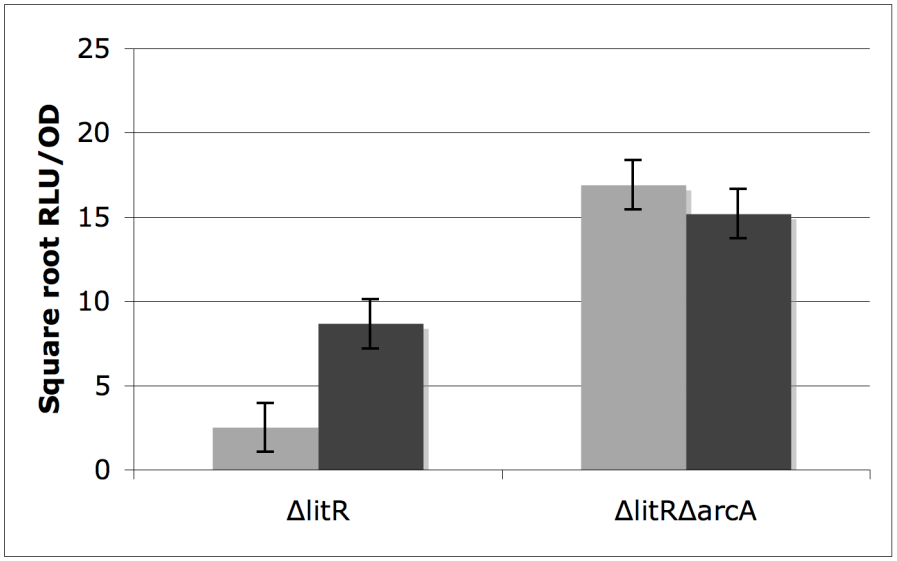

B

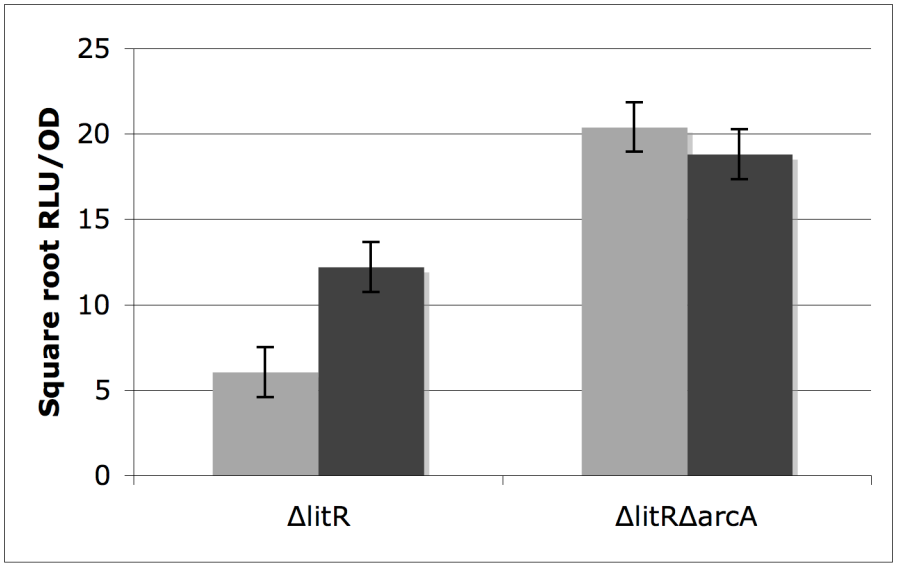

Figure 4.6. Deletion of *arcA* in a Δ*litR* background of *V. fischeri* abolishes the CsrA-dependent increase in luminescence seen in a Δ*litR* single mutant. *V. fischeri* PMF8 (Δ*litR*) exhibits an increase in luminescence that occurs when CsrA level is changed from underexpression (light grey) to overexpression (dark grey), whereas *V. fischeri* JB21 (Δ*litR*-*arcA*) shows no statistically significant change in luminescence as CsrA levels change. The effect is the same at [AI] of 20 nM (A) or 100 nM (B). Data is represented as the square root of RLU/OD. Error bars represent the 95% confidence interval for the mean value. Data was obtained as two independent samples with luminescence readings taken in triplicate.

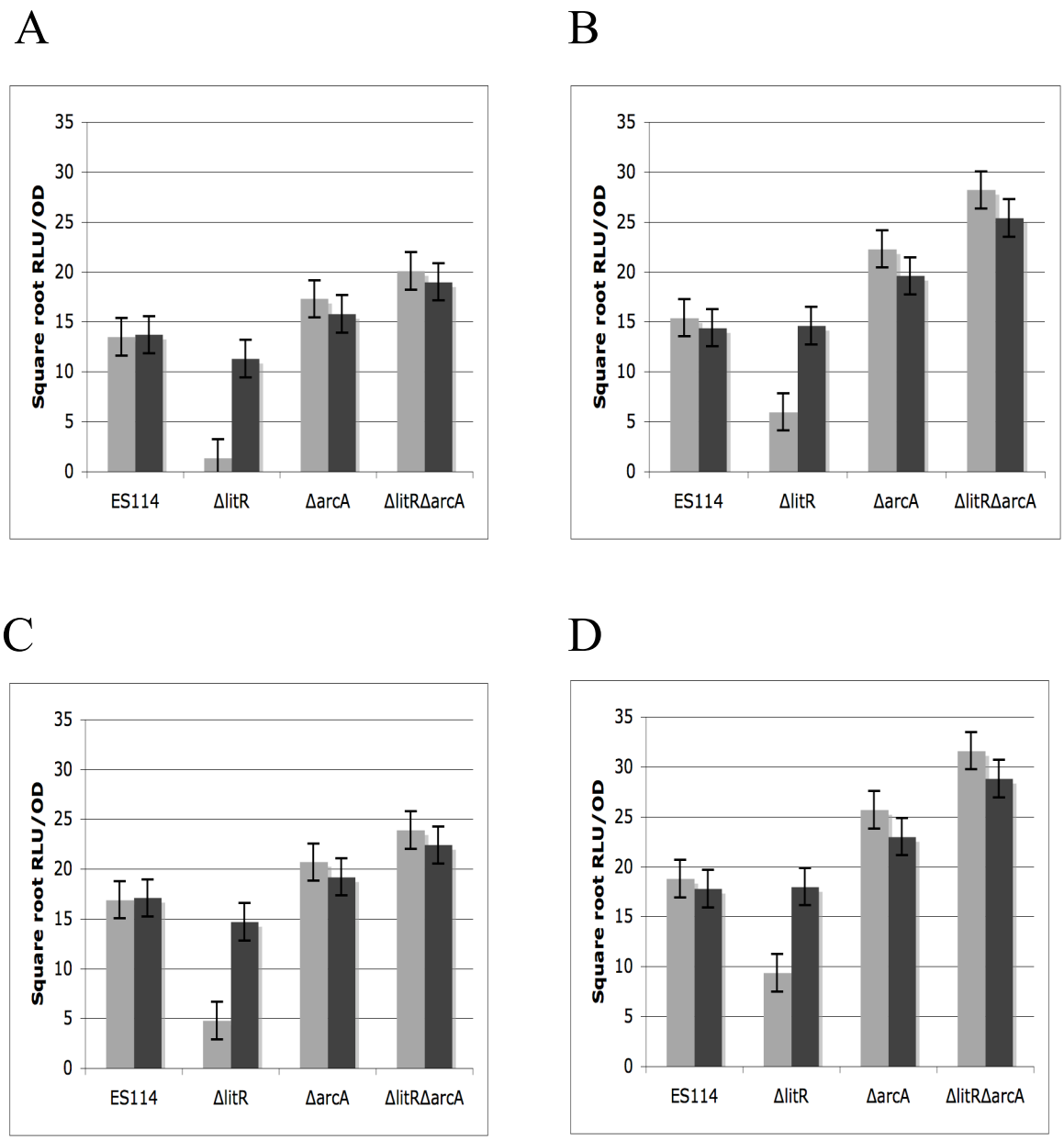

Figure 4.7. Effects of cAMP addition on luminescence values in *V. fischeri* ES114, PMF8, AMJ2, and JB21 expressing different levels of *csrA*. cAMP at wild-type (panels A and C) or added at 5 mM (panels B and D) concentrations to cells either underexpressing (light grey) or overexpressing (dark grey) *csrA*. This was performed when exogenous AI was supplied at 20 nM (panels A and B) or 100 nM (panels C and D). Data is represented as the square root of RLU/OD. Error bars represent the 95% confidence interval for the mean value. Data was obtained as two independent samples with luminescence readings taken in triplicate.

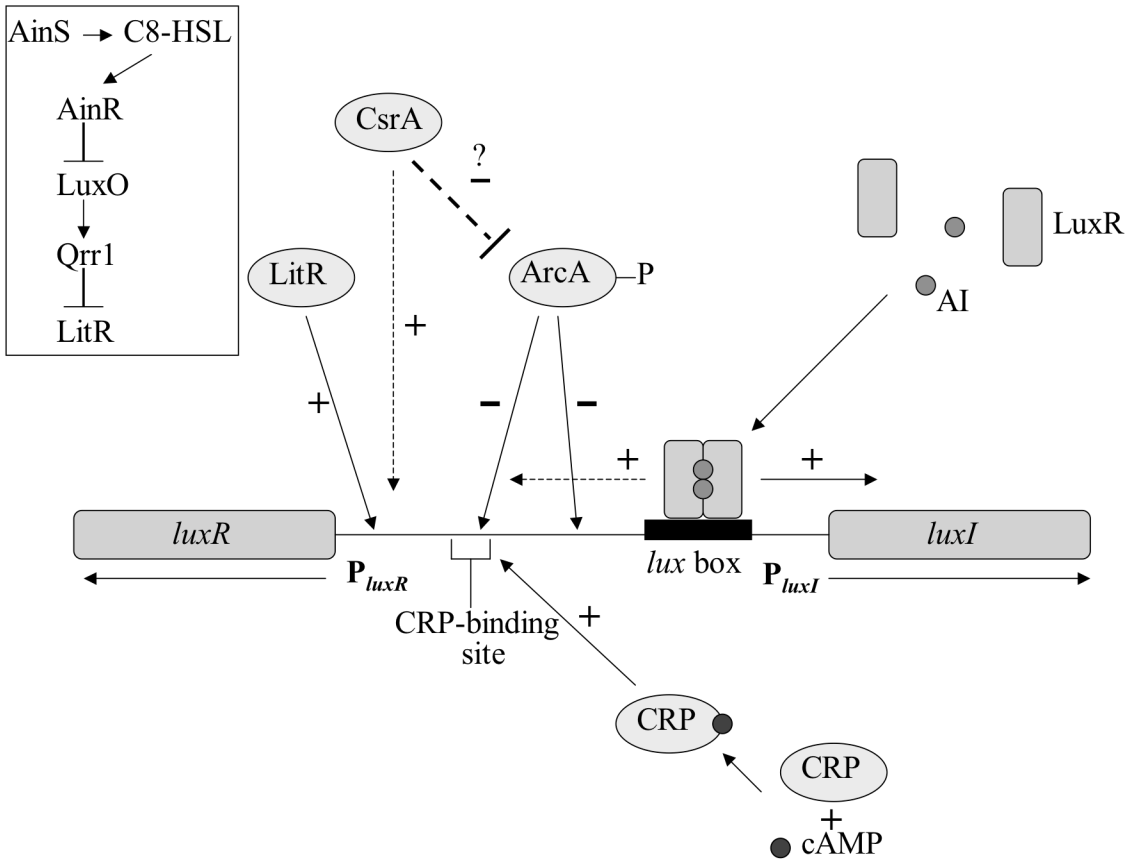

Figure 4.8. Regulatory components from multiple pathways and their influence on *luxR* transcription. Diagram indicates both positive (+) and negative regulators (-) of *luxR* expression, and their relative binding positions in the intergenic region between *luxR* and *luxI*. Note that there are two ArcA binding sites, one of which partially overlaps the proposed CRP-binding site. Dashed arrows indicate that the exact mechanism of action is still unknown. The upstream quorum-sensing regulatory pathway that governs *litR* expression is shown schematically in a box in the upper left corner. See (21) for more details on this pathway.

Chapter 5

Overall conclusions

Hysteresis and bistability in the quorum-sensing response

It has been known for decades that LuxR is the regulator of the quorum-sensing response in *Vibrio fischeri*, and that many other bacterial species that utilize quorum-sensing systems have LuxR homologs that function much in the same manner. Much of the work on understanding quorum-sensing has focused on how the system becomes induced. One goal of this thesis research was to establish how the dynamic process of induction is maintained during signal fluctuation, and how the system returns to a basal state once inducing conditions are no longer present.

LuxR positive transcriptional autoregulation has been demonstrated by past work, but has been largely ignored in mathematical modeling efforts that describe the quorum-sensing response. Our combined modeling and experimental efforts have now shown that LuxR positive autoregulation is critical in maintaining a robust quorum-sensing response that can be stably maintained during fluctuation and loss of AI from the surrounding environment, once the system reaches a critical threshold of AI. This mechanism leads to increased transcription of *luxR* as [AI] increases, such that the system becomes more sensitive to increasing AI, and thus induction is accelerated. However, once full induction is achieved, the system is less sensitive to loss of AI, due to the fact that there is much more LuxR present to respond to less AI. This increase in LuxR levels at high [AI] creates a hysteretic response, and a bistable system that requires a significant dilution of extracellular AI in order to return to the basal state of expression.

The history-dependent quorum-sensing response also creates two distinct sub-populations of cells that may be important in overall fitness of the cell population, much as persister cells are important in a biofilm. By maintaining a small subset of the cell

population at a low, or non-induced state, while the majority of the cells emit bioluminescence, the population may be better adapted to changing conditions. When the squid host vents its culture of *V. fischeri* into the ocean, the portion of the population that has been in a high induction state, which contains significant amounts of the quorum-sensing regulatory proteins and bioluminescence enzymes, will take longer to adapt to the less favorable conditions of the open ocean than the cells which were in a non-induced state, and thus may not survive as well. Also, the portion of the population remaining in the squid that was in the lower state of induction may be better suited to rapidly re-populate the light organ due to their lower energy demands.

Discovery of CsrA-regulating sRNAs in *V. fischeri*

Many Gram-negative proteobacteria are known to encode a functional CsrA which is important in regulating metabolic processes involved in secondary metabolism and the transition to stationary phase. In *E. coli*, CsrA is known to be regulated by multiple sRNAs, which are not easily identified in other species by typical BLAST searches of the genome. By using combined bioinformatic and experimental approaches, we have identified and characterized two CsrA-regulating sRNAs in *V. fischeri*, named CsrB1 and CsrB2. Using northern blotting and transcriptional β-galactosidase fusions, we have established that these sRNAs are expressed at similar levels in the cell, and are very similar in size (predicted to have only a 4 bp difference). By expressing *V. fischeri* CsrA, CsrB1, and CsrB2 in recombinant *E. coli*, we have shown that they function in a similar manner as what has been demonstrated in *E. coli*, and that the system is highly conserved between species of Gram-negative proteobacteria. This work establishes a useful search tool that can be used to locate these sRNAs in many other species in which

they have not yet been identified, as well as experimental methods to determine whether they are functional.

Connections between the CsrA and quorum-sensing pathways

A connection between the CsrA and quorum-sensing pathways has been demonstrated in *V. fischeri* using an experimental approach grounded in statistical analysis of variance. The method has allowed us to determine with greater confidence than traditional experimental methods that CsrA causes an increase in *luxR* transcription when the quorum-sensing regulatory protein LitR is absent. We have also demonstrated that CsrA does not influence any other known regulator of *luxR* expression, with the exception of ArcA. By examining the luminescence response in various quorum-sensing pathway mutants expressing elevated or depressed CsrA levels, we have established that no quorum-sensing component upstream of *luxR* is affected by CsrA, and that CsrA can restore wild-type levels of luminescence in a normally dark *litR* mutant.

It is important to note that LitR and LuxR regulate different behaviors, and are therefore potentially regulated in different ways, rather than a simple linear network as is commonly depicted. LitR is important for colonization of the squid host, while LuxR is more important later at high cell density once colonization has been established. CsrA may help to regulate at what point the luminescence system becomes active in relation to metabolic or redox state, by activating increasing *luxR* transcription in a LitR-independent manner.

The cAMP-CRP complex is both an important secondary metabolism regulator and *luxR* transcriptional activator, so it was surprising to see that CsrA had no effect on either *crp* transcript levels or adenylate cyclase activity. Although cAMP-CRP regulation

was a logical target, experiments demonstrated that CsrA did not impact its activity. This suggests that multiple metabolic cues could impact *luxR* regulation, because CsrA and cAMP-CRP can independently regulate *luxR* expression, thus allowing the response to be controlled by global regulatory networks in a coordinated manner.

Our results suggest that the increase in *luxR* transcription caused by CsrA is mediated through the redox-responsive regulator ArcA. Deletion of ArcA abolished the CsrA-dependent increase in *luxR* transcription, which indicated that CsrA in some way affects ArcA-mediated repression of the *lux* genes. The mechanism involved in this ArcA repression is not yet known, but CsrA may influence transcription rate or transcript stability of either *arcB* or *arcA*, as well as the phosphorylation state of ArcA. This effect could be mediated directly by CsrA, or indirectly through another protein that is affected by CsrA.

Future work

Understanding the mechanism by which CsrA causes an increase in *luxR* transcription will be a crucial goal for future work on this project. It is likely that this mechanism will be conserved in other species of *Vibrio*, and may also shed light on CsrA-based regulation in species that do not utilize quorum-sensing systems. Another important goal for future projects involving CsrA-regulation in *V. fischeri* will be to determine with better efficiency, the CsrA regulon. This could be attempted by performing *in vivo* RNA-pulldown assays (described in appendix II), and determining which RNAs co-purify with CsrA. This method will allow direct identification of CsrA-regulated transcripts, and will help establish the consensus binding site and other binding

requirements for CsrA in *V. fischeri*. This work will enhance efforts to generate computer search algorithms that can identify CsrA-regulated genes in multiple species.

Concluding remarks

The regulation of *luxR* expression in *V. fischeri* serves as a critical point for the integration of multiple regulatory system components. Redox state, metabolic state, and quorum-sensing pathways each play a role in governing when, and to what degree *luxR* is expressed. This is due to the fact that LuxR is the master regulator of the luminescence response, and also regulates other processes in the cell, which requires its production to be tightly and specifically controlled in order to exert the appropriate response to environmental conditions. Because many other quorum-sensing systems contain LuxR homologs, it is likely that they too act as key points of regulation in their corresponding species. Hopefully, the work presented in this thesis will demonstrate the importance of multiple levels of regulation on these LuxR homologs, and serve as an example of how mathematical modeling, statistical analysis, and experimental work can be combined to better understand complex regulatory networks.

Appendix I

Supplemental material for Chapter 2

(see text for details)

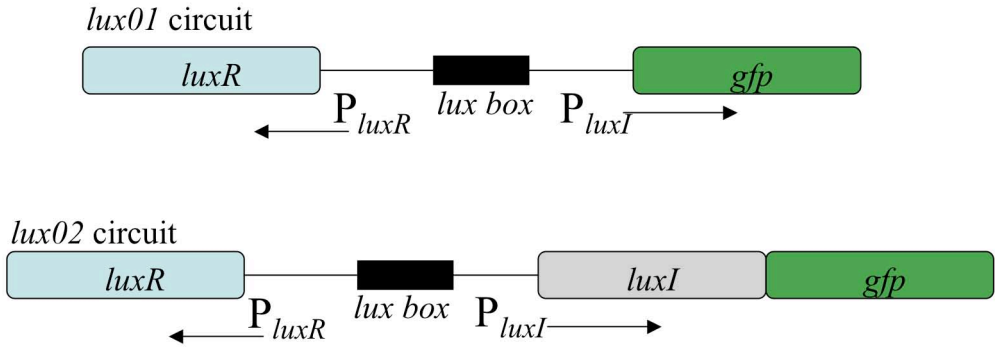

Figure AI.1: Diagram of the *lux01*and *lux02*genetic expression circuits. The *lux01* circuit contains *gfp* under transcriptional control of the *luxI* promoter, and *luxR* under control of its native promoter elements. The intergenic region is also native to *V. fischeri*, containing the *lux box* regulatory region necessary for transcriptional activation by the LuxR-AI complex. This circuit does not produce AI, and therefore transcription of *gfp* will only occur when AI is supplied exogenously. The *lux02* genetic circuit is identical to the *lux01* circuit, except that it contains *luxI,* which is the AI synthase gene, allowing *de novo* synthesis of AI.

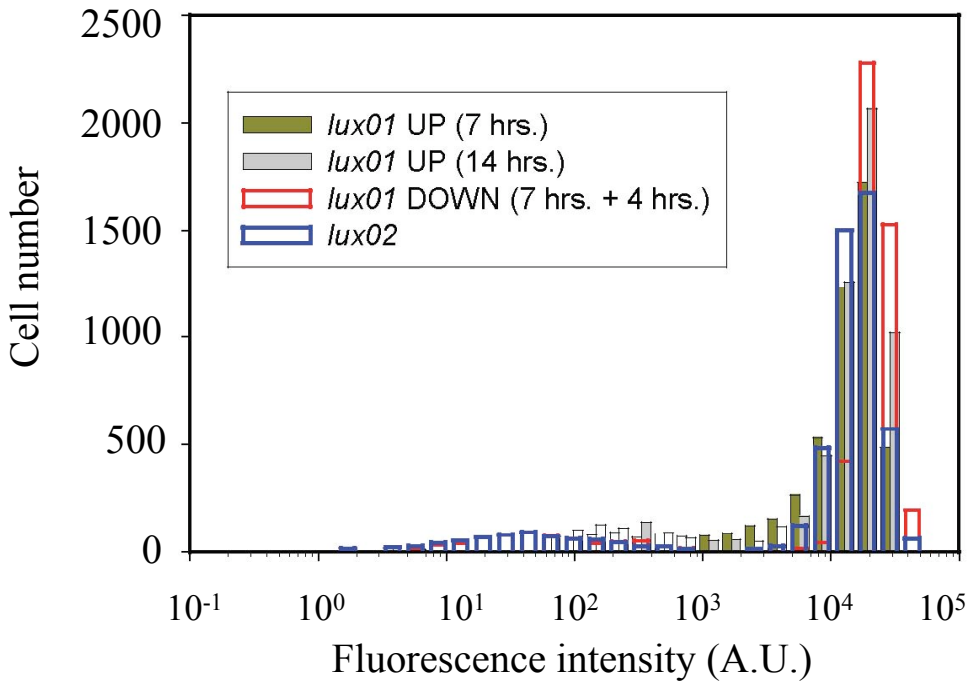

Figure AI.2: Comparison of maximum steady state Gfp expression of the *lux01*and *lux02*circuits over time. Cells were exposed to 100 nM AI for 7-14 hrs, then analyzed with flow cytometry to determine single cell expression levels. After 7 hrs, both the *lux01* circuit (green) and the *lux02* circuit (open blue) reached a maximum level of expression that did not increase significantly for up to a total induction period of 14 hrs (grey). When the *lux01* cells were diluted in fresh medium containing the same [AI] at the 7 hr time point, and analyzed for an additional 4 hrs (open red), there was no significant increase in fluorescence, showing that the maximum level of expression achieved at 7 hrs was not due to metabolic starvation.

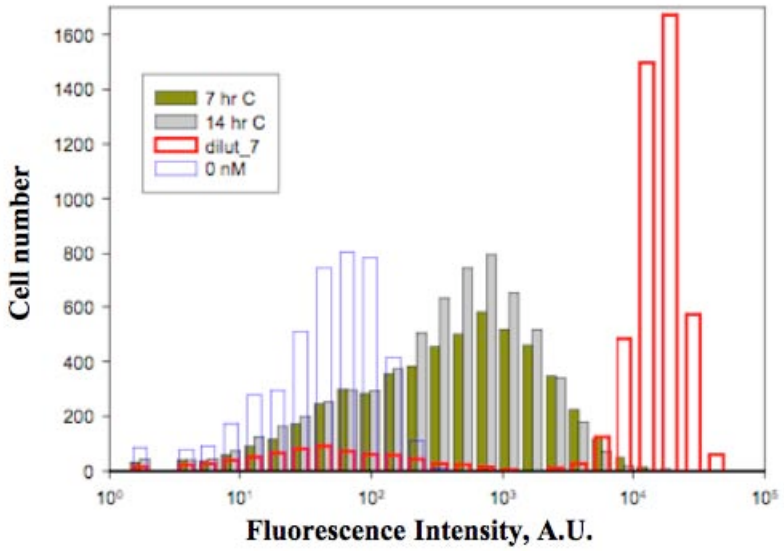

Figure AI.3: Flow cytometry analysis of the *lux01*circuit induced with 5 nM AI.
Cells expressing the *lux01* circuit were exposed to 5 nM AI for 7 hrs (green) or 14 hrs (grey). For comparison, cells in the uninduced state at 0 nM AI (open blue) are shown, as well as cells diluted to ~13 nM from maximum steady state induction of 100 nM (open red). 5 nM AI produces an intermediate level of fluorescence induction that falls between the lower and higher states of expression, and as AI is further increased, bimodality in this system becomes more apparent (see the following figures).

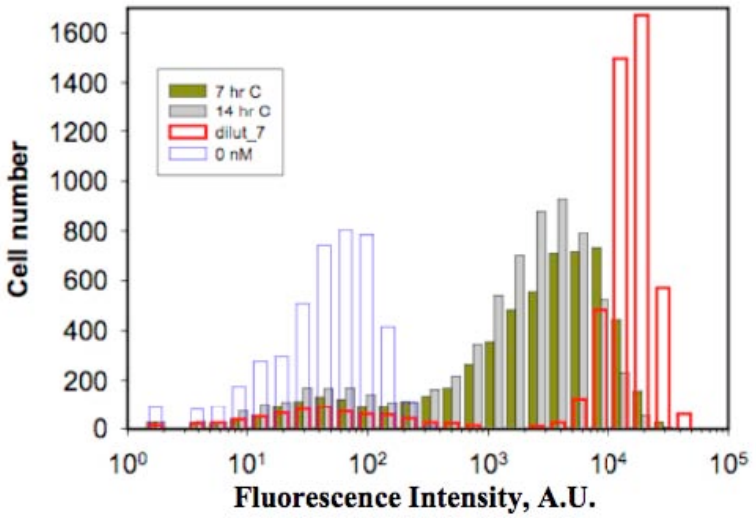

Figure AI.4: Flow cytometry analysis of the *lux01*circuit induced with 10 nM AI. Cells expressing the *lux01* circuit induced with 10 nM AI for 7 or 14 hrs (green and grey respectively) show a much more pronounced shift in cell populations toward a bimodal distribution. At this [AI], most cells are found in the higher steady state of expression, with a subset of the population remaining in the lower steady state corresponding to fluorescence values close to the uninduced level (open blue). Cells diluted from 100 nM to~13 nM AI are shown (open red) for comparison to demonstrate the hysteretic behavior of the system when approximately equal [AI]s are reached from different histories of induction.

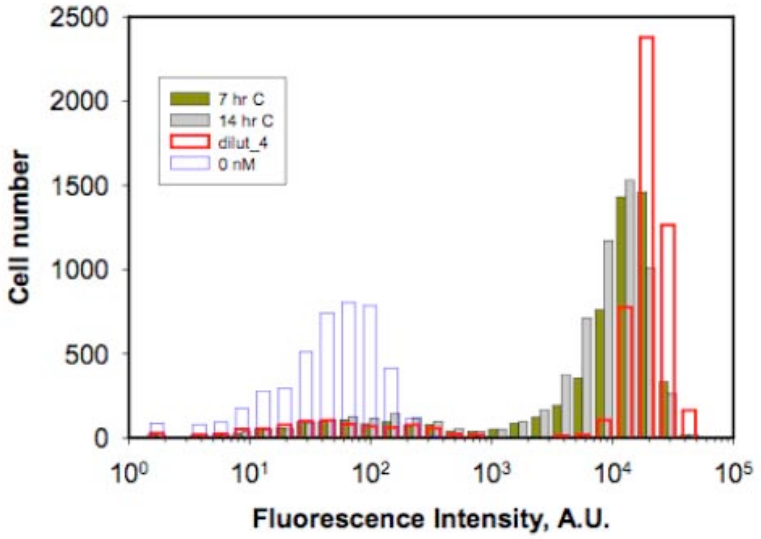

Figure AI.5: Flow cytometry analysis of the *lux01*circuit induced with 30 nM AI. Cells expressing the *lux01* circuit induced with 30 nM AI for 7 or 14 hrs (green and grey respectively) show lower levels of fluorescence intensity than cells diluted from 100 nM to ~31 nM AI (open red), indicating hysteresis in the system. Open blue bars indicate the uninduced response at 0 nM AI.

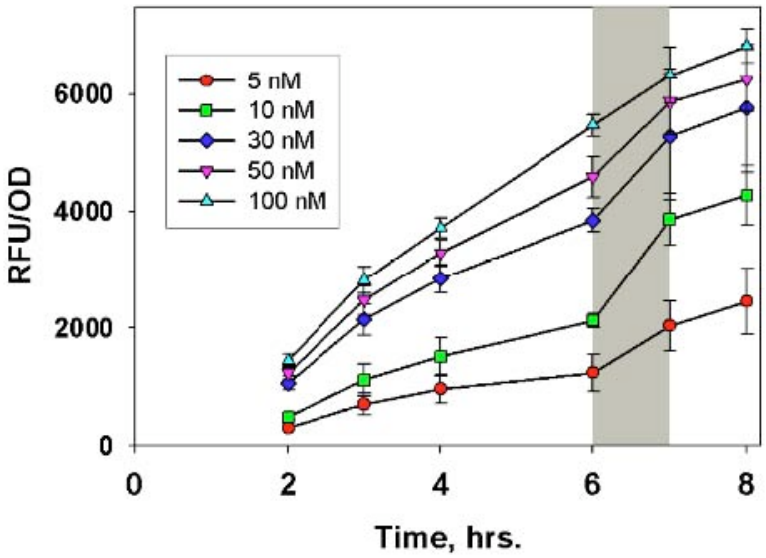

Figure AI.6: Induction of the *lux02* circuit to maximum steady state at different [AI]. Cells expressing the *lux02* circuit were induced up to 8 hrs at the indicated [AI], in order to determine the time necessary to reach maximum steady state Gfp expression. Steady state was reached after approximately 7 hrs exposure to AI, which corresponds to the same time necessary for the *lux01* circuit to reach maximum steady state. Error bars represent the standard deviation of two independent triplicate assays.

Appendix II

Unpublished methods for CsrA purification and RNA-pulldown assays

CsrA purification under native conditions

Cells of *Escherichia coli* (pKK223-3-CsrA) or *Vibrio fischeri* ES114 (pJW3) were grown in 1 L flasks containing LB (10 g tryptone, 5 g yeast extract, 5 g NaCl) or LBS (LB with an additional 15 g NaCl) medium, respectively. Cultures were incubated at 30°C with shaking at 250 r.p.m.

For purification of CsrA from *E. coli*, cultures were grown to an $OD_{600\ nm}$ of 0.2, then IPTG was added to a final concentration of 1 mM. Cells were incubated an additional four hours, and then harvested via centrifugation at 5000 x g for 20 min. For purification of CsrA from *V. fischeri*, the cells were grown to an $OD_{600\ nm}$ of 0.6 without IPTG induction, then harvested in the same manner. Cell pellets were resuspended in 10 ml of wash buffer (50 mM $NaPO_4$ (pH 6.0), 500 mM NaCl, 10% glycerol, 20 mM imidazole). Cells were then lysed using three cycles of a French press set at 15,000 psi.

The cell lysate was centrifuged at 10,000 x g at 4°C for 10 min. and the supernatant was removed, then subjected to ultra-centrifugation at 100,000 x g for 1 hour at 4°C. The supernatant fraction was then passed over a column containing 1 ml of Ni-NTA resin. 40 volumes of wash buffer were passed over the column to remove unbound or non-specifically bound protein. Next, three 1 ml washes were performed using wash buffer with an imidazole concentration of 50 mM, followed by one 1 ml of wash buffer containing 75 mM imidazole. The 6x-His-CsrA protein was then eluted from the column using wash buffer with 250 mM imidazole. Fractions collected during the purification process were analyzed via SDS-PAGE, and samples were stored in aliquots at -80°C.

Purification of RNAs co-purified during the *V. fischeri* CsrA purification protocol

Fractions from the protein purification containing pure CsrA protein isolated from *V. fischeri* (based on SDS-PAGE analysis) were used to isolate any RNA species that were bound to the protein via phenol extraction and ethanol precipitation. The sample was brought to a 200 µl volume with dH_2O, and then 200 µl of phenol/chloroform (pH 4.5) was added. The sample was mixed gently by inversion and placed in a 50°C water bath for 10 minutes, then centrifuged at 13,000 x g for 5 minutes. The top/aqueous layer was removed to a clean tube, and the extraction was repeated once more.

For ethanol precipitation of the nucleic acids obtained from the previous phenol extraction, the sample was brought to a volume of 200 µl, and 20 µl of 3M sodium acetate pH 5.2 was added and mixed. Next, 600 µl (3x volume) of 100% ethanol was added to the sample and mixed well by inversion. The sample was incubated at room temperature for 30-60 minutes and then centrifuged at 13,000 x g. for 15 minutes. The supernatant was discarded, and 800 µl of 70% ethanol was added to wash the pellet. The sample was then centrifuged at 13,000 x g or 10 minutes (sample must be placed into the centrifuge in the opposite orientation as previously so that the pellet travels through the ethanol). The supernatant was discarded, and the pellet was allowed to air dry, before being resuspended in 30-100 µl RNase-free dH_2O (amount of resuspension varies depending on how concentrated the sample needs to be).

Conversion of RNA to cDNA

RNA that was co-purified during the CsrA purification protocol, and subsequently isolated via phenol/chloroform extraction, was converted to cDNA using the applied biosystems High-Capacity Reverse Transcriptase kit, according to the manufacturer's

directions. In order to remove RNA that was bound to the 1st strand of the cDNA, RNaseH (NEB) was added according to the manufacturer's specifications, and the reaction was incubated at 37°C for two hours. The sample was then purified using a Qiagen PCR purification kit. For 2nd strand cDNA synthesis, the purified 1st strand was used as template and DNA polymerase (Klenow fragment, NEB) was added according to the manufacturer's recommendations. Because this reaction leaves blunt-ended products, adenine was subsequently added using *Taq* polymerase, and the product was purified using a Qiagen PCR purification kit. The double-stranded cDNA products were then ligated into the pGEM-T TA cloning vector (Promega), and used to transform *E. coli* Top10. Isolates containing an insert were chosen and the plasmid was purified using a Qiagen miniprep kit. Plasmid samples were then submitted for sequencing of the cDNA insert to the Virginia Bioinformatics Institute Core Laboratory.

Methods and rationale for *in vitro* CsrA-RNA binding assays

CsrA purification from *V. fischeri* is not as efficient as from *E. coli*, and has not yet been optimized so that pure CsrA protein can be isolated from other contaminants which also have interactions with RNA species, such as ribosomal protein subunits. In order to gain a higher concentration of pure *V. fischeri* CsrA, which can then be used for *in vitro* RNA-binding assays, the following methods have been in development and are proposed for future work.

CsrA should be purified from 1 L of *E. coli* (pKK223-3-CsrA) according to the previously stated methods. The major problem with purifying *V. fischeri* CsrA from a recombinant *E. coli* strain, is that the *V. fischeri* and *E. coli* Csr systems function similarly, and therefore, the *E. coli* Csr sRNAs that regulate CsrA will be co-purified

with the CsrA protein, as well as any *E. coli* genes that are regulated by CsrA. To address this problem, once the 1st round of CsrA purification has been completed, the protein must be incubated with RNase, in order to degrade any RNA species that were co-purified from *E. coli*. Once this RNase digestion reaction has been completed, the protein sample must be diluted in wash buffer containing 20 mM imidazole (see previous purification section for recipe). At this point, the protein, which should now be free of any RNA contaminants, should be re-purified using Ni-affinity chromatography as described previously. The column must be washed extensively in order to remove any RNase contamination prior to elution of CsrA. The elution fraction should be analyzed with SDS-PAGE, and fractions containing pure CsrA can be used for the *in vitro* binding assay.

Once *V. fischeri* CsrA has been purified from recombinant *E. coli*, and co-purified RNA species have been removed, the CsrA protein sample should be dialyzed against the binding reaction buffer (10 mM Tris-HCl, pH 7.5, 10 mM $MgCl_2$, 100 mM KCl, 7.5% glycerol, 20 mM dithiothreitol (DTT)). This buffer is a modified version of the binding reaction buffer used in RNA-mobility shift assays (1).

To obtain RNA for use in the binding assay, a culture of *V. fischeri* ES114 should be grown to an $OD_{600\ nm}$ of 0.6, and total RNA should be isolated according to the Qiagen RNeasy mini kit protocol. RNA should be used immediately in order to avoid degradation.

For the binding reaction, variable amounts of CsrA may be used for a set concentration of RNA. RNA should be denatured by heating to 85°C, and renatured by slow cooling to room temperature prior addition to the binding reaction buffer. RNase

inhibitor should also be added to the binding reaction buffer to prevent any degradation of the RNA sample. Once the desired concentration of CsrA has been added to the binding reaction, it should be incubated at 30°C for 30 minutes, then placed on ice.

Once the CsrA-RNA binding reaction has been performed, the reaction should be diluted in 10-15 ml of wash buffer containing 20 mM imidazole (see CsrA purification section for recipe). Once the protein binding reaction sample has been added to the Ni-NTA column, the column should be washed extensively (with at least 40 volumes of wash buffer) in order to remove any RNA that is not associated with CsrA. At this point the CsrA protein which has bound RNA from *V. fischeri* can be purified once more according to the previously described methods. Upon completion of this round of purification, the fraction containing pure CsrA should be used for RNA extraction, conversion to cDNA, and cloning into the pGEM-T sequencing vector as stated in the previous sections.

References:

1. **Weilbacher, T., Kazushi, S., Dubey, A.K., Wang, X., Gudapaty, S., Morozov, I., Baker, C.S., Georgellis, D., Babitzke, P., Romeo, T. 2003.** A novel sRNA component of the carbon storage regulatory system of *Escherichia coli*. Molec. Microbiol. **43**:657-670.

Appendix III

Supplemental material for Chapter 4

Table AIII.1 Factors and treatment levels for factorial design experiments

Experiment/factors	Low level[a,b]	High level[a,b]	Center level[b]
Experiment 1			
Factors:			
ainS	Off	On	
luxO	Off	On	
CsrA	NE	OE	
AI	20	100	
Experiment 2			
Factors:			
litR	Off	On	
arcA	Off	On	
CsrA	UE	OE	NE
cAMP (mM)	0	5	2.5
AI (nM)	20	100	60

[a] "off" = mutant strain for indicated gene, "on" = wild-type expression of indicated gene
[b] "OE" = overexpression, "UE" = underexpression, "NE" = wild-type expression

Table AIII.2. *V. fischeri* strains used in the factorial design experiments

Experiment 1				
Factors	*ainS*[a]	*luxO*[a]	CsrA[b]	Strain
Treatments				
1	Off	Off	OE	CL64 (pJW3)
2	Off	Off	NE	CL64
3	Off	On	OE	CL21 (pJW3)
4	Off	On	NE	CL21
5	On	Off	OE	CL42 (pJW3)
6	On	Off	NE	CL42
7	On	On	OE	ES114 (pJW3)
8	On	On	NE	ES114
Experiment 2				
Factors	*litR*[a]	*arcA*[a]	CsrA[b]	Strain
Treatments				
1	Off	Off	OE	JB21 (pJW3)
2	Off	Off	UE	JB21 (pJW4)
3	Off	On	OE	PMF8 (pJW3)
4	Off	On	UE	PMF8 (pJW4)
5	On	Off	OE	AMJ2 (pJW3)
6	On	Off	NE	AMJ2 (pJW4)
7	On	On	OE	ES114 (pJW3)
8	On	On	UE	ES114 (pJW4)

[a] "off" = mutant strain for indicated gene, "on" = wild-type expression of indicated gene
[b] "OE" = overexpression, "UE" = underexpression, "NE" = wild-type expression

Table AIII.3. ANOVA of results from experiment 1

ANOVA for selected factorial model

Analysis of variance table [Partial sum of squares - Type III]

	Sum of		Mean	F	p-value	
Source	Squares	df	Square	Value	Prob > F	
Block	0.05	1	0.05			
Model	1168.86	8	146.11	123.05	< 0.0001	significant
A-ainS	295.36	1	295.36	248.75	< 0.0001	
B-luxO	425.55	1	425.55	358.39	< 0.0001	
C-CsrA	0.00	1	0.00	0.00	0.9594	
E-C6	26.52	1	26.52	22.33	0.0001	
AB	419.58	1	419.58	353.37	< 0.0001	
AC	0.66	1	0.66	0.55	0.4645	
BC	0.58	1	0.58	0.49	0.4906	
CE	0.60	1	0.60	0.51	0.4841	
Residual	26.12	22	1.19			
Lack of Fit	3.91	6	0.65	0.47	0.8208	not significant
Pure Error	22.21	16	1.39			
Cor Total	1195.03	31				

Table AIII.4. ANOVA of results for experiment 2

ANOVA for selected factorial model

Analysis of variance table [Partial sum of squares - Type III]

	Sum of		Mean	F	p-value	
Source	Squares	df	Square	Value	Prob > F	
Block	2.21	1	2.21			
Model	3348.57	12	279.05	81.73	< 0.0001	significant
A-litR	8.02	1	8.02	2.35	0.1304	
B-arcA	1510.46	1	1510.46	442.38	< 0.0001	
C-AI	185.85	1	185.85	54.43	< 0.0001	
D-cAMP	279.34	1	279.34	81.81	< 0.0001	
E-CsrA	21.37	1	21.37	6.26	0.0150	
AB	442.18	1	442.18	129.50	< 0.0001	
AD	28.82	1	28.82	8.44	0.0051	
AE	92.97	1	92.97	27.23	< 0.0001	
BD	38.74	1	38.74	11.35	0.0013	
BE	172.20	1	172.20	50.43	< 0.0001	
DE	6.35	1	6.35	1.86	0.1774	
ABE	94.94	1	94.94	27.81	< 0.0001	
Curvature	14.31	4	3.58	1.05	0.3901	not significant
Residual	211.69	62	3.41			
Lack of Fit	187.18	54	3.47	1.13	0.4640	not significant
Pure Error	24.51	8	3.06			
Cor Total	3576.78	79				